NOTE TO USERS

SOLAR-DRIVEN VAPOR FLOW IN WOOD-FRAME WALLS WITH WETTED CLADDING

Shan Huang

A thesis

in

The Department

of

Building, Civil and Environmental Engineering

Presented in Partial Fulfillment of the Requirements
For the Degree of Masters of Applied Science at
Concordia University
Montreal, Quebec, Canada

August 2005

Your file Votre référence
ISBN: 0-494-10219-5
Our file Notre référence
ISBN: 0-494-10219-5

ABSTRACT

SOLAR-DRIVEN VAPOR FLOW IN WOOD-FRAME WALLS WITH WETTED CLADDING

Shan Huang, M. A. Sc.

Solar radiation on wet porous claddings may produce inward vapour flow and condensation. In warm and humid climates, such phenomenon must be considered in the building envelope design. Although no major failure due to solar-driven moisture condensation in cold climates have been reported, such moisture transport may occur, and it is not known to what extent summer condensation must be prevented in Canadian climates. The objective of the project presented in this thesis is to investigate the phenomenon and the factors that influence it. The thesis presents an experimental protocol including test specimen design, monitoring instrumentation and loading conditions. Varied parameters include a wet cladding subjected to simulated solar radiation, location of the vapour retarder and ventilation of the air cavity. Solar radiation is simulated using heat lamps. Experimental results on the hygrothermal performance of walls with wet cladding subjected to simulated solar radiation are presented. Experimental results are further analyzed with the dew-point method and a commercial heat and mass transport model.

Acknowledgements

I would like to thank Dr. Dominique Derome, my thesis supervisor, who guided me with patience and good humor. Doing experiments is really time-consuming and sometimes the results are frustrating. I could always get her encouragement all along. Her thought-provoking suggestions let me never to lose sight of the light at the end of the tunnel.

I would like to thank NATEQ and NSERC for the support in this project, and also gratefully acknowledge the contributions of the following individuals:

Luc Demers and Jacques Payer for providing laboratory technical support,

Hua Ge, Jiwu Rao and Anik St-Hilaire for their comments on the research,

Li Jun Bai for his assistance in the laboratory, and

My parents for their understanding and encouragement.

Table of contents

List of tables

List of figures

Nomenclature

Symbol	Parameter	Units
A	cross-sectional area normal to flow	[m^2]
c	specific heat	[J/kg·K]
D_ϕ	liquid conduction coefficient	[kg/m·s]
E_t	total solar radiation incident on surface	[$W/m^2 \cdot K$]
g_v	Density of moisture flow rate	[$kg/m^2 s$]
H	total enthalpy	[J/m^3]
h_v	latent heat of phase change	[J/kg]
k	thermal conductivity	[$W/(m \cdot K)$]
L	thickness of element – length of path	[m]
q	heat flow rate	[W]
t	time	[s]
T	absolute temperature	[K]
te	sol-air temperature	[K]
p	vapor pressure	[Pa]
w	mass of vapor transferred over unit time	[$ng/s \cdot m^2$]
W	total mass of vapor transferred	[ng]

Greek Alphabet Symbols

α	absorptance of surface for solar radiation	
β	Surface coefficient of vapor transfer	[s/m]

ε	emissivity of surface	
ϕ	relative humidity	[%]
λ	thermal conductivity	[W/m·K]
μ	vapor permeability	[ng/Pa·m·s]

Subscripts

in	indoor
o	outdoor
r	radiation
sat	saturation

Abbreviations

OSB	oriented strand board
RH	relative humidity of the air
WRC	western red cedar

CHAPTER 1 RESEARCH PROBLEM AND OBJECTIVES

1.1 Introduction

Building envelope assemblies have to sustain loads of different types: structural (dead load, wind load), thermal (air temperature gradient, solar radiation), hygric and hydric (vapor pressure gradient, wind-driven rain, rising damp, moisture in material), etc. The capacity of the assemblies to sustain these loads will affect the durability of the envelope. Examples of deterioration of mismanaged moisture loads could be corrosion of fasteners, development of mold on surfaces of the materials, and fungal deterioration of wood and wood-based components.

In studying moisture loads, it is recognized that, although movement of liquid water can result in a very significant amount of moisture introduced into the building envelope and air can also transport a significant amount of moisture, diffusive vapor flow can also lead to wetting of assemblies. In cold climates, the indoor vapor pressure is, most of the year, greater than the outdoor vapor pressure and, as a result, current design solutions of envelope assemblies integrate a vapor barrier towards the inside of the assembly. It is also recognized that, in summer time, the vapor differential is reversed and results in moisture flows towards the inside. In addition, as heat and moisture transfers are highly interrelated processes, vapor movement can be induced by a thermal differential. This

thesis will focus on vapor transfer in summer conditions, particular by looking at solar radiation combined with the use of air conditioning.

1.2 Current state of knowledge

This project looks at one type of loading on the building envelope, especially the wall assembly. The building envelope includes the elements that separate the indoor of a building from the outdoor environment, including the walls, windows and doors, the foundation walls and basement slab, the roof, and skylights, etc. The wall assembly is a major component of a building envelope. Often, it covers the largest area in the building enclosure. If the wall is not designed or constructed reasonably, discomfort may be felt by occupants and degradation of the assemblies may occur.

Since indoor and outdoor conditions are different, differentials in terms of partial vapor pressure, air pressure and temperature produce driving potentials for moisture, air and heat transfer across the whole building envelope system. Moisture in vapor form can be transported by: 1) diffusion, as the result of a differential in partial vapor pressure; or 2) convection, where air movement is the result of a differential in air pressure. In addition, vapor movement can be due to a gradient of temperature. Of the three modes of heat transfer, conduction, convection and radiation, the latter, from the sun, can cause major temperature gradients across a wall. There has been a lot of research work focusing on

the influence of conduction and/or convection on moisture movement, but radiation, especially solar radiation, and its impact on moisture movement has not yet been fully characterized.

The control of the transport of water vapor by diffusion is primarily done with the introduction of a vapor barrier. Vapor barrier membranes have been used in North America since World War II (Rose 1997). Previously, oil-based paints have been playing this role. As its function is to control vapor flows, the choice and location of the vapor barrier must be done in light of the loading conditions. Unfortunately, solutions for cold climates have been duplicated in southern US and there has been a lot of attention given to the problems that followed this misunderstanding of basic knowledge. This situation has led to discussions on whether using low-permeance vapor barriers on the interior of walls and roof systems in large parts of North America is reasonable or not, in light of the possible occurrence of solar-driven vapor flows, also named solar-driven condensation (Straube 2001).

From Chapter 24.7 of the ASHRAE Handbook of Fundamental 2001, it is mentioned that "in mixed climates, the need for low-permeance vapor retarders in most types of buildings is less pronounced than in heating climates or in warm, humid climates. If a vapor retarder is deemed necessary in a mixed climate zone, its placement presents somewhat of a dilemma" (ASHRAE 2001). As presented in more details in Chapter 2,

several works from an initial study of Wilson (1965), to works done in Canada (Straube and Burnett 1995), Sweden (Sandin 1993) and Denmark (Andersen, 1988), tend to demonstrate that damaging solar-driven summer condensation can occur in cold climates as well as in mixed climates.

In terms of vapor diffusion towards the interior, the main questions that remain to be addressed are:

1. Whether such summer vapor flow, of which magnitude varies with geographical location, is sufficient to cause damage and, if so,
2. What would be solutions to prevent such damage.

This project looks at the summer conditions found in a cold climate (Montreal) as the loading conditions for a wood-frame wall assembly with wetted cladding and investigates the risks associated with solar-driven vapor flow.

1.3 Proposed approach

Even though simulation models are becoming widely used to study moisture movement, available models do not yet incorporate air movement, like the natural convection flow behind the cladding, and any model development would still require calibration against experimental data. When the full complexity of heat and mass flows is taken into account,

experimental work is still a complete and accurate mode of investigation of moisture transfer in envelope assemblies. The work presented here is mainly experimental. A test protocol was developed specifically in relation with the research objectives.

This project studies the moisture movement and accumulation in timber-frame wall assemblies from an experimental approach. Factors considered include exterior climate, interior climate, solar absorptance and rainwater absorption. Parameters that were investigated include type of sheathing, presence or absence of polyethylene sheet, presence or absence of ventilation behind the cladding and duration of loading.

1.4 Research objectives

It is possible that solar-driven summer condensation imposes an undue wetting load on the assembly. Although inward vapor diffusion is clearly a design issue, sources of guidelines, like the Canadian Mortgage and Housing Corporation publications or the ASHRAE Handbook of Fundamental (2001), do not provide the design professionals with a means to access the likelihood and severity of the problem, nor do they suggest control measures. The present project looked at the summer-driven vapor flow in terms of extreme loading for wood-frame walls with wood cladding.

In general terms, the scope of this project is to develop a better understanding of the nature and significance of solar-driven inward vapor diffusion through the investigation of hygrothermal performance of different wood-framed wall assemblies under summer conditions, with considerations of a cold climate for loading and assembly design.

Specifically, the objectives of this research are as follows:

- To develop an experimental procedure to simulate and monitor solar-driven moisture flow;
- To run an experimental program using four different test panels in a test hut under simulated solar radiation conditions for a cold climate;
- To analyze the data from the experiments to establish if condensation and/or mold growth occur;
- To perform a parametric analysis of the presence or absence of interior vapor barrier in wood-frame walls under different summer loading schemes using a model calibrated with the experimental results.

In this project, vapor diffusion and the effect of air movement in the air cavity behind the cladding are considered; capillary suction between the cladding and the sheathing is not taken into account. This project is for residential wood-frame buildings in cold climates in North America.

When the moisture behavior of external wall assemblies due to diffusion is analyzed, the most important criteria are amount of water vapor condensation and mold growth in the wall assembly (Vinha, *et al.* 2003). In this study, the research was focused on the first area.

The next chapter reviews the basic building science principles and previous experimental and model work performed to understand and predict the hygrothermal performance of timber-frame wall assemblies under summer conditions. The third chapter presents the methodology of the experimental work, the test set-up and procedure. The fourth chapter describes the experimental results and their analyses. The fifth chapter presents the modeling work done to reproduce the experimental data and the results of the parametric analysis. The last chapter provides the summarized conclusions and main contributions of this study while proposing future work.

CHAPTER 2 LITERATURE REVIEW

2.1 Introduction

In developed countries, there are two main types of residential building structural systems: wood frame and masonry. Wood-frame buildings have been widely used in North America for residential purpose for a long time (Hens and Fatin 1995). The solutions to control of heat, air and moisture flow across the assembly are dependent on the climatic loads. Depending on different climatic conditions, the composition of wall assemblies of wood-frame residential buildings may vary substantially. This chapter starts by a brief review of wood frame systems, followed by functions and ways to fulfill them and will then review the literature on solar-driven vapor flow.

2.2 General overview

2.2.1 Composition of wood-frame wall assemblies

For the rain screen base system, which is widely used under Canadian climates, the wall components from outside to inside are as follows:

- Exterior veneer (e.g. brick, wood siding, aluminium, stucco etc.)
- Air space (19 mm as minimum)
- Weather barrier (e.g. spun bonded polyolefin membrane, construction paper)
- Sheathing (e.g. fiberboard, plywood, OSB etc.)

- Wood stud (38 mm x 89 mm or 38 mm x 140 mm)
- Insulation (e.g. glass fiber, mineral wool, extruded polystyrene, expanded polystyrene, polyurethane, cellulose fiber etc. applied between wood studs, outside of sheathing materials or both; insulation on inside of studs is used almost only in case of retrofitting)
- Vapor barrier (polyethylene sheet, kraft paper)
- Interior finishing (gypsum board and paints; possible use of paint as vapor retarder)

2.2.2 The functions of building envelope walls

The overall function of a building envelope is to provide a barrier between indoor and outdoor environments, so the indoor conditions can be maintained within acceptable limits. Hutcheon (1963) has provided the list of principal requirements for walls. Hence, walls must:

- Control heat flow;
- Control air flow;
- Control water vapor flow;
- Control rain penetration;
- Control light, solar and other radiation;
- Control noise;
- Control fire;
- Provide strength and rigidity;

- Be durable;
- Be aesthetically pleasing;
- Be economical.

The control of heat flow is mainly performed by the insulation. The control of air flow requires the integration of the air barrier approach to the system. For the rest of this thesis, the discussion will focus on airtight wall assemblies. Control of rain penetration is achieved by cladding systems where water is allowed to run off the façade surface, and by proper flashing details to prevent the infiltration of water. Cladding may get wet though. Next, a more detailed explanation of heat and vapor diffusion flow mechanisms and control options is presented.

2.3 Review of heat transfer

Heat transfer is due to a temperature difference. There are three modes of heat transfer: conduction, convection and radiation. Each one plays a role in the problem that will be later studied.

2.3.1 Thermal conduction

In ASHRAE Fundamental 2001, conduction is defined as the mechanism of heat transfer whereby energy is transported between particles or groups of particles at the atomic level.

Steady-state one-dimensional conduction is used to calculate heat loads for HVAC design. In terms of building envelope design, it is used to calculate the surface and interior layer temperatures, which are needed for vapor flow/ condensation calculations.

For steady-state heat conduction in one dimension, the Fourier law is:

$$q = -(k\ A)\ d_t/d_x \qquad (2.1)$$

where q: heat flow rate [W]

k: thermal conductivity [W/(m · K)]

A: cross-sectional area normal to flow [m^2]

d_t/d_x: temperature gradient [K/m]

-: heat flow is positive in the direction of decreasing temperature

The thermal conductivity, k, may be assumed constant over the temperature range for a building envelope. Steady-state one-dimensional conduction is used to calculate the surface and interior layer temperatures, which are needed for vapor flow/ condensation calculations. To control heat flows by conduction, insulation is used. Minimum R-values are set in government regulations (e.g. Règlement sur l'efficacité énergétique in Québec) and model codes (e.g. Model Energy Code of Canada), etc.

During the design process, heating degree days are widely used to decide the minimum thermal resistance of walls and roofs. Heating degree days are calculated based on the indoor temperature and daily average outdoor temperature. For example, for one particular day if the average temperature is -10°C and the indoor temperature is 18°C, the

difference in temperature from indoor to outdoor is 28°C. Therefore, that day represents 28 heating degree days. Summing the heating degree days for the entire year will yield the total heating degree days for that region.

2.3.2 Thermal convection

In ASHRAE Fundamental 2001, thermal convection is defined to be energy transfer by fluid movement and molecular conduction (Burmeister 1983, Kays and Crawford 1980).

As air is warmed against a warm surface, it becomes lighter and moves up. Also, when air is in contact with a cold surface, it gets colder, heavier and thus moves down. This movement is called convection and transfers heat from one place to the other. In a building envelope, convection may take the form of a closed loop in an enclosed space, e.g. in an stud space without insulation or with low-density insulation. Convection may also be air movement across the envelope or behind the cladding. In an air cavity, convection may result from air in contact with cladding at a different temperature or be induced by air pressure differentials created by wind. When wind blows over a building, positive and negative air pressure gradients form, which may induce air movement into or out of the air spaces.

In the building envelope, this transfer of heat at the inside and outside surfaces of the assembly is taken into account with surface coefficients. The film coefficients are

denoted ho and h_i, and include both the convection coefficient and an equivalent radiative coefficient.

$$q = h\ A\ (T_{surf} - T_{air}) \qquad (2.2)$$

where $h = h_c + h_r$

2.3.3 Thermal radiation

With conduction and convection, heat transfer takes place through matter. In ASHRAE Fundamental 2001, thermal radiation is defined as a change in energy form from internal energy at the source to electromagnetic energy for transmission, then back to internal energy at the receiver.

As cavities or air spaces are found within the envelope assemblies, the radiative exchange between the surfaces of these air layers is often required. The ASHRAE Fundamental has tables that list equivalent conductance for different emissivities and orientations of air between parallel plates.

The radiative component is calculated using:

$$q_r = A\ \sigma\ f_{1\text{-}2}\ (T_1^4 - T_2^4) \qquad (2.3)$$

where: q_r: radiative heat flow [W]

$f_{1\text{-}2}$: $\dfrac{1}{1/\varepsilon 1 + 1/\varepsilon 2 - 1}$

ε : emissivity of surface

T: absolute temperature [K]

This is linearized to yield

$$q_r = A\ \sigma 4\ T_m^3\ f_{1\text{-}2}\ (T_1\text{-}T_2) \quad (2.4)$$

simplified to

$$q_r = A\ h_r\ (T_1\text{-}T_2) \quad (2.5)$$

where $h_r = 4\sigma\ T_m^3\ f_{1\text{-}2}$

In cavities, this is combined with the convective coefficient to yield the convective surface coefficient, as presented in the previous section.

2.3.3.1 Solar radiation

When there is solar radiation, the surface temperature is raised above the ambient air temperature. The concept of sol-air temperature was developed to provide the air temperature that would result in the same surface temperature that would result from solar radiation exposure. The definition of sol-air temperature is shown in the following equation.

$$ho \cdot (te - to) = \alpha \cdot Et \quad \text{(ASHRAE Fundamental 2001)} \quad (2.6)$$

where:

α : absorptance of surface for solar radiation

Et : total solar radiation incident on surface [W/m^2·K]

te : sol-air temperature [K]

to : outdoor air temperature [K]

However, this concept cannot be used in all situations and the exact solar radiation on a surface may be required. From solar radiation calculation (Appendix B), the solar intensity that falls on a south facing vertical wall surface on July 21 in Montreal is 433 W/m². When the air temperature is 22 °C, the resulting sol-air temperature would be 45°C.

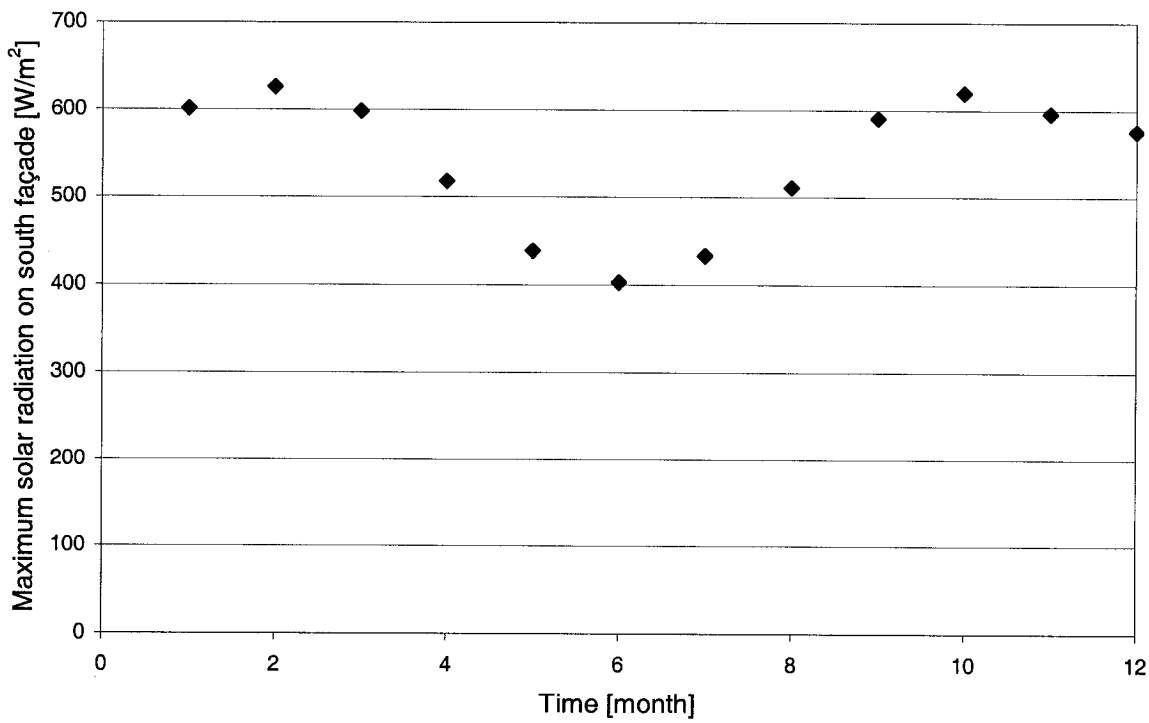

Figure 2.1. Maximum monthly solar radiation on a south facing vertical wall surface—for Montreal calculated based on data from 21st of each month

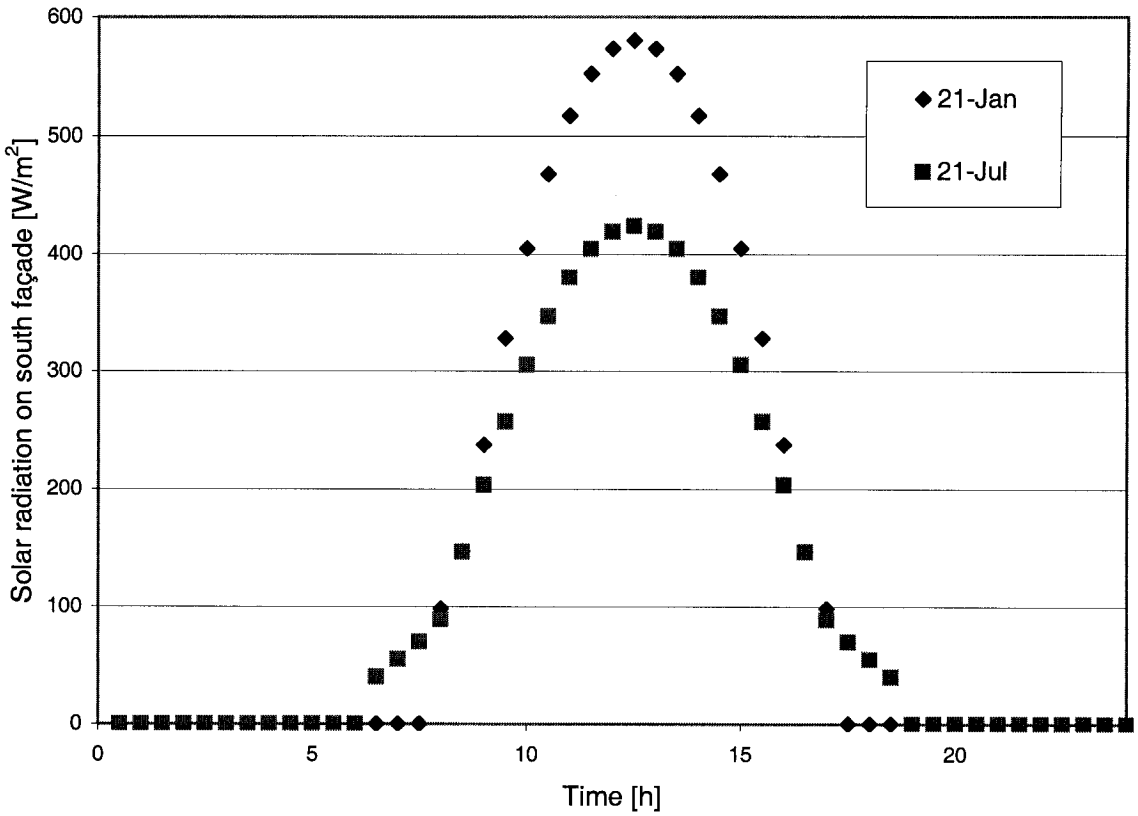

Figure 2.2. Daily solar radiation intensity on a south face wall surface--Montreal

2.4 Review of moisture transfer

The moisture transfer through an envelope assembly occurs either via the slow process of diffusion through the material or via the faster movement of moisture laden air through the discontinuities in the building materials. Kumaran (1992) explains the complexity of moisture transfer in its different phases: ice, water, vapor and adsorbate film. For this building envelope study, there are two main moisture transfer modes: diffusion and convection of vapor, but, as some condensation may occur, some liquid uptake can also occur. Also, the wetting of cladding is mainly through water uptake of wood and some absorbate water redistribution. The study here will not focus on the wetting mechanisms

of the cladding and will start the analysis with a wet cladding. Also, the cladding is used as a reservoir of water and a simplified evaporation mechanism will be assumed.

2.4.1 Moisture diffusion

Although, for most cases, rain penetration or air leakage is more important than vapor diffusion during the process of moisture transfer, vapor diffusion must always be seriously considered (Latta and Beach 1964). Vapor transfer through continuous building materials may occur through two processes: gas phase diffusion in air contained in the interrelated pores of materials, and by adsorption by the inner surfaces of the pores of polar materials.

Fick's equation is widely used to calculate water vapor transfer through materials.

$$w = -\mu \delta p / \delta x \qquad (2.7)$$

where w= mass of vapor transferred over unit time [ng/s·m^2]

μ = permeability [ng/Pa·m·s]

p = vapor pressure [Pa]

x = distance along the flow path [m]

Permeability is a function of vapor pressure and temperature. It is not a constant. However, an average permeability can be used for approximate purpose.

$$W = \bar{\mu}\theta A (P_1-P_2) / L \quad (2.8)$$

where W = total mass of vapor transferred [ng]

A = cross section area of flow path [m^2]

θ = time of flow [seconds]

P_1-P_2 = vapor pressure difference [Pa]

L = thickness of element – length of path [m]

$\bar{\mu}$ = average permeability [ng/ Pa·s·m]

For a component of fixed thickness, the permeance, M, is defined as below.

$$M = \bar{\mu} / L \ [ng/ Pa\ s\ m^2] \quad (2.9)$$

2.4.2 Moisture movement by convection

Moisture-laden air can be introduced into the building envelope through small holes. The driving potential for this process is air pressure difference caused by either the stack effect or mechanically-driven air movement.

Convective mass transfer is analogous to convective heat transfer where geometry and boundary conditions are similar (ASHRAE Fundamental 2001).

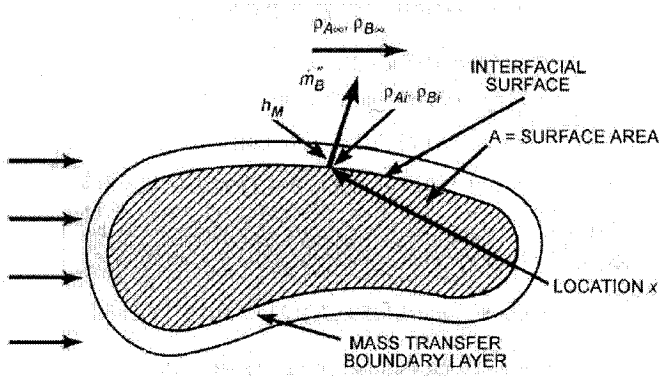

Figure 2.3. Nomenclature for convective mass transfer from external surface at location x where surface is impermeable to gas A (from ASHRAE Fundamental 2001)

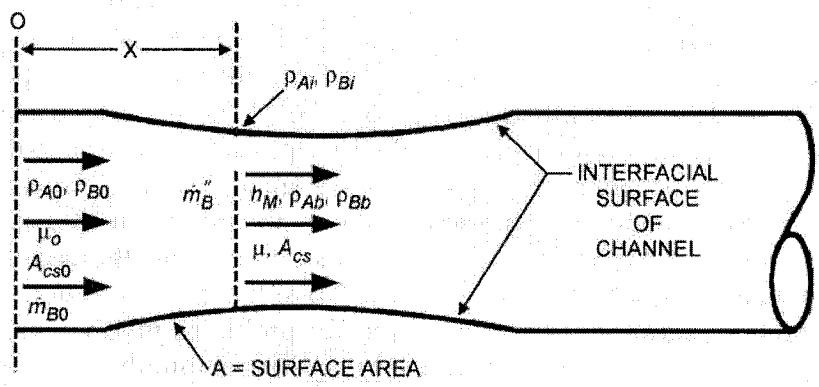

Figure 2.4. Nomenclature for convective mass transfer from internal surface impermeable to gas A (from ASHRAE Fundamental 2001)

Most external convective mass transfer problems can be solved with an appropriate formulation that relates the mass transfer flux (to or from an interfacial surface) to the concentration difference across the boundary layer. This formulation gives rise to the convective mass transfer coefficient, defined as

$$h_M \equiv \frac{\dot{m}''_B}{\rho_{Bi} - \rho_{B\infty}} \tag{2.10}$$

h_M = local external mass transfer coefficient [m/s]

$\dot{m}''_B$ = mass flux of gas B from surface [kg/ (m^2·s)]

ρ_B = density of gas B at interface (saturation density) [kg/m^3]

$\rho_{B\infty}$ = density of component B outside boundary layer [kg/m^3]

Moisture movement by natural convection:

As discussed above in the thermal convection section, air convection forms in air space, and wind pressure on buildings may induce air movement into or out of air spaces. During this process, relatively dry outside air takes the place of moist air, and moist air is transported to the outside.

Moisture accumulation in materials and conditions that lead to fungi growth:

Problems with high moisture content appear in the wooden framework. The problems in the timber-frame wall assemblies are first and foremost mold and decay of organic materials. The most important boundary conditions for the growth of fungi are temperature, humidity and substrate conditions, which have to be simultaneously available over a certain period of time.

2.5 Condensation

2.5.1 Principle of Condensation

Relative humidity is an expression of the partial pressure of water vapor in air:

$$RH = Pw / Psat \times 100 \quad (2.11)$$

Where RH= relative humidity [%]

Pw= partial vapor pressure in air for a given temperature [Pa]

Psat= saturation vapor pressure for the same given temperature [Pa]

When the temperature changes, a given volume of moist air keeps the same amount of moisture, but the relative humidity changes. When temperature is increased, RH decreases, and when temperature is decreased, RH increases. At one point, RH=100%, and this means that the partial vapor pressure equals the saturation vapor pressure. Once saturated, the air cannot support more vapor, and the excess vapor will condense.

2.5.2 Main occurrence of condensation in cold climate

In winter, indoor vapor pressure is higher than outdoor vapor pressure; the moisture movement is from the interior to the exterior. At a point where the actual vapor pressure is higher than the saturation vapor pressure at the same temperature, condensation occurs. Usually, vapor barriers are used behind the interior gypsum board. Control of winter

condensation is the reason why vapor barriers were introduced into the modern building envelope (Rose 1997).

2.5.3 Vapor Barrier

The vapor barrier is a membrane or system to retard the diffusion of moisture into building cavities. Vapor barriers have been used in North America since World War II (Rose 1997). Rose provided a history on both the conceptual development and physical application of vapor barriers in the United States. Nowadays, polyethylene sheet is widely used as vapor barrier for the building envelope system.

Straube (2001) specified the function and requirement as: "The function of a vapor barrier is simply the control of water vapor diffusion to reduce the occurrence or intensity of condensation. As such, it has one performance requirement: it must have the specified level of vapor permeance and be installed to cover most of the area of an enclosure. If a small crack or perforation occurs in a vapor barrier, its performance is not substantially reduced and such imperfections can be accepted."

In Straube's paper (2001), in the "Example Calculations" part, the author uses the dew-point method to calculate vapor diffusion through several wall assemblies under the weather conditions of Omaha, Nebraska. These calculations are in order to prove the author's point of view which is summarized as follows: with a vapor barrier, there are

moisture problems; without a vapor barrier, no moisture problem or only minor moisture problem occurs. The calculation analysis part is shown in Appendix C.

Table 2.1 is a summary of the calculation analysis for Omaha, Nebraska (a cold climate). The calculations by Straube (2001) are complemented by more calculations, performed by the author, for different conditions and assemblies, using the same methodology as described in Straube's paper. The detailed calculation process is shown in Appendix C.

According to the analysis results (Table 2.1), it is shown that applying a low permeance vapor retarder towards the inner side of the insulation is not the only reason for condensation in wall assemblies under a cold climate. Vapor retarder cannot only be regarded as several kinds of building materials, of which their vapor permeance is lower than 60 ng/Ps·m^2·s. A wall assembly is a system. The hygrothermal performance of a wall assembly depends on the climate loading, thermal resistance, vapor permeance of its components, etc.

Table 2.1 provides the moisture content rise of the bottom plate for each wall assembly after the calculation duration of one month. From the analysis results, the wall assemblies with a low permeance vapor retarder may have no moisture problems, and the wall assemblies without a low permeance vapor retarder may still have moisture problems.

Summary

Calculation for Omaha, Nebraska (a cold climate)

Wall 1	**Temperature**	**Temp: 21/ -19°C**		**Temp: 21/ -4°C**	**Temp: 21/ 5°C**	**Temp: 22/ 40°C**
	Element	Table 1	Table 9	Table 2	Table 7	Table 14
	Inside film	Condensation	Condensation	Condensation	Condensation	Condensation
	Vapor retarder	Rate: 0.172 g/m2h	Rate:0	Rate: 0.10 g/m2h	Rate:0	Rate: 0.370 g/m2h
	Batt insulation	Mvapor retarder:**60**	very small	MR (plywood)=1.05%	very small	MR(spruce)=1.75%
	Plywood	Mplywood:**40**	Vapor retarder: **M=1.5**			
	Outside film	MR (plywood)=2%				
Wall 2	Element	Table 3	Table 13	Table 15	Table 16	Table 17
	Inside film	No condensation	Condensation	No condensation	No condensation	Condensation
	Painted drywall	in door RH=30%	Rate: 0.092 g/m2h	in door RH=30%	in door RH=30%	Rate: 13.1 g/m2h
	Batt insulation	Mpainted drywall:**180**	in door RH=40%			MR (painted drywall)= 87.33%
	Fiberboard	Mfiberboard:**1666**	MR (fiberboard)=1.69%			
	Outside film					
Wall 3	Element	Table 18		Table 4	Table 19	Table 20
	Inside film	Condensation		No condensation	No condensation	Condensation
	Vapor retarder	Rate: 0.270 g/m2h		Vapor retarder: **M=180**		Rate: 1.48 g/m2h
	Batt insulation	Mvapor retarder:**180**				MR (spruce)=7.01%
	EPS sheathing	Meps:**150**				
	Outside film	MR (spruce)=1.28%				
Wall 4	Element	Table 21		Table 22	Table 23	Table 5
	Inside film	No condensation		No condensation	No condensation	Condensation
	Vapor retarder	Mvapor retarder: **60**				Rate: 13.64 g/m2h
	Batt insulation	Mfiberboard: **1666**				MR (spruce)=64.61%
	Fiberboard					
	Outside film					
Wall 5	Element	Table 10		Table 12	Table 11	Table 24
	Inside film	Temp: 21/ -19°C		Temp: 21/ -4°C	Temp: 21/ 6°C	Temp: 22/ 40°C
	Gypsum drywall	Condensation		Condensation	No condensation	No condensation
	Batt insulation	Rate: 0.508 g/m2h		Rate: 0.291 g/m2h		
	Plywood	Mgypsum:**180**		MR(plywood)=3.06%		
	Outside film	Mplywood:**40**				
		MR (plywood)=5.33%				

Note:
- [thick box] means tables the author mentioned in the paper
- [thin box] means tables the author only mentioned their results in the paper
- [no box] means relevant tables the author didn't mentioned in the paper
- MR: Moisture Content Rise For One Month

Table 2.1 Dew point calculation results for cases in Straube 2001 and complementary conditions

2.5.3 Summer Condensation

2.5.3.1 Reason for summer condensation

Sun-driven moisture flow is a phenomenon that occurs when walls are wetted and then heated by solar radiation. For wood-frame wall assemblies with masonry veneer, in summer, the temperature in the masonry can rise from 40 to 50 °C. If the masonry is wet, e.g., by heavy rain, the vapor concentration will become very high. At the same time, the indoor temperature and vapor concentration are much lower than in the masonry. This will result in vapor transport from the exterior towards the interior. This inward vapor movement has been called "solar vapor flow reversal", since the direction of the vapor movement is opposite to the direction usually considered for a cold climate building envelope design. If there is a vapor barrier on the inner side of the wall, the relative humidity will become very high. In extreme conditions, summer condensation can take place on the outside of the vapor barrier

The condensation water may run down and accumulate at the base of the wall assembly, and damage to the wood members may occur. During the warm season, especially in summer, the thermal gradients that could promote drying are relatively small, when no sun radiation is present. The drying potential is relatively small, too. As well, whenever the temperature is above 5 °C and less than 40 °C, the relative humidity is above 80%,

wood members may be vulnerable to fungal growth. If moisture accumulates in a wall during cold weather, it may not necessarily be damaging since the wall may dry out before temperatures conductive to decay occur (Pressnail 2003).

2.5.3.2 Severity of summer condensation

The results of summer condensation should be seriously considered. Straube (2001) explained this for the following two reasons:

1. When summer condensation occurs, the temperature of condensation plane is warm enough for fungal growth, and the rate of corrosion is much higher than with condensation in winter conditions;
2. The summer condensation plane is often close to the interior, a location within an enclosure that is rarely built with moisture-tolerant materials (drywall interior finishes are unlike cladding and sheathing products, which are often assumed to receive some wetting);

2.5.3.3 Typical indoor/outdoor environmental conditions under summer conditions in Canada

Building envelopes and mechanical systems should be designed for a specific hygrothermal region, rain exposure zone and interior climate class. The following is a

proposal for classifying loading conditions. It has been developed by Lstiburek and Pettit (2004).

Figure 2.5. Hygrothermal region map by Lstiburek and Pettit (2004).

Hygrothermal Region:

- Very cold
- Cold
- Mixed-humid
- Hot-dry/ Mixed Dry
- Hot-humid

Rain exposure zone:

- Extreme (above 60 inches annual precipitation)
- High (40 to 60 inches annual precipitation)
- Moderate (20 to 40 inches annual precipitation)
- Low (less than 20 inches annual precipitation)

Interior climate classes:

1) Temperature moderated;
    a) Vapor pressure uncontrolled;
    b) Air pressure uncontrolled (warehouses, garages, storage rooms);
2) Temperature controlled
    a) Vapor pressure moderated;
    b) Air pressure moderated (houses, apartments, offices, schools, commercial and retail spaces);
3) Temperature controlled
    a) Vapor pressure controlled;
    b) Air pressure controlled (hospitals, museums, swimming pool enclosures and computer facilities).

Such classification systems may one day be part of building codes and could be used to provide guidelines to designers when deciding on the best approach to control summer-driven moisture flows.

2.5.3.4 Hygrothermal transfer modeling

The following section presents two examples of heat and moisture transfer model for building envelope assemblies.

1. WUFI -ORNL/IBP

WUFI-ORNL/IBP is a windows-based PC program for the hygrothermal (heat and moisture) analysis of building envelope construction (ASTM MNL 40). It is widely used as a transient hygrothermal model by building envelope designers in North America.

WUFI allows realistic calculation of the transient hygrothermal behavior of multi-layer building components exposed to natural climate conditions, and at the same time, indoor/ outdoor environmental conditions may be changed to suit the desired simulation conditions. The WUFI model can handle contributions from rain, solar radiation, and other crucial weather events on an hourly basis. Both vapor and liquid transport are included along with the sorptive capacity of building construction materials.

The governing equations employed in WUFI ORNL/IBP model for mass and energy transfer are as follows:

for moisture transfer

$$\frac{\partial w}{\partial \phi}\cdot\frac{\partial \phi}{\partial t} = \nabla\cdot(D_\phi \nabla\phi + \delta_p \nabla(\phi p_{sat})) \qquad (2.11)$$

for energy transfer

$$\frac{\partial H}{\partial T}\cdot\frac{\partial T}{\partial t} = \nabla\cdot(\lambda \nabla T) + h_v \nabla(\delta_p \nabla(\phi p_{sat})) \qquad (2.12)$$

where

ϕ = relative humidity

t = time [s]

T = temperature [K]

c = specific heat [J/kg·K]

w = moisture content [kg/m^3]

Psat= saturation vapor pressure [Pa]

λ = thermal conductivity [W/m·K]

H = total enthalpy [J/m^3]

D_ϕ = liquid conduction coefficient [kg/m·s]

δ_p = vapor permeability [kg/m·s·Pa]

h_v = latent heat of phase change [J/kg]

The WUFI-ORNL/IBP software offers a user-friendly interface for data input. The definition of the component geometry is performed by a graphical interface with automatic grid generation. The software comes complete with weather data for 53 North American cities. Results, such as temperatures, relative humidities and water contents, can be analyzed with the help of preconfigured or user-defined diagrams. All the computed profiles can be displayed in rapid succession as a film that shows the transient thermal and hygric processes occurring in the enclosure. The film is ideal for gaining insights into the hygrothermal processes and for developing insight for the situation. The reactions of the different materials to the changing climatic conditions can be visualized directly.

2. HygIRC

Kumaran (2003) stated, "The computer model hygIRC was used to investigate the hygrothermal responses of wall assemblies. The model predicts (not in absolute terms but

on a relative basis) real-time response of the wall to change environmental conditions and hygrothermal loads. It simulates simultaneous heat, air and moisture transfer. The model hygIRC provided the hygrothermal response of the wall assembly, at each hour. These responses at any selected point were quantified in terms of a temperature, moisture content (or RH) and a pair of airflow velocity vectors. The following four mechanisms of moisture transfer were considered in hygIRC analyses:

- Vapor diffusion due to vapor pressure differences across the wall, as defined by the weather records and indoor conditions;
- Wind-driven rain impinging on the exterior face of the cladding, as defined by the weather records and a prediction method to convert vertical rainfall to rain deposition on a vertical surface due to the prevailing wind;
- Unintentional rainwater leakage into the stud space, as derived from testing of full-scale wall specimens in a dynamic wall test facility and adjusted to the weather records;
- Vapor transport that accompanies natural and unintentional airflow across the wall, as defined by the weather records and through specified airflow paths respectively;"

Lawton and Brown (2003) used NRC's HygIRC to simulate the performance of a wall assembly for Vancouver climate. HygIRC uses rain and wind data to calculate the

amount of rain that will hit a vertical surface and uses radiation and cloud index data to calculate radiant heat transfer between the wall and the surrounding sky.

2.5.3.5 Experimental work and other sun-driven moisture flow related topics

Condensation under summer conditions has been reported for many years. Hutcheon (1953) described such phenomenon fifty years ago: "When a vapour barrier is used, the wall can lose moisture only to the outside. In summer, hot sun following a rain drives moisture as vapour to the inside of the wall, and condensation behind the vapour barrier can occur."

Through field measurements of masonry walls in residential construction in Canada, Wilson (1965) demonstrated that summer condensation could occur in the insulation and on the vapour barrier of walls incorporating permeable insulation. Two solutions were provided to address summer condensation:

- Use of an exterior cladding that is not readily wetted by rain, which means the siding materials having only small moisture capacities;
- Ventilation with outside air between the masonry and inner components where absorptive masonry is used.

Christensen (1985) made a series of tests, which were based on traditional insulation systems in Denmark, and proposed different ways to prevent summer condensation.

- Using overhang to prevent driving rain from hitting the wall;
- Siliconating the wall thus preventing the absorption of moisture;
- Using cladding materials having only small moisture capacities;
- Placing asphalt paper on the outside of the insulation and a vapour barrier is then placed on the interior side of the insulation as usual.
- In brick veneer walls, ventilation can be arranged between bricks and the airtight layer protecting the insulation material.
- Using insulation materials with high moisture diffusion resistance to reduce the moisture flow inwards.

Anderson (1985) described the summer condensation problems in Denmark. He advised several ways to solve them:

- Using water-repellent cladding;
- Incorporating a ventilated space between brick facings and the insulation behind them;
- Installing an asphalt felt between the bricks and the insulation;

Anderson also concluded "It is likely that problems associated with summer condensation are related more to air leakage, rain penetration, and solar heating than classic vapour drive. In most cases, the installation of vapour retarders (near the outside) is not the solution to such problems, but in some areas vapour retarders may be needed."

In the United Kingdom, the Building Research Establishment (1989) believed that omitting the vapour barrier should not be considered an acceptable solution since summer condensation can also occur behind low-permeability internal finishes.

Sandin (1993) clearly explained the reason of summer condensation for wooden frame walls with masonry veneer. He evaluated the value of the air space and vapour barrier in a cavity wall in terms of their moisture transfer function. Sandin finally provided a simple measure, excluding the vapour barrier on the inner side of the wall, to deal with the extreme climate (heavy driving rain followed by sunshine and cooling of the indoor air). He specified two preconditions for excluding the vapour barrier: there should be no vapour-tight layer on the outer side of the wall; the vapour concentration of the indoor air should not be extremely high.

Whether using low-permeance vapour barriers on the interior of wall and roof systems in large parts of North America is reasonable or not has become a focus of discussion in building envelope design. Straube and Burnett (1998) mentioned the problem of summer condensation and, in their conclusion, they questioned the current practice of installing very low-permeance vapour diffusion retarders. One of the most compelling reasons for not providing a low-permeance vapour retarder on the interior of some enclosures even in cold climates is the phenomenon of solar-driven summer condensation (Straube 2001).

In addition to the discussions on summer condensation problems in "cold" climates as reported above, others researchers have proven that such problems occur in warm climates and may cause moisture problems. Looking at condensation of moisture in exterior wood-frame walls, Tenwolde and Mei (1985) indicated "in a warm, humid climate, an interior vapour retarder is undesirable unless an exterior vapour retarder is installed as well".

When a vapour barrier is used, the wall can lose moisture only to the outside. In summer, sun radiation on the cladding wetted by rain drives moisture as vapour to the inside of the wall, and condensation on the vapour barrier can occur. Straube (2001) described several ways to control inward vapour drives for many cool and temperate climates:

- Avoiding rainwater absorption of cladding (on both the front and back side, since rainwater that penetrates most cladding can drain down the back and be absorbed) or the wetting of outer layers of the enclosure;
- Using a moderate vapour permeance component on the exterior (e.g., a vapour permeance in the order of 100 to 200 ng/(Pa·s·m^2) combined with a moderate vapour retarder on the interior, in the order of 150 to 300 ng/(Pa·s·m^2)).

Solar-driven summer condensation is a phenomenon that occurs when absorptive wall components are wetted by rain, and then heated by solar radiation. For wood-frame wall assemblies with wood siding, in summer, the temperature on the surface of the wood

siding can rise to 40-50°C. If the wood siding is wet, e.g., by heavy rain, then heated by sun radiation, the wood siding will dry to all the directions. The vapour pressure will become very high in the air layer. At the same time, the indoor temperature and vapour pressure are much lower than in the air cavity (indoor: 21°C, 40%). This vapour pressure difference will result in vapour transport from the exterior towards the interior. The moisture flow is from wet wood siding to air space, sheathing membrane, sheathing, insulation, vapour barrier and gypsum board. If there is a vapour barrier on the inner side of the wall, moisture will be "blocked" on the exterior of the vapour barrier. In extreme conditions, condensation appears on the outside of the vapour barrier.

Pressnail, et al. (2003) analyzed the consequences of summer condensation. Condensation water may run down and accumulate at the base of the wall assembly, and damage to the wood members may occur. During the warm season, especially in summer, the thermal gradients that could promote drying are relatively small. As well, whenever the temperature is above 5°C and less than 40°C, and the relative humidity above 80% RH, wood member may be vulnerable to fungal growth. Mold growth will occur ultimately followed by wood decay. At higher relative humidity levels, over a long period of time, the risk of fungi growth will increase. In unfavourable circumstances, mold may produce an unpleasant smell (Santin 1991). If moisture accumulates in a wall during cold weather, it may not necessarily be damaging since the wall may dry out before temperatures conducive to decay occur.

Another reason that summer condensation should be seriously considered is that "the summer condensation plane is often close to the interior, a location within an enclosure that is rarely built with moisture-tolerant materials (drywall interior finishes are unlike cladding and sheathing products, which are often assumed to receive some wetting)" (Straube 2001).

Pressnail, et al. (2003) did a series of tests in order to find ways to control sun-driven moisture. The tests were based on two basic wall systems: one is a wall system with an exterior air cavity; the other one is a wall system that incorporated low permeance exterior sheathing. In order to simulate solar radiation, a set of heat lamps in front of the test panels were used to produce a net surface temperature increase of approximately 25K. After the tests, two solutions were provided to control sun-driven moisture: one is the use of low vapour permeance insulated sheathing, e.g., extruded polystyrene, and the other one is the use of a vented air cavity. Pressnail (2003) investigated several various cavity widths, 25 mm (1"), 37.5 mm (1.5"), 50 mm (2") and concluded that a 25 mm vented air gap can be used to manage solar-driven moisture. From the test results and computer modelling, it was also demonstrated that even without an air space, low permeance insulated sheathing can very effectively control sun-driven moisture.

In Pressnail's paper (2003), there is one main type of wall construction without an air cavity where the wet siding was placed in direct contact with the spun-bonded polyolefin

air barrier. In such cases, it should be recognized that vapour diffusion is not the main mechanism to transport moisture. Capillary suction is the main mechanism of moisture transportation instead.

The work presented above has provided insights on the occurrence of solar-driven moisture flows. However, the work performed so far was very limited in scope and the data produced is scarce and difficult to analyse in detail due to lack of information on all conditions during the measurements.

2.6 Conclusions

The above literature review shows, after a review of the building envelope components and functions and of basic heat and mass transfer processes, the current knowledge on solar-driven summer condensation. The review shows that such phenomenon needs more investigation to understand its mechanisms and that, maybe, more solutions to solve the problem should be provided. In the project presented in this thesis, the author aimed to evaluate the magnitude of solar-driven summer condensation. Tests were carried out to determine the influence of the different parameters on the hygrothermal performance of the wall assemblies, including types of sheathing, moisture content of cladding, location of vapour barrier and ventilation of air cavity. Part of the objectives of the tests was to

evaluate the validity of the proposed test set-up to produce reproducible results. The experimental procedure is detailed in the following chapter.

CHAPTER 3 METHODOLOGY

From the literature review, the previous experiments did not reflect Canadian field construction. For example, in Pressnail's paper (2003), there is one main type of wall construction without air cavity where the wet siding was placed in direct contact with the spun-bonded polyolefin air barrier. In such cases, it should be recognized that vapour diffusion is not the main mechanism to transport moisture. Capillary suction is the main mechanism of moisture transportation instead. The proposed work aimed at reproducing realistic conditions.

3.1 General methodology

Solar-driven moisture flow occurs under specific conditions. The aim of the experimental work was to reproduce these conditions. The chosen approach focused on reproducing solar radiation on a wet cladding and studying the moisture flow in the few hours (6 to 18 hours) that followed each wetting event. An important development effort was required to determine the appropriate test conditions. In many early attempts, no moisture content variation could be measured. Also, special attention was put into developing a multi-component gravimetric specimen for monitoring. Once the testing protocol was developed and the test setup built, test panels were built and a series of experiments were carried out to investigate the phenomenon and the factors that influence solar-driven vapor flow. This chapter describes some of the development

efforts and the final experimental protocol. Chapter 4 reports the experimental results. Analyses based on the test results are found in Chapter 5.

3.2 The experimental procedure development

The test setup and test procedure were developed specially for this investigation. No existing standard method could be used to address this issue. The developed procedure was based in part on previous works performed at Concordia, and in part on information gathered during the literature review. Several tentative preliminary tests were performed during test procedure development.

3.2.1 Environmental conditions

During the experimental process, the exterior conditions were the environmental conditions of the Concordia laboratory. The interior conditions were air-conditioned. In a first preliminary setup the test hut was not air conditioned, and the effect of the heat lamps resulted in an increase in temperature of the warm air in front and behind the test panel. No moisture accumulation was measured according to a series of preliminary tests. Then, an air conditioner (6000 BTU) was installed in the test hut, and a cardboard box with holes on three sides (top/left/right) was used to cover the air conditioner to create a mixed airflow within the test hut. Nine thermocouples were installed evenly near the interior gypsum board of the test panel at a distance of 5 mm to measure the air temperature. In the first trial, the thermometer of the air conditioner was inside the cardboard box, and air inside the cardboard box reached the temperature set point faster than air outside the cardboard box. The air temperature near the gypsum drywall was

always 4 to 5 degrees higher than the temperature set point, which was 19 °C for all experiments. Then the thermometer of the air conditioner was extended to the outside of the box within the test hut, thermocouples showed that temperature differences were within ±1 °C during the tests.

3.2.2 Wetting of the cladding

The main challenge in the wetting of the cladding was to provide a uniform initial moisture source where water would be in a material that would release moisture at a realistic rate. Therefore, extremely porous materials like autoclaved aerated concrete or absorbing fabric were not considered. Materials considered were unpainted wood siding (commonly West Coast Cedar) and brick veneer.

Also, the manipulation of the cladding element was an issue. Due to laboratory constraints, no crane or lift device was available to move the cladding. This is the main reason why brick veneer was not selected.

Finally, the cladding panel was developed to be able to undergo dimensional movement due to moisture content variations, allow easy weighing and installing on the test hut and provide a mechanism to let the air cavity be open or closed.

The movement of water and vapor in wood is slow. After the wood siding was totally soaked in water for 48 hours in a preliminary test, a piece of western red cedar was cut

in the middle. It showed on the cross section that water moved into 1 mm from the surface towards the inner part of the siding piece. Another preliminary soaking test, which lasted for five days, showed a similar result. In order to shorten the sample preparation time, the wood siding was fully immersed in water for 48 hours before each test. Although the wood siding was soaked in water for 48 hours, the amount of water absorbed by the siding was still reasonable. Brick cladding can absorb the same amount of water in much shorter time.

3.2.3 Gravimetric sample

There is no existing equipment to measure moisture flow. Since moisture accumulation can be easily monitored, maximum moisture accumulation was recorded for all the experiments as the most important finding to evaluate the hygrothermal performance of the wall assemblies.

In order to measure moisture accumulation, a 150 x 150 mm sample was cut from the top right of the testing panel when viewed from the outside, as shown in Figure 3.15. It included:

- 12.7 mm gypsum board;
- with or without 6 mil PE-membrane;
- 89 mm glass fiber batt;

In order to make the whole gravimetric sample "isolated" from the surrounding, and easy to be taken out for weight measurement, this sample was wrapped with fiber mesh

tape, and was provided with a small gutter at the bottom to collect water accumulation. Air leakage around the gravimetric sample was small enough to be considered negligible.

3.2.4 Preliminary tests

Once all these developments seemed to provide a satisfactory performance, preliminary tests were carried out to test the parameters and procedures of the experiments of this research project. The following section will present two preliminary tests, which have each two runs. Reproducibility of the tests with different parameters was demonstrated.

For a typical test panel, the wall components from outside to inside were as listed below:

- Wet wood siding (red cedar siding);
- Air space (19 mm);
- Spun bonded polyolefin membrane (SBPO);
- Fiberboard sheathing (11 mm);
- 38 mm x 89 mm (2" x 4") stud with 89 mm glass fiber inside;
- Polyethylene (PE) sheet (6 mil);
- Interior gypsum board (12.7 mm).

3.2.4.1 Running the preliminary tests

Before each test, the wood siding was soaked in water for 48 hours. On average, the wood siding would go from 6.6 kg (before wetting) to 8.2 kg (after 48 hours of wetting), i.e., an average increase in moisture content of around 24%. Then the wood

siding was installed on the test panel. The distance between the tip of the heat bulbs and the surface of the wood siding was 42 cm.

Laboratory environmental conditions were not constant from test to test, but overall, during one test, conditions were reasonably stable. The siding would lose moisture during the process of installation. Since the duration was just several minutes and similar for each test, it only slightly influenced the final results. The test duration was 12 hours, according to the preliminary tests, which showed that 12 hours were long enough to get the maximum moisture accumulation. The gravimetric sample was taken out every two hours for measurements.

3.2.4.2 Test results of the preliminary runs

For the test hut, the outdoor air temperature was 24±2°C, the indoor air temperature was 21±1.5°C, which is a typical indoor air-conditioning temperature in summer; the outdoor relative humidity was 35% ~ 45%, and the indoor relative humidity was 30%~ 40%. When the air gap was sealed with construction tape, the gravimetric sample weight increased over the first 6 hours, and then decreased over the next 6 hours as shown in Table 3.1.

Table 3.1. Gravimetric sample weight with closed air cavity (in grams)

Time	12:30 am	2:30 pm	4:30 pm	6:30 pm	8:30 pm	10:30 pm	12:30 pm
Run 1	200.35	200.43	200.50	200.51	200.49	200.46	200.41
Run 2	200.35	200.38	200.52	200.54	200.50	200.47	200.41

The maximum condensation accumulation was 0.16 g. The gravimetric sample measured 150 mm x 150 mm (0.0225 m^2), so the total condensation was equivalent to 7.11 g/m^2. By the end of the 12-hour test under constant radiation, around two-thirds of the maximum condensation had dried up.

When the air gap was open to the outside and natural ventilation allowed to occur, the gravimetric sample weight was constant as shown in Table 3.2. There was no condensation on the gravimetric sample.

Table 3.2. Gravimetric sample weight with open air cavity (in grams)

Time	12:00 am	2:00 pm	4:00 pm	6:00 pm	8:00 pm	10:00 pm	12:00 pm
Run 3	200.34	200.34	200.34	200.34	200.34	200.34	200.34
Run 4	200.36	200.36	200.37	200.37	200.36	200.36	200.36

The curves of temperature, relative humidity and vapour pressure near the PE-membrane and in the air cavity were established and provided in Figures 3.1 to 3.6.

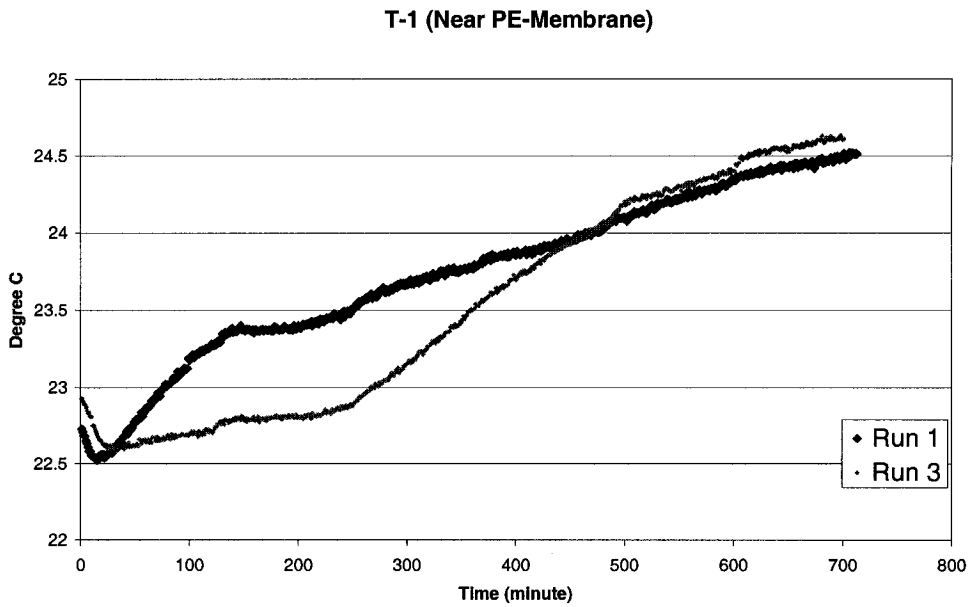

Figure 3.1. Sensor No. 1 temperature: Run 1 & Run 3

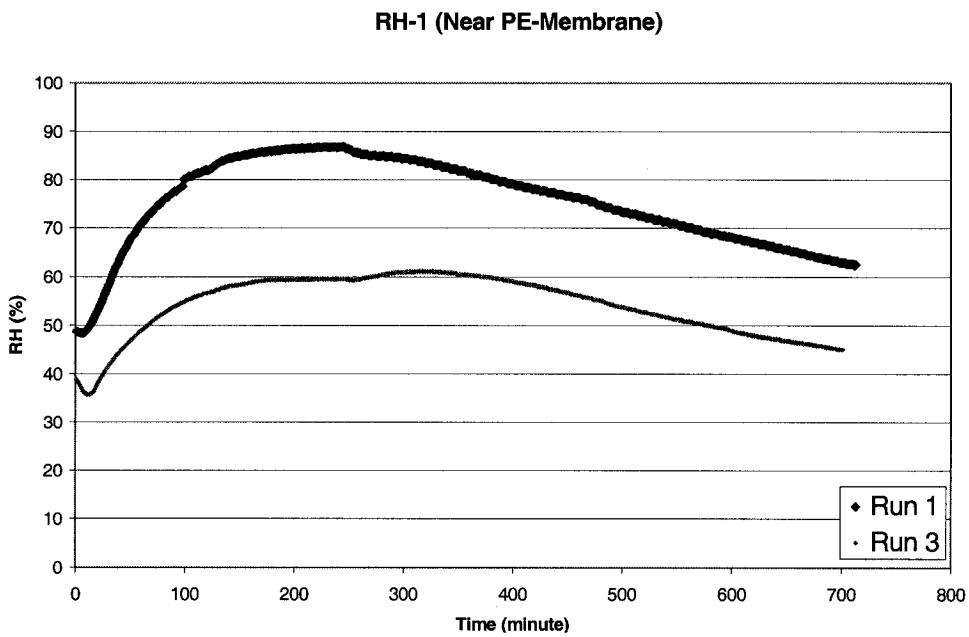

Figure 3.2. Sensor No. 1 relative humidity: Run 1 & Run 3

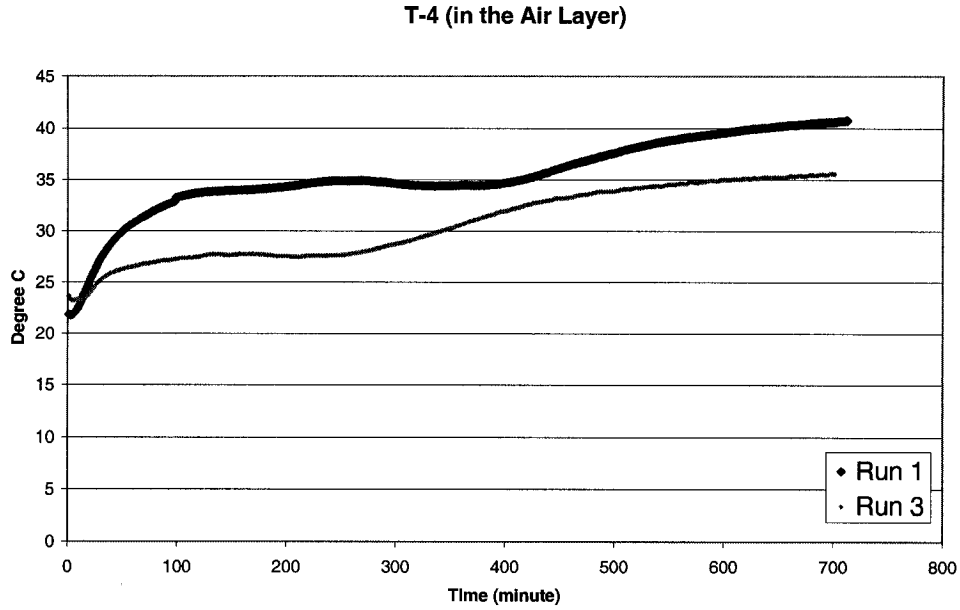

Figure 3.3. Sensor No. 4 temperature: Run 1 & Run 3

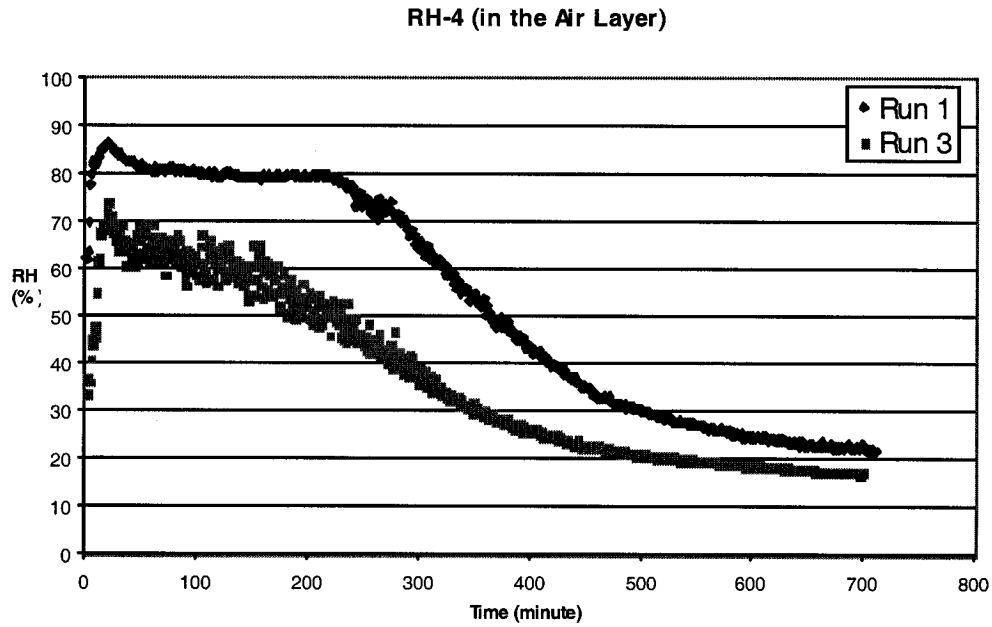

Figure 3.4. Sensor No. 4 relative humidity: Run 1 & Run 3

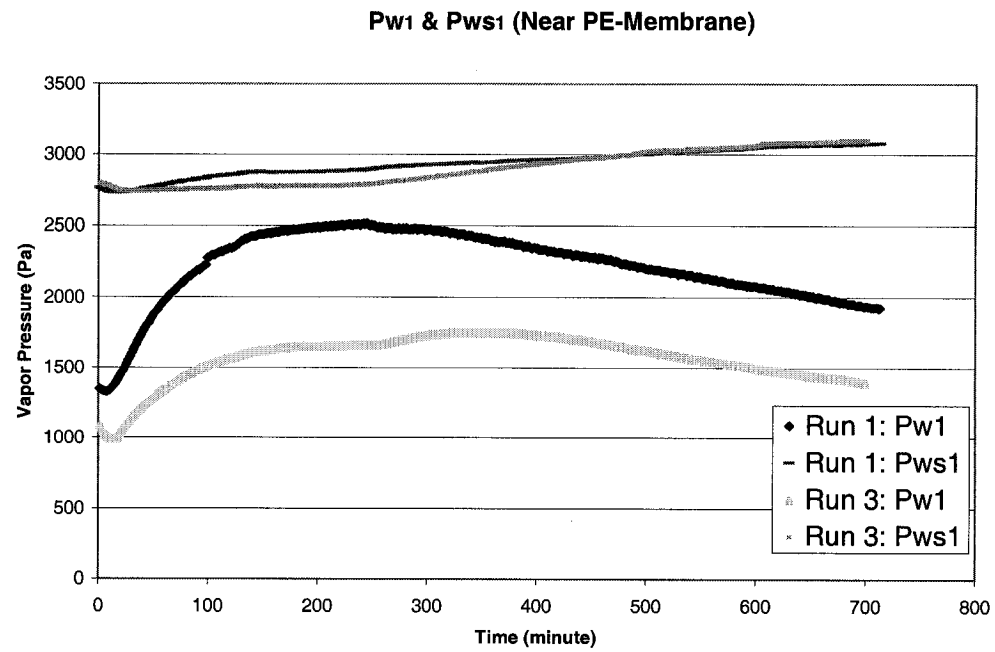

Figure 3.5. Sensor No. 1 actual vapor pressure and saturation vapor pressure: Run 1 & Run 3

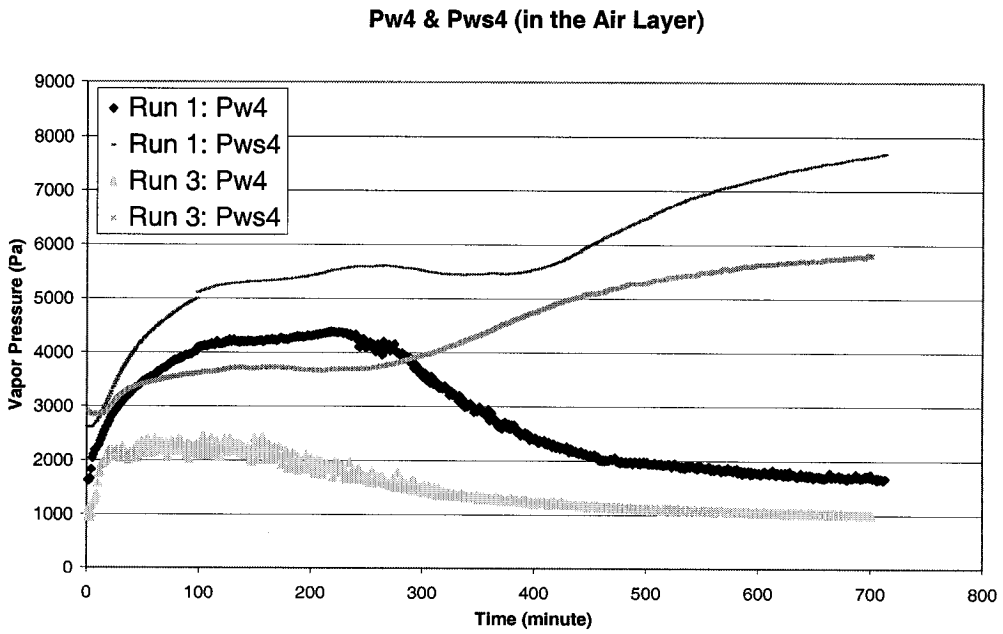

Figure 3.6. Sensor No. 4 actual vapor pressure and saturation vapor pressure: Run 1 & Run 3

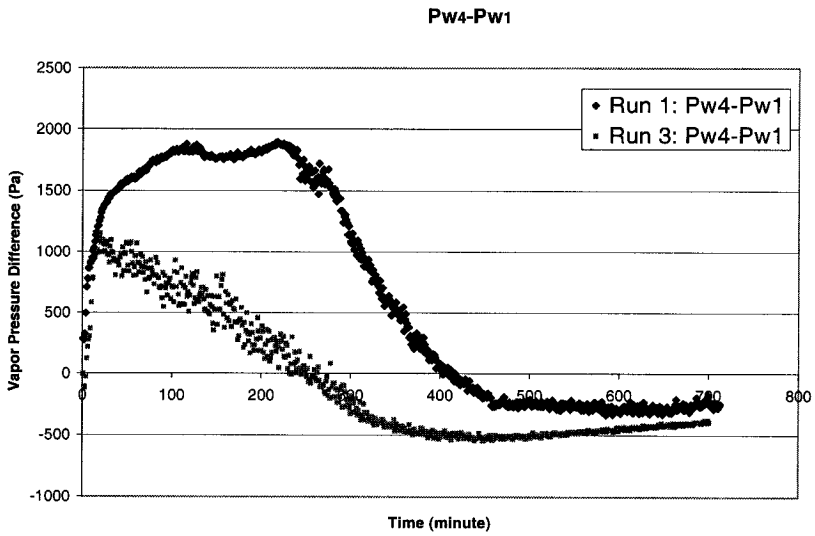

Figure 3.7. actual vapor pressure difference between sensor No. 4 and sensor No. 1, Run 1 and Run 3.

Figures 3.1, 3.2 and 3.5 show the temperature, relative humidity and vapour pressure on the outside of the PE-membrane. The specimen with the unvented air space experienced higher values in all cases. The same situation is observed in the air space itself, as shown in Figures 3.3, 3.4 and 3.6. Figure 3.7 clearly demonstrates that vapour pressure differential in the wall with unvented air space first increases, to later decrease but is always higher than the vapour pressure differential across the wall with the vented air space.

With these preliminary tests, it was clearly established that:

- the loading conditions could lead to moisture accumulation
- the loading conditions induced produced different profiles of temperature and relative humidity whether the air space was open or closed, as expected
- the gravimetric specimen developed was effective in measuring moisture content variation due to vapour flow

- It was therefore possible to continue along the same path and develop the systematic test protocol according to the parameters of interest.

3.2.5 Experimental setup

This section presents the experimental protocol including test specimen design, monitoring instrumentation and loading conditions. Varied parameters include a wet cladding subjected to simulated solar radiation, with/without vapour retarder and ventilation of air cavity. Solar radiation is simulated using heat lamps.

3.2.5.1 Test panel

Each wall specimen was 840 mm wide by 1075 mm high. All the test panels were constructed with two 38 mm x 89 mm (nominal 2" x 4") wood studs spaced at 400 mm on centre, plus another stud at 200 mm on each side, as shown in Figure 3.8. The monitoring was just performed in the central stud space.

For the typical test panel, the wall components from outside to inside were as follows:

- Wet wood siding (western red cedar);
- Air space (19 mm);
- Spun bonded polyolefin membrane (SBPO);
- Fiberboard sheathing (11 mm);
- 38 mm x 89 mm (2" x 4") stud with 89 mm glass fiber inside;
- Polyethylene (PE) sheet (6 mil);
- Interior gypsum board (12.7 mm).

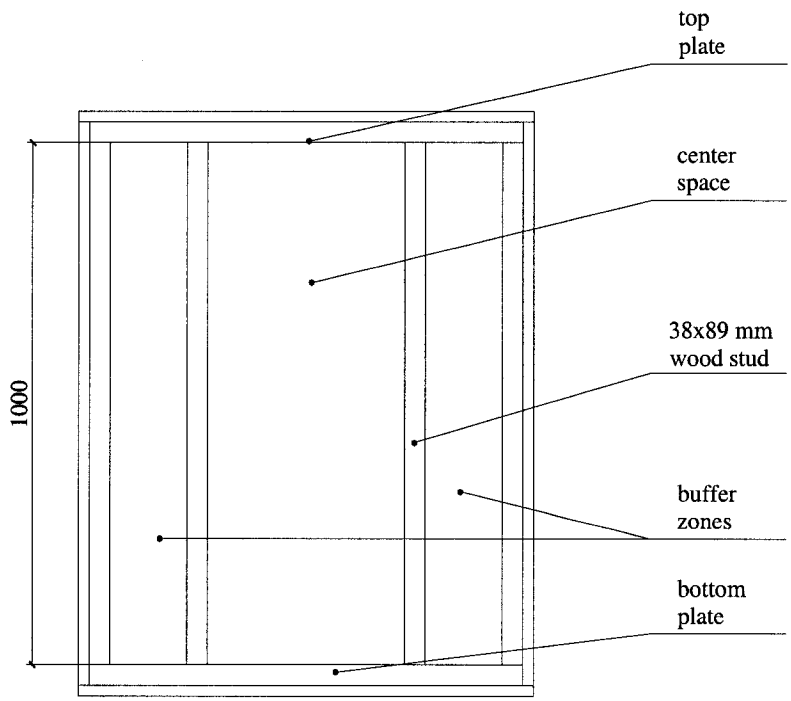

Figure 3.8. Test panel frame

3.2.5.2 Test hut

The wall specimen was installed on one side of the test hut. During the construction process of the test hut, 38 mm x 63 mm (2" x 3") wood studs were used to build the frame of the test hut, and plywood was used as the sheathing material. On the outside of the plywood, 50 mm extruded polystyrene was used as the rigid insulation. According to a preliminary test, a test hut without insulation could not produce an even temperature inside the hut. The test hut was 1500 mm wide, 1500 mm long and 1212 mm high. The configuration of the test hut was based on the configuration of the test panel and previous works performed at Concordia University, where test panels were 1075 mm high. In order to move the test hut easily, four wheels were installed under the bottom frame of the test hut. In order to access to the inside for gravimetric sample

measurement during the experiments, a door was designed on one side of the test hut. Rubber weather strips were used at all junctions of the test hut to avoid air leakage as much as possible. Figures 3.9 to 3.14 show the development of the test hut.

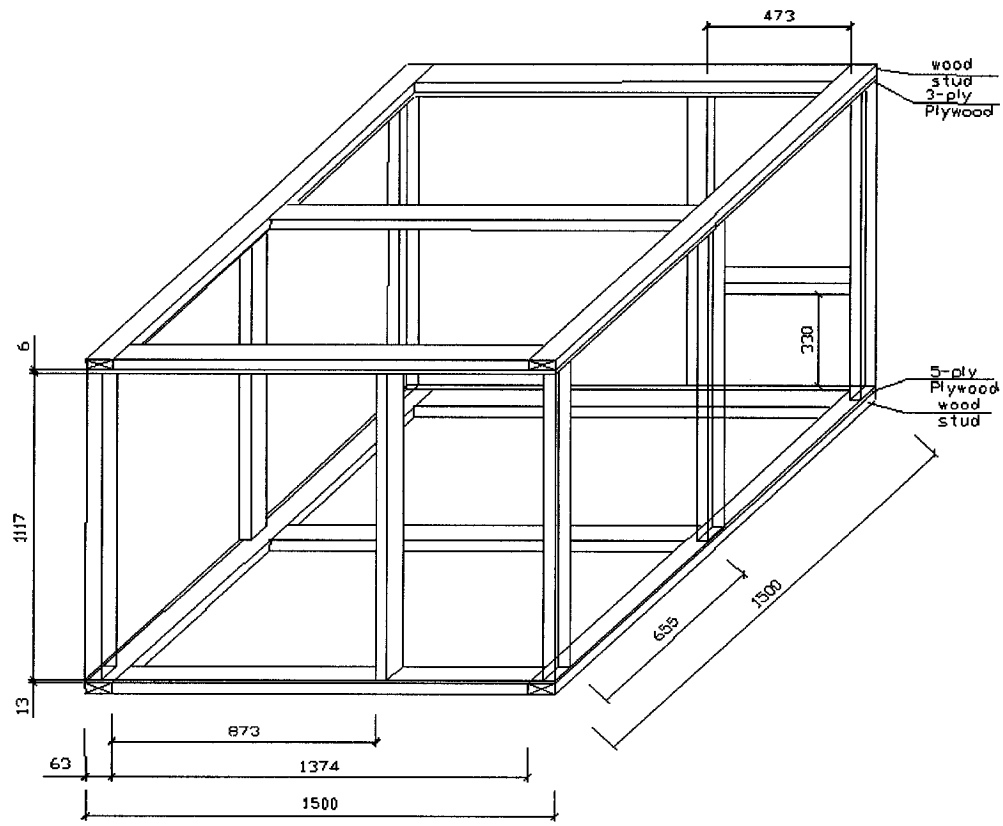

Figure 3.9. View from the front of the testing hut

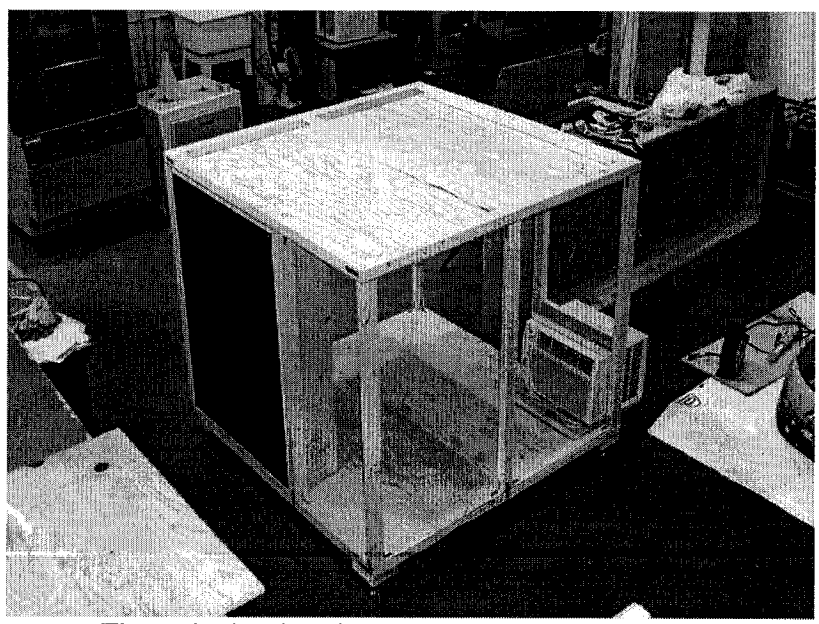
Figure 3.10. View from the front of the testing hut

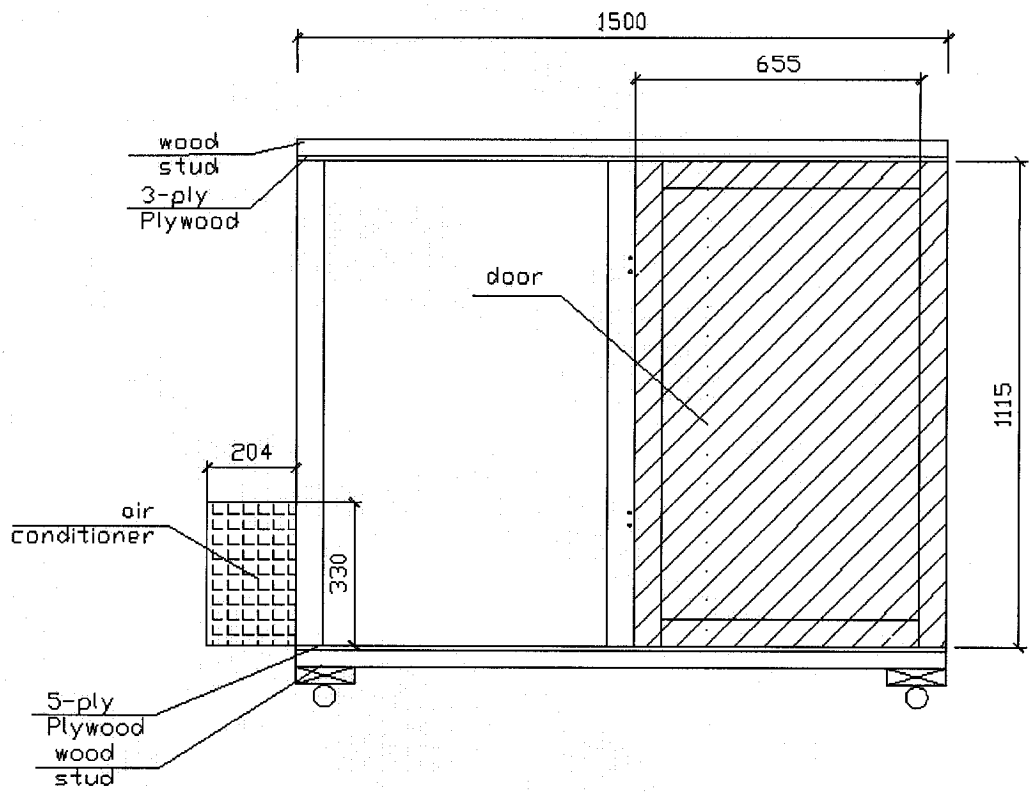

Figure 3.11 View from the side of test hut

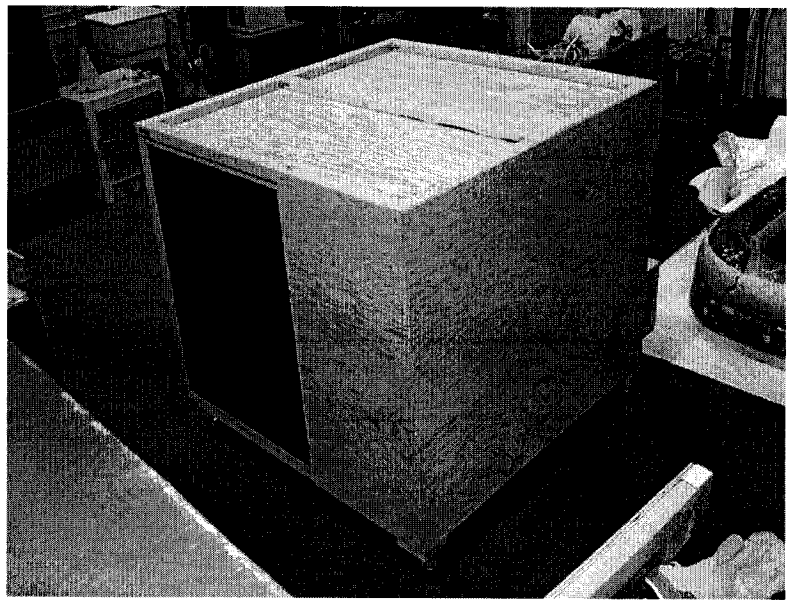

Figure 3.12 View from the side of test hut

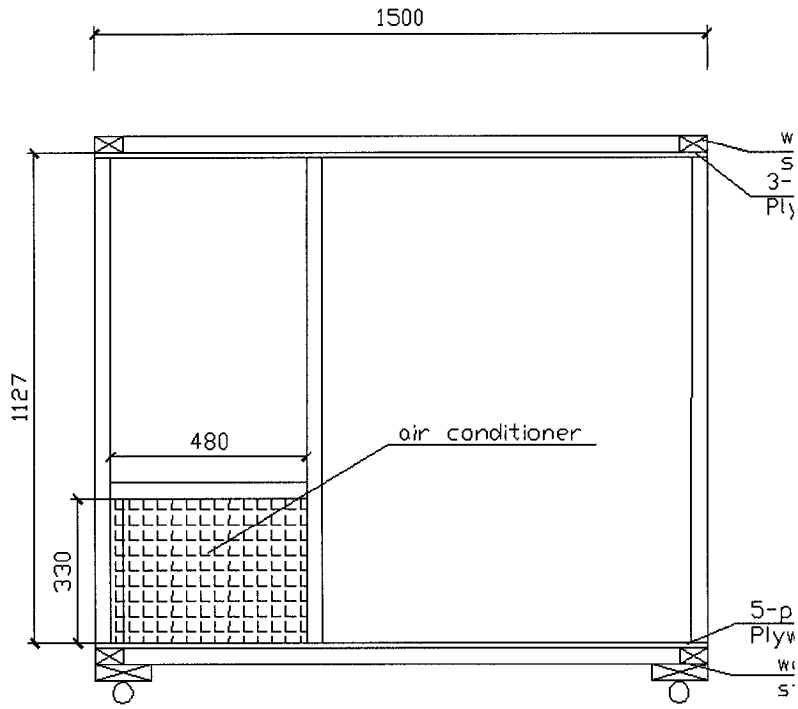

Figure 3.13 View from the back of the test hut

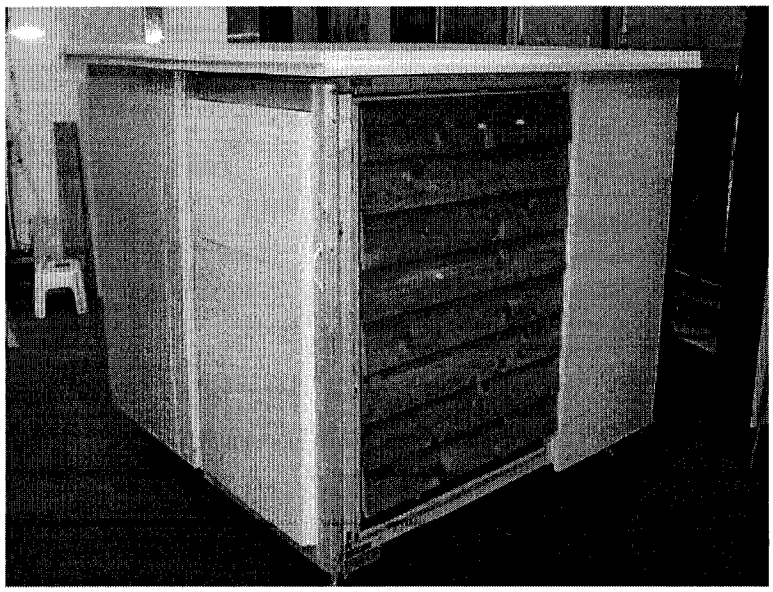

Figure 3.14 Finish view of the test hut

This hut could be used to test one panel at a time. A data logger of a total capacity of 60 points was used for readings and acquiring data (temperature and relative humidity). The time interval between adjacent readings was one minute.

3.2.5.3 Heat lamps

Heat lamps were placed in front of the wood siding to simulate solar radiation, as shown in Figure 3.16. The amount of wattage used in this test to generate sol-air temperature was estimated based on Kan (1999) and Kan (2002). In the experiments, each testing panel is 0.8 m^2 (1.0 m by 0.8 m). To linearly scale up the wattage used by Kan (1999), the provided wattage should have been 1920 W; to linearly scale up the wattage used by Kan (2002), the provided wattage should have been 1110 W. Finally, a total of 1050 W (or nominally 1313 W/m^2) was supplied in the experiments (6x175 W infrared heat lamps). The direction of heat, which was generated by those heat lamps, was not completely perpendicular to the siding surface. From solar radiation calculation, the solar intensity that falls on a vertical surface facing wall surface at noon of July 21 in Montreal is 433 W/m^2. When the air temperature is 20 °C, the resulting sol-air temperature would be 43°C. The calculation process is shown in Appendix B.

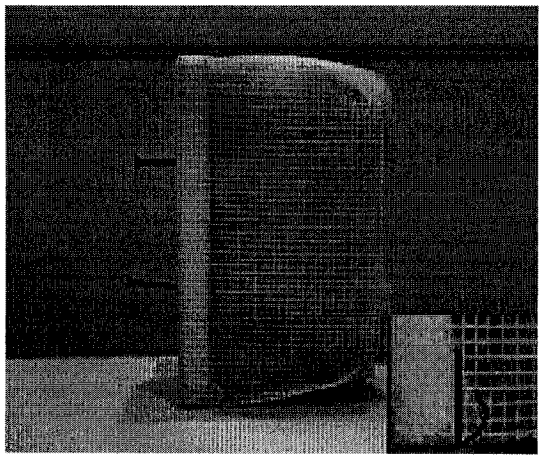

Figure 3.15. Gravimetric sample

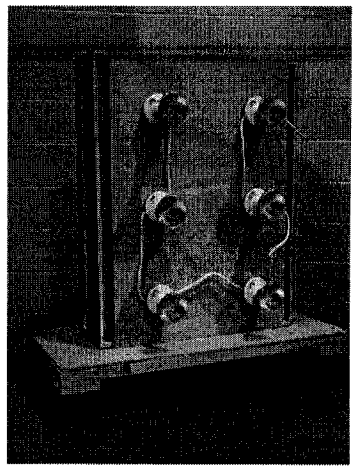

Figure 3.16. Heat lamps

Figure 3.17 is an infrared thermogram, which was taken during the first several hours of an experiment. The temperature distribution on the wet wood surface was not even during the drying process. It is because the heat lamps together did not generate a uniform radiation as solar radiation is. However, using heat lamps was still an easy and efficient way to simulate solar radiation.

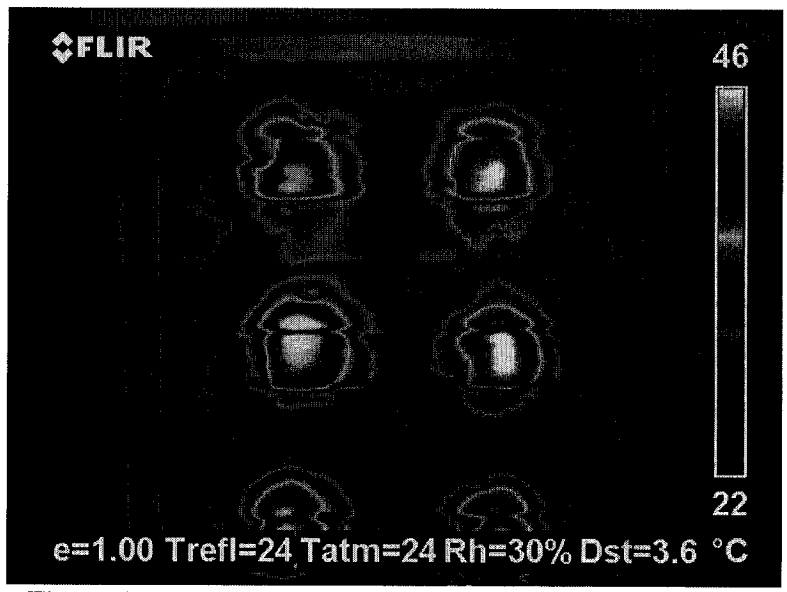

Figure 3.17. Infrared thermogram of the wood siding

3.2.6 Monitoring Plan

This monitoring plan presents the instrumentation used for heat and moisture transfer monitoring. All the air temperature measurement near the gypsum board of the test panels used type-T thermocouples, (copper and constantan) gauge 30, with 0.5°C accuracy, with a reference junction having 0.2°C accuracy. The thermocouples used in the experiments were calibrated using a constant temperature bath before the tests. The readings of these indoor air temperatures were taken every minute.

The relative humidity and temperature transmitter had a range of measurements from 0 to 100% RH and -10°C to +60°C with ±3% RH accuracy and with better than ±1% RH stability per year, based on the claims of the manufacturer. A stand-alone RH calibrator, more specifically a dew-point hygrometer, was used for the sensors calibration. The sensors were put into the calibrator, and then the set relative humidity value was increased step by step from 20% to 90%. The readings of the T/RH sensors were recorded. A calibration curve, which shows the differences between the set RH values and the sensor readings, was thus established. Three transmitters were installed on the exterior surface of the PE-membrane (top/middle/bottom), with sensors No. 1 to 3, as shown in Figure 3.18. Three other transmitters were installed in the air cavity, with sensors No. 4 to 6 on the top/middle/bottom taped on the exterior surface of SBPO, as shown in Figure 3.19. Sensor No.7 was installed to measure the indoor T/RH, and the outdoor conditions were provided by sensor No. 8. The readings of temperature and RH were taken every minute.

The weigh scale used to weigh the gravimetric sample had a capacity of 6100 g and an accuracy of 0.01g. The gravimetric sample was weighed every two hours from the beginning of the experiments. Moisture flowed to the inside of the test hut in the process of removing the sample. Since each time it took just one minute to measure the sample weight, the influence of the intermittent flow was found negligible. The weigh scale used to weigh the wood siding had a capacity of 99.99 kg, and the accuracy of 0.01 kg. The wood siding was weighed before and after each test.

Monitoring of temperature and relative humidity is performed in the 400 mm central portion between the wood studs, which is assumed to be vertically symmetrical on each side of its central axis. Sensors at the top, middle or bottom of the test panel were not installed in line, so that there was no influence between each other.

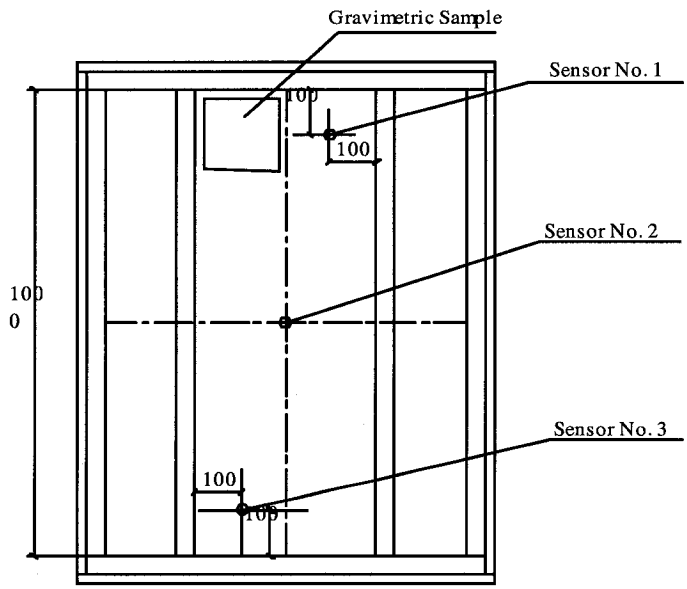

Figure 3.18. Sensors No. 1 to 3 on the PE membrane (view from exterior)

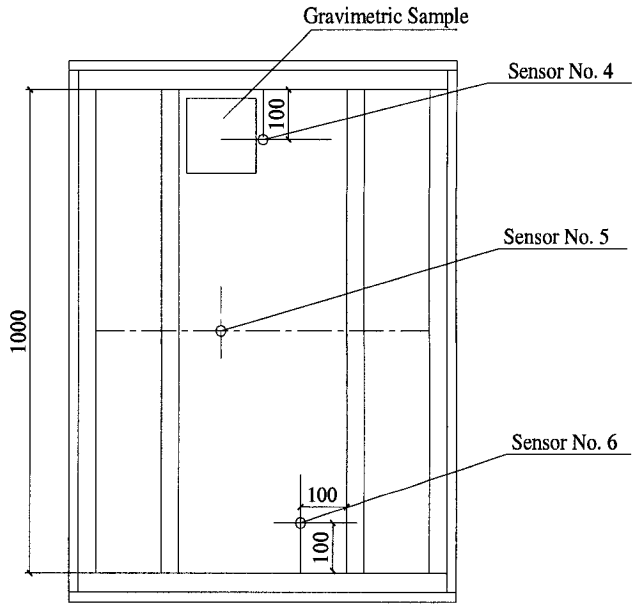

Figure 3.19. Sensors No. 4 to 6 in the air layer (view from exterior)

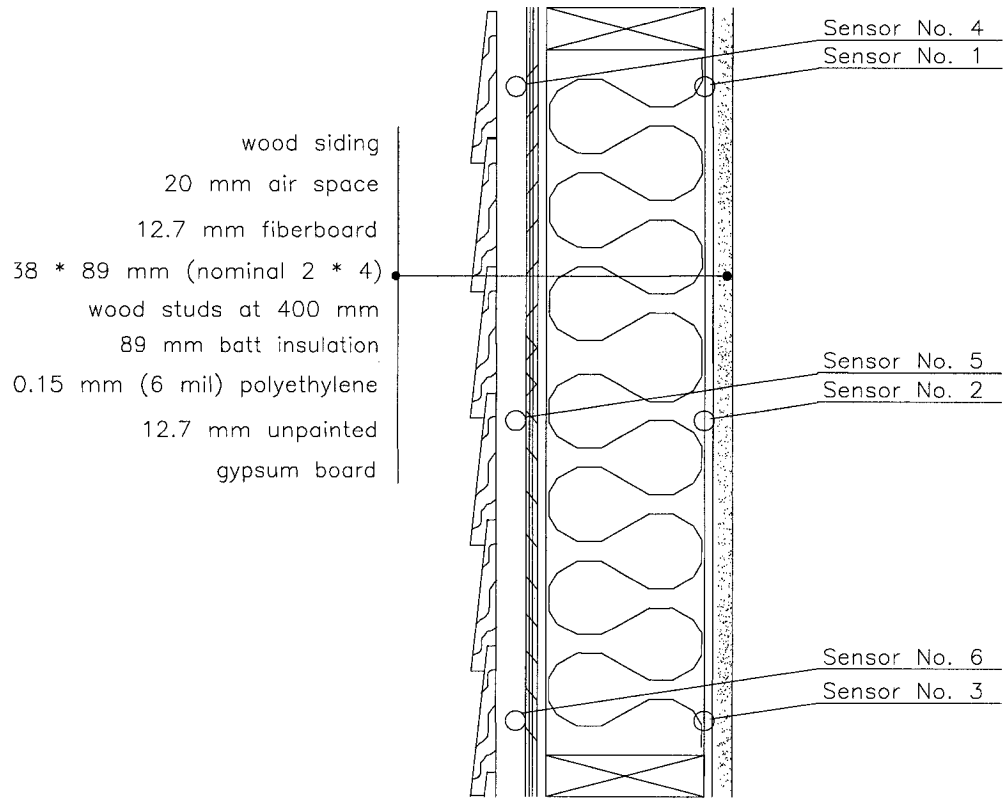

Figure 3.20. Cross section of the test panel

A unidirectional anemometer was used to measure the air velocity in the air space: the measurements were taken at one-hour interval during one experiment, and each measured air velocity value was the average values for one minute.

3.2.7 Optimization of Test Duration

In the preliminary experiments, the test duration was 12 hours, and the heat lamps were always on. According to the preliminary tests, 12 hours were long enough to get the maximum moisture accumulation. For the final experiments, in order to make the simulated conditions close to the real environmental conditions in Canada, the heat lamps were on for 3 hours or 6 hours, and the experimental duration was extended to 18 hours in order to monitor moisture redistribution after the occurrence of radiation.

3.2.8 Laboratory Wall Configurations

Four different wall configurations were tested for the laboratory part of this research project. The difference among the first three was wood sheathing materials. The fourth panel was the same as the first one, except that panel No. 4 did not have polyethylene membrane installed inside the insulation as vapor barrier.

Table 3.3. Test panel configurations

No.	Veneer	Air Space	Weather Barrier	Wood Sheathing	Insulation Material	Vapor Barrier	Interior Sheathing
1	Western Red Cedar (lap siding)	20 mm	Spun Bonded Polyolefin	Wood Fiberboard (11 mm)	Fiber glass (89 mm)	PE-membrane (6 mil)	Unpainted Gypsum board (12.5 mm)
2	Western Red Cedar (lap siding)	20 mm	Spun Bonded Polyolefin	Plywood (11 mm)	Fiber glass (89 mm)	PE-membrane (6 mil)	Unpainted Gypsum board (12.5 mm)
3	Western Red Cedar (lap siding)	20 mm	Spun Bonded Polyolefin	OSB (11 mm)	Fiber glass (89 mm)	PE-membrane (6 mil)	Unpainted Gypsum board (12.5 mm)
4	Western Red Cedar (lap siding)	20 mm	Spun Bonded Polyolefin	Wood Fiberboard (11 mm)	Fiber glass (89 mm)	N/A	Unpainted Gypsum board (12.5 mm)

Veneer

Wood and brick are both water reservoirs. Compared with brick, wood may gain and lose moisture more slowly than brick. However, wood was retained, as it was a lighter material to manipulate. Western Red Cedar was applied as the siding material for all test panels, because it is commonly used in residential buildings in Canada.

Air Space

1"x1" (19x19 mm) wood furring formed the air space between the wood siding and spun bonded polyolefin as shown in Figure 3.21. This 19 mm air space was used in all the testing panels. Figure 3.22 shows the air flow route for the open air cavity in the experiments.

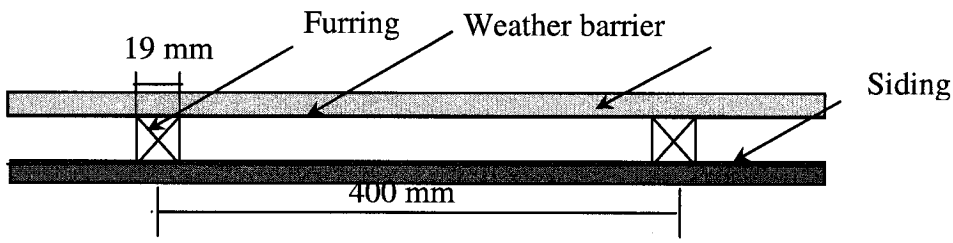

Figure 3.21. Cross section of the air cavity

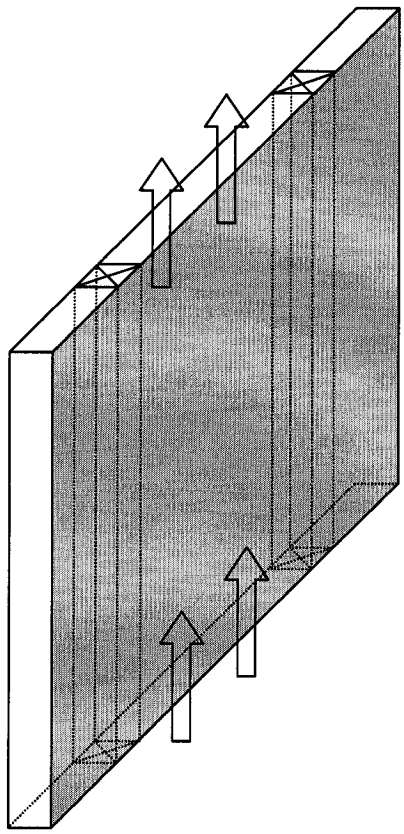

Figure 3.22. Air flow route through the air cavity

Weather Barrier

A spun bonded polyolefin membrane was applied to all the testing panels as weather barrier.

Wood Sheathing

In the experiments, three kinds of wood sheathing were used: wood fiberboard, plywood and OSB (oriented strand board).

Table 3.4 Physical Characteristics of Wood Sheathing (11 mm) (Kumaran *et al.* 2002)

Wood Sheathing	Density (kg/m^3)	Thermal Conductivity ($W/m \cdot k$)	Water Vapor Permeance - dry cup ($ng/m^2 \cdot s \cdot pa$)
Fiber board (11 mm)	320±10	0.052	1666
Plywood (11 mm)	470±5	0.086	416
OSB (11 mm)	650±30	0.102	280

Insulation

Glass fiber insulation (89 mm) was used for all the testing panels.

Vapor Barrier

A polyethylene membrane (6 mil) was applied to the testing panels from No.1 to No.3.

Interior Finish

Unpainted gypsum board (12.5 mm) was applied to all the testing panels.

3.2.9 Series of tests carried out in the lab

The maximum solar radiation after a rain shower does not last over 6 hours at the latitude of major Canadian cities. Therefore, in the tests, the heat lamps were on for 3 hours or 6 hours. Totally, there were 12 experiments carried out in this project. Three sets of test conditions are listed in table 3.5.

Table 3.5. Parameter arrangements

No	Ventilation	3-Hour Radiation	6-Hour Radiation
1	Yes	Yes	No
2	No	Yes	No
3	No	No	Yes

3.3 Limitations

The objective of the work presented was to study conditions that could lead to condensation. The following limitations should be taken into account:

- The experimental setup did not include strong air pressure forces, resulting from wind, which would be present in the field. In the field, lap siding is fairly well ventilated, even without an air space, but an air space does help.
- The wetting pattern of wood lap siding is likely to be very different in the field.
- The simulated radiation was constant for 3 hours or 6 hours.
- The test panel cavity was less than half the height of a typical cavity. Ventilation rates and eventual convection loop within the glass fiber must have been influenced.
- The results were specific to the parameters of the test. Whether or not these results could be applied to other parameters needs to be investigated.

The experimental results are given out in Chapter 4, and the data analyses of all the tests carried out is presented in Chapter 5.

CHAPTER 4 EXPERIMENTAL RESULTS

As described in Chapter 3, three sets of data were collected for each of the four test panels. These data include moisture accumulation in the gravimetric sample, as well as temperature and relative humidity inside and outside each wall assembly.

4.1 Experimental conditions

There are twelve experiments in this research project. During the experiments, temperature and relative humidity were recorded. The following figures show the indoor/ outdoor environmental conditions of all tests presented together to illustrate the small variations of loading conditions from test to test.

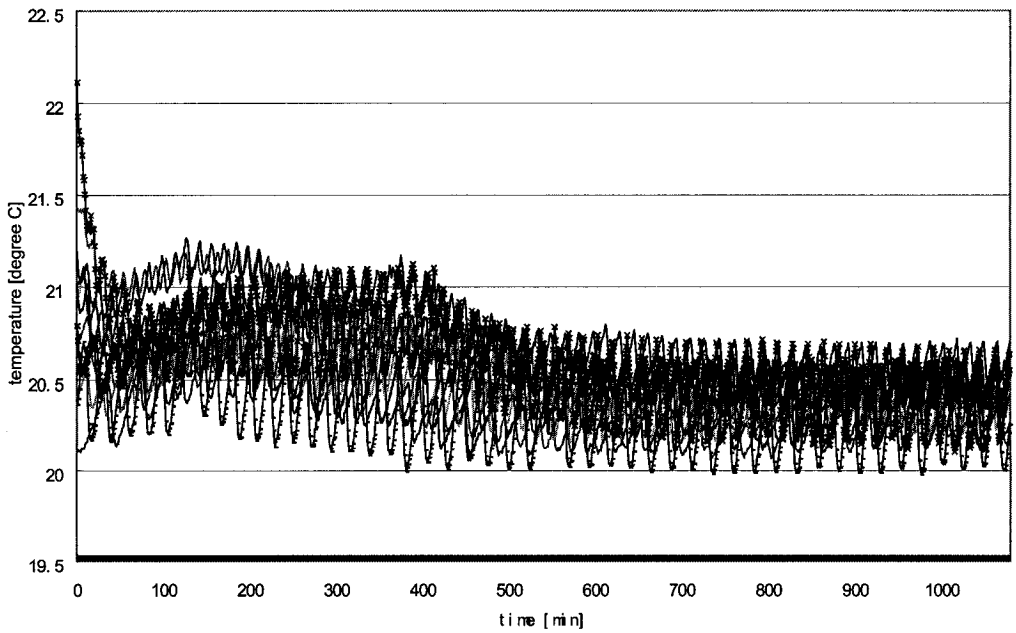

Figure 4.1. Indoor air temperature readings from the twelve main experiments

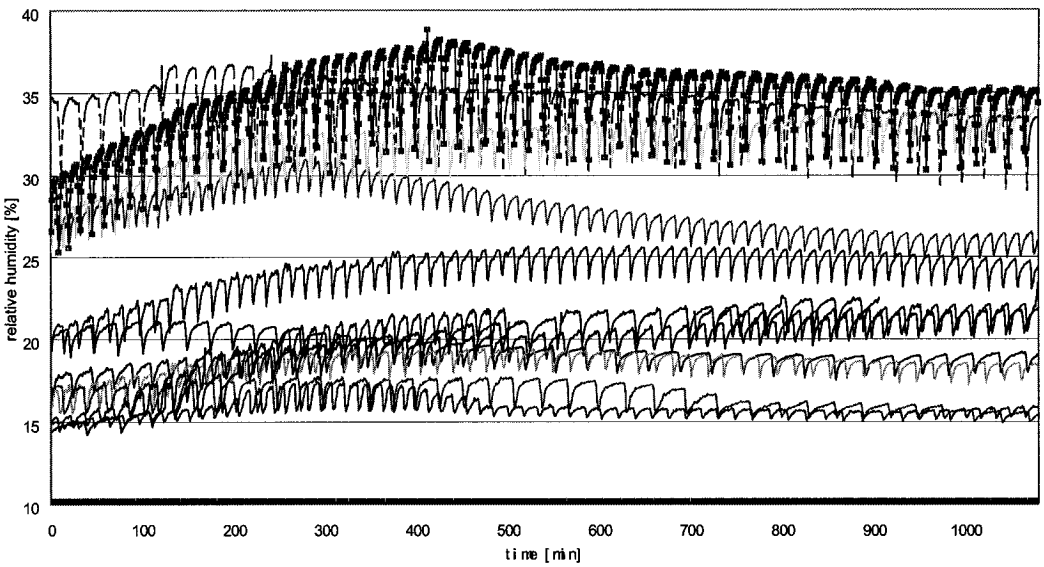

Figure 4.2. Indoor air relative humidity readings from the twelve main experiments

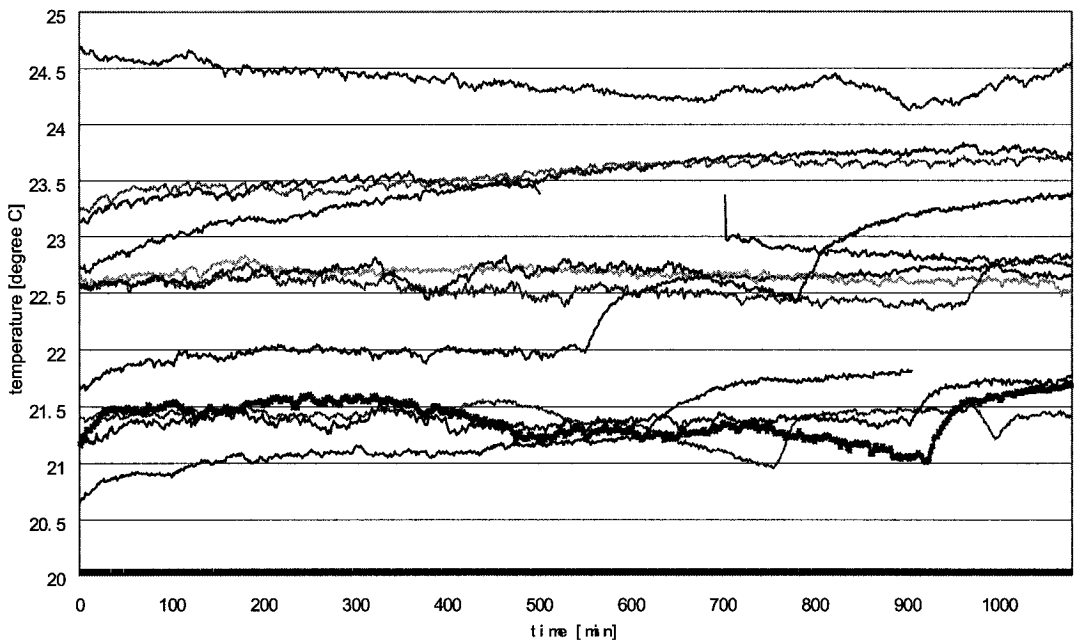

Figure 4.3. Outdoor air temperature readings from the twelve main experiments

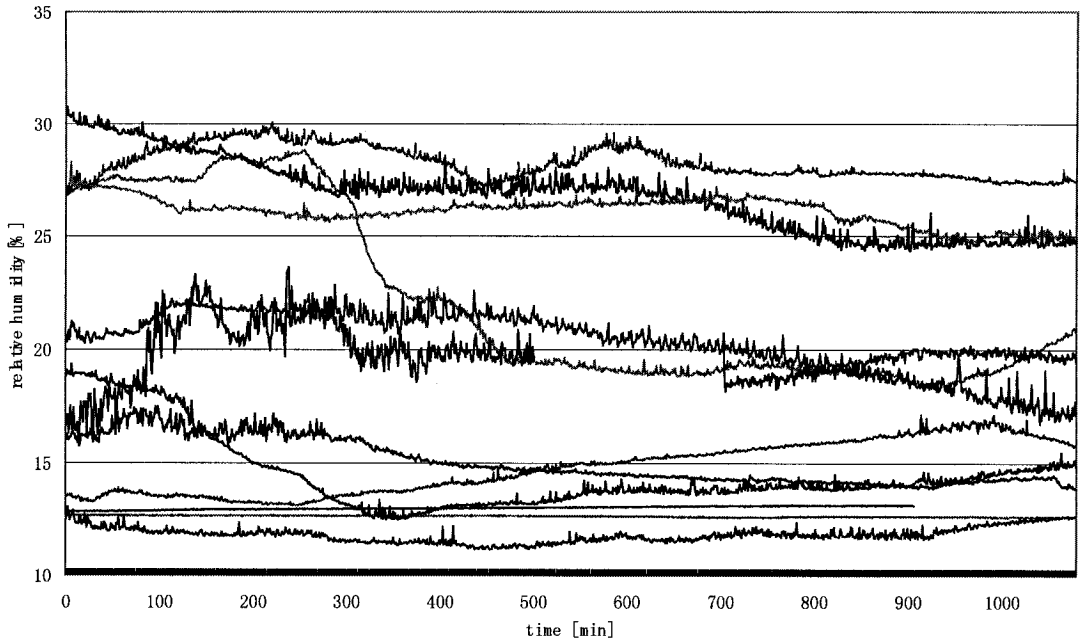

Figure 4.4. Outdoor air relative humidity readings from the twelve main experiments

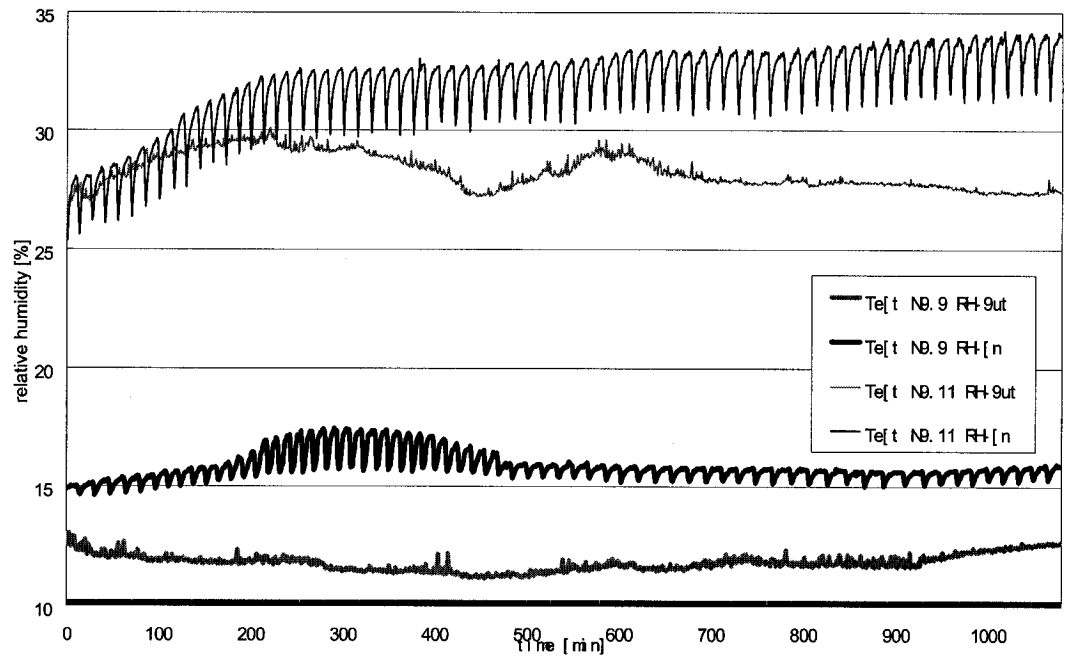

Figure 4.5. Indoor/outdoor relative humidity in two tests

For the test hut, the indoor air temperature was 21±1°C, which is a typical indoor air-conditioning temperature in summer conditions. The inside conditions, being temperature controlled, are very similar from test to test in terms of temperature within an initial spread of one degree Celsius that reduces to 0.75 degrees after around 500 minutes (around 6 hours). For the test hut, the indoor relative humidity was 15%~40% (Figure 4.2). The inside relative humidity conditions are of 25 % RH plus or minus 10% RH. The test hut was not within a controlled environment; as a result, more variation of conditions can be observed in the outdoor temperature (Figure 4.3) with an average spread of 3.5 degrees Celsius. The variation of relative humidity is similar to the RH variation in the test hut. Since the relative humidity was not controlled during the experiments, Figures 4.5 shows the influence of the outdoor relative humidity on the indoor relative humidity. Since there is only a small temperature difference between the inside and the outside, the higher the outdoor relative humidity; the higher the indoor relative humidity. Therefore, the differentials of conditions across the specimens were similar from test to test. Since the similarity of the conditions of all tests has been established, it is now possible to continue with the analysis of the data.

Technical problems occurred in the data acquisition system during two experimental processes, some T/RH data were lost. This consideration was taken into account in the data analyses as shown in Chapter 5.

4.2 Moisture accumulation in the gravimetric sample

According to the experimental procedure, the gravimetric sample was weighed every two hours from the beginning of each experiment. The gravimetric sample weight changes are very important data to evaluate the performance of the wall assemblies.

Table 4.1. The Experimental Results of the Maximum Moisture Accumulation of Gravimetric Sample (g)

	3h/open	3h/closed	6h/closed
Assemblies with polyethylene Membrane Fiberboard	0.04	0.17	0.13
Plywood	0.03	0.09	0.08
OSB	0.00	0.08	0.06
Without polyethylene Membrane Fiberboard	0.17	0.37	0.55

The dimension of the gravimetric sample was 150 mm x 150 mm (0.0225 m^2), so the moisture accumulations on each square meter were equivalent to the values as shown in table 4.2.

Table 4.2. Experimental Results: Maximum Moisture Accumulation of the Gravimetric Sample (g/m^2)

	3h/open	3h/closed	6h/closed
Assemblies with PE membrane Fiberboard	1.78	7.56	5.78
Plywood	1.33	4.00	3.56
OSB	0.00	3.56	2.67
Without PE membrane Fiberboard	7.56	16.44	24.44

This set of data represents the first set of controlled and monitored data on moisture flow induced by simulated solar radiation. This set clearly establishes that, in certain conditions, solar-driven moisture flows can result in moisture accumulation within the interior components of the wall. The data also illustrates clearly two relationships:

1. The moisture gain is null or very small in the walls with an open air cavity. When the air space is not allowed to vent, a noticeable increase of moisture accumulation occurs.

2. When moisture accumulation occurs, its magnitude is related to the permeance of the sheathing. Hence, the high permeable fiberboard has the highest amount of moisture accumulation, followed by plywood and than OSB, the least vapor permeable material of the three.

This set of data also presents a surprising result. All assemblies without polyethylene membrane had a higher moisture accumulation than the assemblies with a PE-membrane. When thinking in terms of condensation point, this result is surprising as the removal of the PE membrane result in all vapor pressure to remain below the saturation vapor pressure (below dewpoint), in the assemblies. What is happening, under the conditions of the test, is that the assemblies without polyethylene membrane undergo a higher moisture flow and more hygroscopic adsorption of moisture occurs. Therefore, moisture accumulation is higher but due to moisture absorption and not vapor condensation.

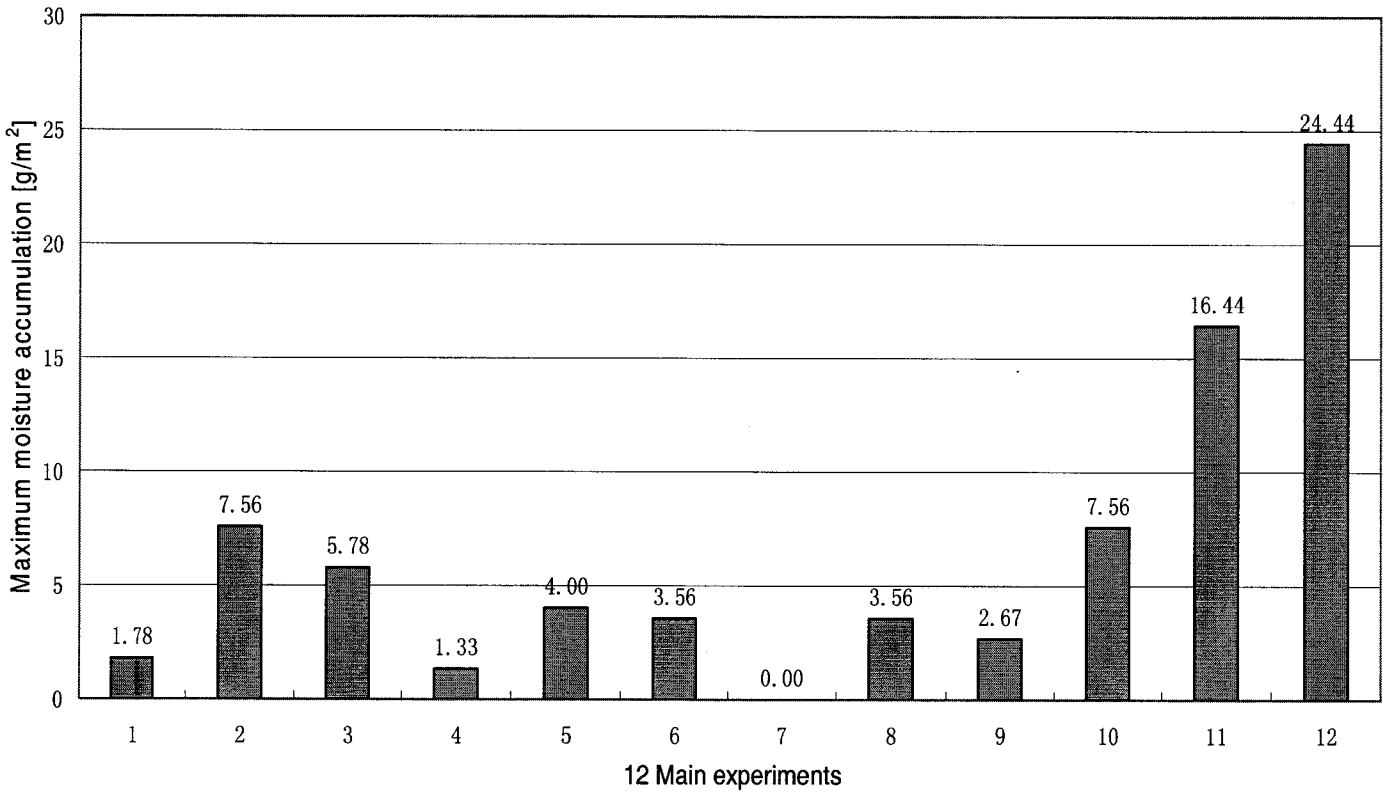

1. Fiberboard-3h-open
2. Fiberboard-3h-closed
3. Fiberboard-6h-closed
4. Plywood-3h-open
5. Plywood-3h-closed
6. Plywood-6h-closed
7. OSB-3h-open
8. OSB-3h-closed
9. OSB-6h-closed
10. Fiberboard-no PE-3h-open
11. Fiberboard-no PE-3h-closed
12. Fiberboard-no PE-6h-closed

Figure 4.6. Maximum moisture accumulation of 12 main experiments

4.3 Temperature and Relative Humidity in the Test Panel

As described in the experimental procedure, temperature and relative humidity of the exterior environment, in the air cavities, at the location near the polyethylene sheet or near the paper faced gypsum board and of the interior environment were measured and recorded every minute through the data acquisition system to the computer. According to T/RH values, saturation vapor pressure and actual vapor pressure profiles over time were established as shown in Appendix D. The heat lamps expedited the drying process of the wet wood siding. At the beginning of the tests, the wet wood siding released moisture to the air space, the temperature and relative humidity in the air cavity increased. The saturation vapor pressure inside the air space corresponds to the temperature. When the actual vapor pressure increase rate became lower than the saturation vapor pressure increase rate, the relative humidity began to decrease as shown in the figures in Appendix D.

4.4 Air Velocity in the Air Space

Air velocity is an important factor that influences the hygrothermal performance of the wall assemblies. Although convection is not the research emphasis in this project, air velocity inside the air space still needed to be known. In order to determine the air velocity, an unidirectional anemometer was used. During the measurements, the anemometer was extended into the air space to measure the air velocity inside the air cavity. When the air space was sealed during the experiments, the air velocity in the air

cavity was 0 m/s. When the air space was open to the outside during the experiments, the air velocity in the air cavity was 0.14 m/s for the first three hours of radiation, which was within the typical range of well-vented wall systems in field measurements (Straube 1998), and then gradually decreased in the following hours. The accuracy of the anemometer is ±0.015 m/s. The measurements of air velocity were all performed in one day, every half hour from the beginning of the experiment.

These measurements clearly indicate that the open-air cavity underwent air movement that led part of humidity released by the cladding out of the assembly. To investigate further the conditions in the air space, the evaporation rate of the cladding needed to be assessed. This is done in the following section.

4.5 Surface Coefficient of Vapour Transfer

At the start of each test, the wet wood siding would lose moisture in two directions. Some moisture evaporated to ambient air outside the test hut; some moisture evaporated to the air cavity. The amount of moisture evaporated to the air cavity is an important factor that influenced the hygrothermal performance of the wall system. In order to determine the amount of moisture evaporated into ambient air and the air cavity, two experiments were carried out to determine the "surface coefficient of vapor transfer", β, (s/m). The unit of β can be written as (kg/m^{2}sPa), i;e; vapor transfer rate for each square meter under the vapor pressure difference of 1 Pa. The values of the surface coefficient of vapor transfer

are compared with the surface coefficients resulting from the analysis in the moisture balance calculations in Chapter 5.

For drying, surface condensation and hygroscopic sorption and desorption, the surface film coefficient for diffusion plays a decisive role (de Wit, 2004).

$$g_v = \beta \cdot (p - p_s) \tag{4.1}$$

where

g_v = Density of moisture flow rate [kg/m^{2}s]

β = Surface coefficient of vapor transfer [s/m]

p = Vapor pressure outside the boundary layer [Pa]

p_s = Vapor pressure on the surface [Pa]

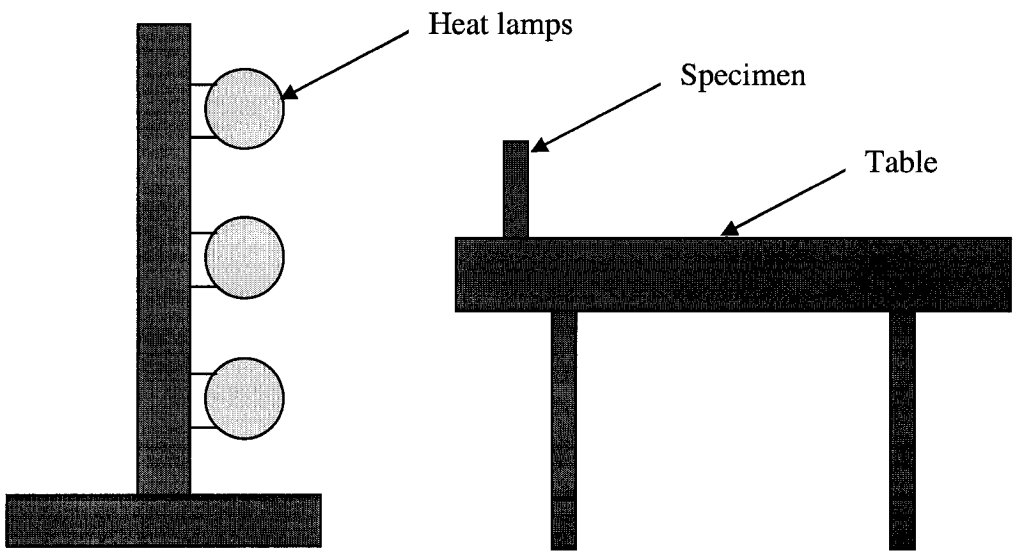

Figure 4.7. Diagram of experimental set-up for surface coefficient (Beta) determination

Two pieces of western red cedar samples (E, F) were used in the experiments. Each sample was 724 × 134 mm. In the main experiments, the two surfaces of the siding material have different surface coefficients of vapor transfer. This is because the exterior surface of the siding was facing the heat lamps and ambient air outside, while the interior surface of the siding was facing the air cavity. Since T/RH outside the test hut and inside the air cavity are very different during the experimental procedure, the density of moisture flow rate from the siding surface to ambient air and to the air cavity are different. Surface coefficient of vapor transfer to ambient air is referred to as $\beta room$; surface coefficient of vapor transfer to the air cavity as βcav .

In order to calculate β , siding samples had one side soaked in water for 48 hours, which was the same duration as the main experiments. After the siding samples were taken out of water, they were placed 42 cm from the heat lamps, which was the same distance as the main experiments. During the experimental process, the samples were weighed every half an hour.

Table 4.3. Experimental Configurations (β)

	β_{room}	β_{cav}
3-hour Radiation	Wet surface faced the heat lamps	Dry surface faced the heat lamps
6-hour Radiation	Wet surface faced the heat lamps	Dry surface faced the heat lamps

For western red cedar, the desorption data are shown in the table 4.4 (Kumaran et al. 2002).

Table 4.4. Western red cedar-Desorption Data

RH [%]	Temperature [°C]	Moisture Content [%]
99.78	22	113.0
88.70	23	13.3
70.50	23	9.0
50.00	23	1.0

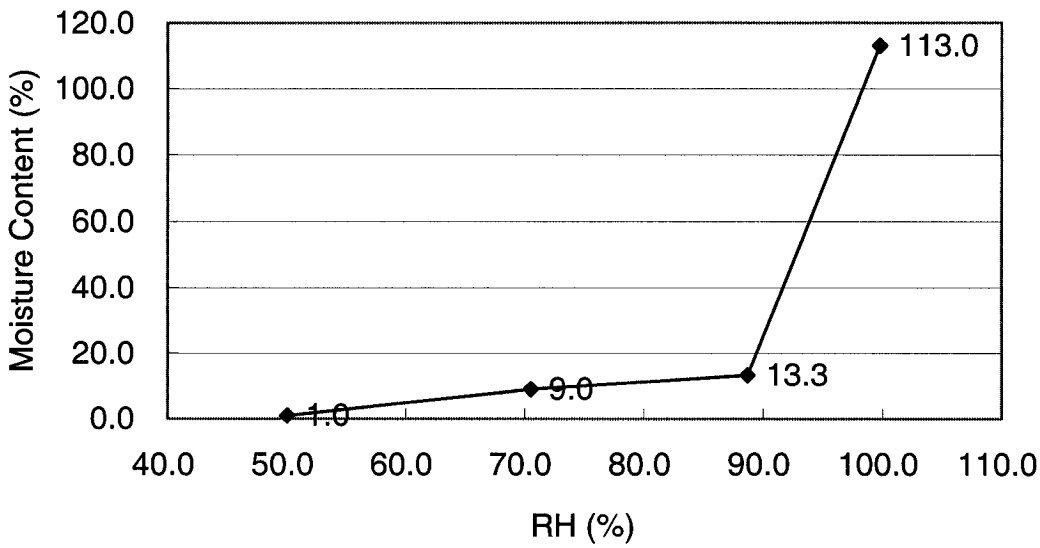

Figure 4.8. Desorption curve of western red cedar

From Figure 4.8, when moisture content is above 113%, relative humidity is 100%. Moisture content from 13.3% to 113% can be assumed to have a linear correlation with relative humidity. If a moisture content value in this range is known, assuming equilibrium was attained, then the relative humidity value can be calculated. Density of moisture flow rate g_v was based on the experimental results, ambient air temperature and relative humidity were measured, the surface temperature was measured and relative humidity was calculated based on the correlation as shown in Figure 4.8. According to

the equation $g_v = \beta \cdot (p - p_s)$, surface coefficient of vapor transfer β was calculated, and its profiles were established in figure 4.9 and 4.10.

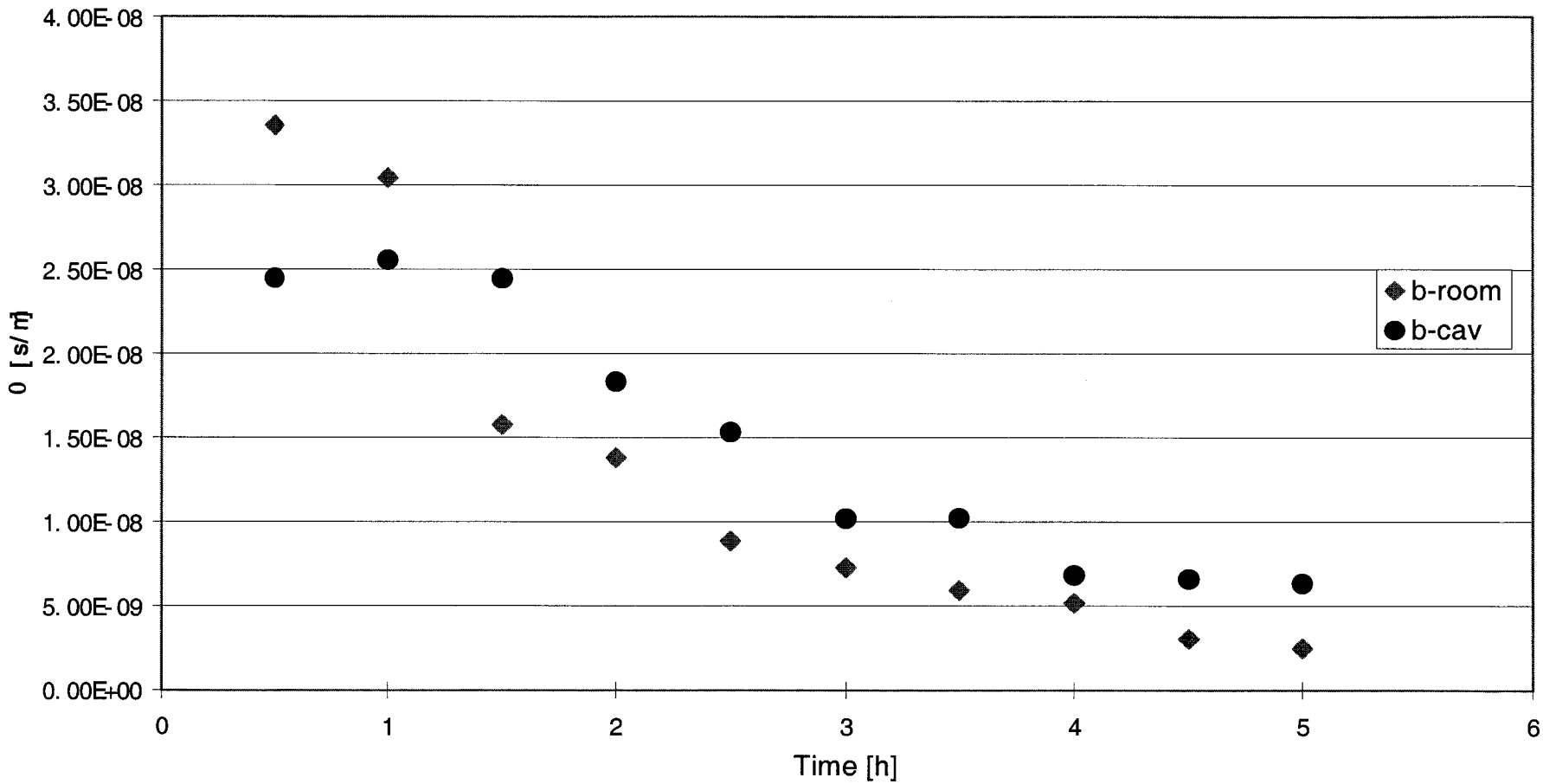

Figure 4.9 Surface coefficient of vapor transfer β-6h Radiation

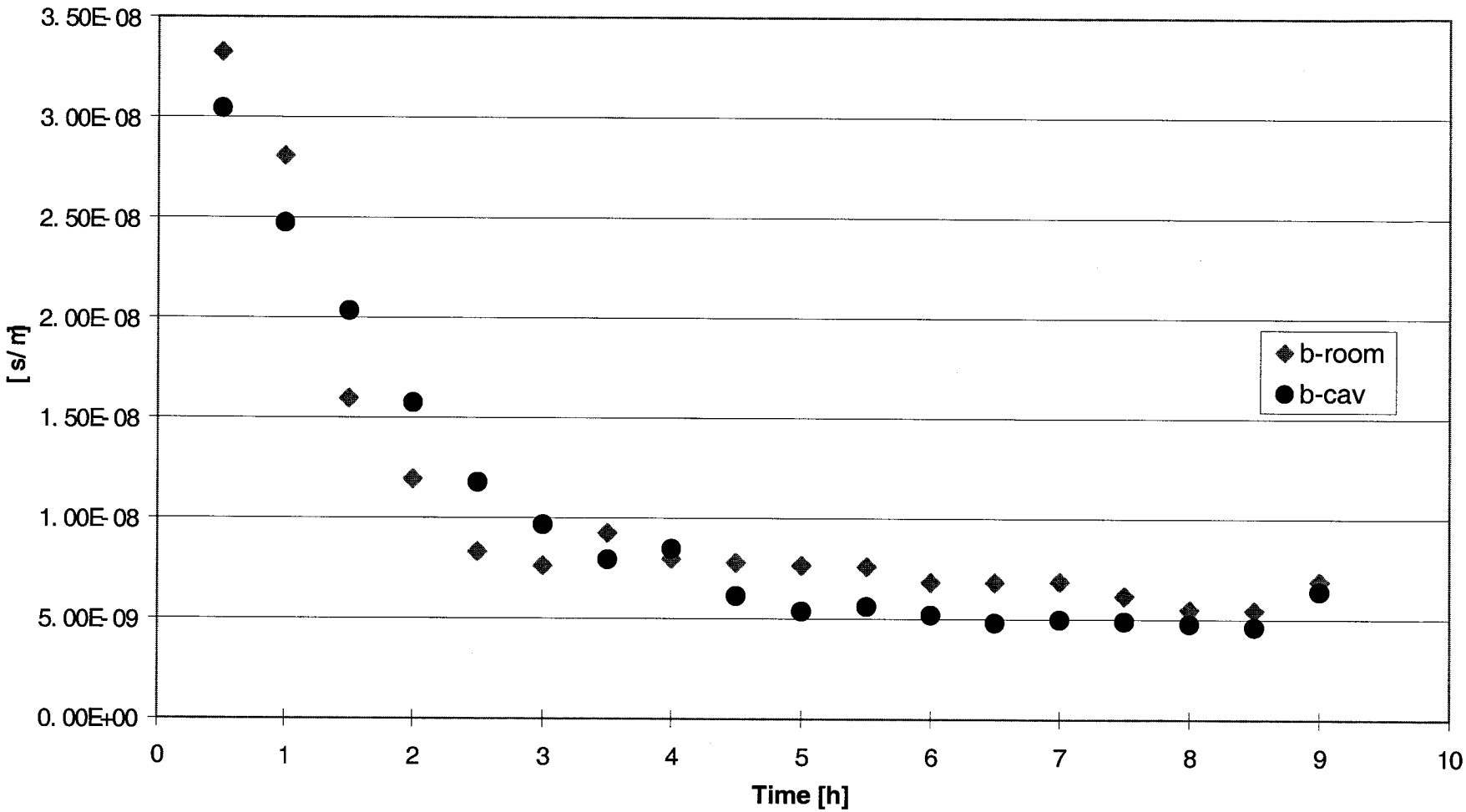

Figure 4.10 Surface coefficient of vapor transfer β-3h Radiation

4.6 Sources of experimental error

There are twelve experiments carried out in this research project. Before these experiments, preliminary tests were applied to determine the experimental parameters and to develop the experimental procedures, which were based on the literature review and the research work previously done at Concordia. Best efforts were used to minimize errors.

There is one factor that could have influenced the moisture accumulation, temperatures and relative humidity. When there is a closed air cavity in the wall assembly, moisture was assumed to transport only in the direction perpendicular to the surface of the wall panels. The air gap was sealed with moisture impermeable construction tape. Since the cables for the sensors had to go through the bottom of the air space to connect with the data acquisition system, construction tape was used to seal the top, left, right and part of the bottom of air space when no ventilation of the air space was planned. Besides this small opening, there may be small flaws that may have resulted in two dimensional heat and moisture flow. This heat and moisture flow would finally influence the moisture accumulation on the gravimetric sample.

Also errors may occur because of drying of samples during weighing, but these errors should be the same error for all tests. From test to test, actual vapor pressure differences between the inside of the test hut and the outside of the test hut are similar (Appendix D).

This chapter presented the experimental results from this research project; the test results will be analyzed and verified in the next chapter.

CHAPTER 5 EXPERIMENTAL DATA ANALYSES

This chapter aims at understanding further the phenomenon of solar-driven moisture flow. The experimental data collected was for a very specific set of loading conditions. First, two different analysis tools are used with the aim of reproducing the data. The tools are: the dew-point method and the hygrothermal model WUFI. This work has led to a better understanding of the different parameters at play. Second, a brief parametric analysis opens the way to a more complete study of the phenomenon, where all loading conditions can be eventually included. Even though such complete study is beyond the scope of this research, the parametric analysis points out interesting avenues. Finally, a study of the moisture content in the air cavity is performed to highlight the importance of the evaporation rate of the water in the cladding during solar-driven moisture flow.

5.1 Dew-point method calculation for the wall assemblies with low permeance polyethylene membrane on the inner side

There were three sets of data recorded during the experimental procedure. The first set of data was moisture accumulation. Moisture accumulation was measured by weighing the gravimetric sample every two hours from the beginning of the experiments. The second set of data were temperature and relative humidity, which were measured with thermocouples and T/RH sensors at the selected locations.

The amount of moisture accumulation predicted by the dew-point calculation, in this section, and WUFI simulation, in the following section, can be used to verify the amount

of moisture accumulation measured from the experiments. Comparisons between the experimental results and the calculation output are presented.

As the experiment was running, the cladding was drying and the hot and humid air in the air space had much higher vapor pressure than air inside the test hut, especially at the beginning of the tests. The steady state application of Fick's law, known as the dew-point method, provides the vapor pressure profile across the assembly. Comparison with the saturation vapor pressure indicates conditions leading to condensation. This steady-state method is an easy and effective way to analyze the experimental conditions and results using the measured air conditions inside and in the air space. As the measurements were providing the air space conditions, the role of the cladding need not be included and the calculations focused on moisture movement in the back wall.

During the experiments, the temperature and relative humidity inside the air space and inside the test hut were measured every minute. In the calculation process, the hourly average values of temperature and relative humidity were applied. From the temperature and relative humidity values recorded during the experimental process, together with the water vapor permeance of each wall component, the actual vapor pressure at the boundary layers of each wall component can be calculated. If the actual vapor pressure is higher than the saturation vapor pressure at the same temperature, moisture condensation occurs. In the calculation, the rate of condensation was used to determine total moisture condensation over time; this total amount that is considered equivalent, in this section, to moisture accumulation. The moisture accumulation under each hour was added until at a certain point the moisture accumulation value during that hour became negative. Using a

steady state method, there is no point of calculating the conditions with open air cavity where air flow is occurring. Table 5.1 shows the calculation results.

Table 5.1. The dew-point calculation results: the maximum condensation accumulation (g/m^2) vs. the maximum moisture accumulation of the gravimetric sample (g/m^2)

Wall assemblies with sheathing	3h/closed		6h/closed	
	Experimental data	Calculated results	Experimental data	Calculated results
Fiberboard	7.56	9.48	5.78	18.72
Plywood	4.00	5.08	3.56	10.14
OSB	3.56	2.05	2.67	3.07

Generally speaking, the order of magnitude and the tendencies between the theoretical estimation and the experimental results agree for the three-hour data and for the OSB data. The 3-hour calculation is much closer to the experimental data than the 6-hour calculation. The best results are found for OSB in both the tests. The higher resistance of vapor flow of OSB could explain this result. In materials with fiberboard and plywood, moisture can be absorbed by the sheathing before entering the wall. The quantities of moisture of Table 5.1 do not account for any moisture content changes in the sheathing. In fact, moisture absorption is not included in this calculation.

The occurrence of moisture accumulation without condensation is also likely in assemblies without PE-Membrane, where some moisture could be absorbed in the hygroscopic material, e.g. unpainted gypsum board in the sample wall assembly, during the experimental process. Calculations using steady state diffusion, i.e. Fick's Law,

cannot take into account moisture transfer combined with absorption. The next section uses a tool that does not have this limitation.

5.2 WUFI-pro simulation using experimental data

WUFI-ORNL/IBP has more advantages than the dew-point method. The dew-point method, described in ASHRAE Fundamental, has been a common method to assess the moisture balance of a building component by considering vapor diffusion transport through a building envelope. However, the dew-point method does not consider capillary transport in the component, nor for its sorption capacity, both of which have a strong influence on the risk of damage in case of condensation. Furthermore, since the dew point method only considers steady-state transport under heavily simplified boundary conditions, it cannot reproduce individual short-term events or allow for rain and solar radiation. So the dew-point method can only provide a general assessment of the hygrothermal suitability of a component and cannot produce a simulation of realistic heat and moisture transfer in the building envelope.

WUFI 3.3-pro is a commercial heat and mass transport model, which can be used to simulate the process of one-dimensional moisture transfer through the wall assemblies with/without polyethylene membrane, but WUFI cannot be used to deal with the building envelope system with vented air space. In combination with WUFI, a weather generator tool can be used to generate the input file of the experimental conditions, which were based on the temperature and relative humidity values inside/outside the test hut

measured during the experimental process. The governing equations of the WUFI model were presented in chapter 2. Using the transient state, this model allows one to take into account permeance as a function of relative humidity, the change of moisture versus time of the cladding and the absorption in the hygroscopic range.

The first set of input data in WUFI is the description of the assembly, in terms of dimension, type and initial conditions of materials, together with the hygrothermal properties of each material. For the tested assembly, the western red cedar siding was simulated as three layers of spruce with different initial water content. The model does not include contact resistance between materials, such that the three layers are in continuity. This layered composition allows one to initialize each layer with a different moisture to reflect the conditions in the wood after soaking in water for 48 hours. In the soaking experiments for Beta determination (section 4.5), measurements of the depth of liquid water in wood were made and moisture content in the central part of the wood was measured with moisture pins. These measured moisture conditions were used as the starting point in WUFI.

Another material required a three-layered description. Gypsum board consists of three components: back finishing paper, gypsum plaster and front finishing paper. In order to make the WUFI simulation process close to the experimental process, these three layers were used instead of the uniform gypsum board found in the WUFI material database. There is no finishing paper of gypsum board in the material database; kraft paper was selected as the base for data input and sorption isotherm and permeance were modified

with data from the literature. Roels and Carmeliet (2005) analyzed sorption isotherm of gypsum board. The sorption isotherm was determined for the different constituents of the gypsum board: the finishing papers at the front and back side and the interior gypsum layer. In addition, the sorption isotherms of the two types of finishing coats were determined as shown in Appendix E. The permeance as a function of relative humidity is listed in Table 5.2.

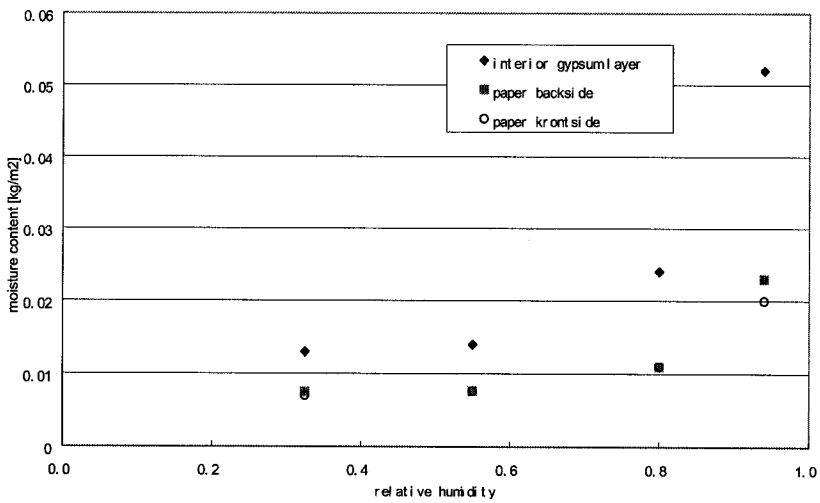

Figure 5.1. The measured sorption data under the same temperature of the different constituents of gypsum board plotted in kg/m^2. (data from Roels and Carmeliet 2005)

Table 5.2. Water vapor diffusion resistance factors of finishing paper (data from Roels and Carmeliet 2005)

Relative Humidity [-]	Vapor Diffusion Resistance Factor [m]
0.0	4.8
0.1	4.7
0.2	4.5
0.3	4.3
0.4	4.0
0.5	3.6
0.6	3.2
0.7	2.7
0.8	2.2
0.9	1.7
1.0	1.3

Given the particular precautions taken for the wood cladding and the gypsum board as described above, the composition of the simulated wall assembly is listed below and the conditions at the start of the simulations are in Table 5.3.

- Spruce (1 mm)
- Spruce (17 mm);
- Spruce (1 mm);
- Air space (20 mm);
- Spun bonded polyolefin membrane (SBPO);
- Fiberboard sheathing (11 mm);
- Glass fiber (89 mm);
- Polyethylene (0.15 mm) – when used in the test specimen
- Kraft paper (0.5 mm);
- Gypsum plaster (11.5 mm);
- Kraft paper (0.5 mm).

Table 5.3. Initial conditions of the different layers

Number	Material Layer	Density (kg/m^3)	Thickness (m)	Initial Water Content (kg/m^3)
1	Spruce	400	0.001	294
2	Spruce	400	0.017	32
3	Spruce	400	0.001	294
4	Air Space	1.3	0.02	0
5	Spun Bonded Polyolefin	590	0.001	0
6	Wood Fibreboard Plywood OSB	300 500 600	0.011 0.011 0.011	10 15 25
7	Fibre Glass	30	0.089	0
8	Polyethylene	130	0.00015	0
9	Back Paper	120	0.0005	10
10	Gypsum Plaster	1721	0.0115	1
11	Front Paper	120	0.0005	10

The second set of the data input is the loading conditions. A sample weather data file, which was from a main test, was provided in Table 5.4.

Table 5.4. Typical weather data file

$WUFI$ 30.5.2005_0.0 - 30.5.2005_18.0
101300.000

1	0	850	22.57	0.27	21.14	0.27
2	0	850	22.60	0.27	21.05	0.28
3	0	850	22.64	0.28	21.11	0.29
4	0	0	22.65	0.28	21.10	0.30
5	0	0	22.61	0.28	20.96	0.30
6	0	0	22.57	0.24	20.83	0.30
7	0	0	22.51	0.22	20.71	0.29
8	0	0	22.53	0.21	20.63	0.29
9	0	0	22.46	0.19	20.59	0.28
10	0	0	22.54	0.19	20.54	0.28
11	0	0	22.51	0.19	20.52	0.27
12	0	0	22.49	0.19	20.51	0.27
13	0	0	22.45	0.19	20.53	0.27
14	0	0	22.43	0.19	20.50	0.26
15	0	0	22.41	0.19	20.48	0.26
16	0	0	22.39	0.19	20.50	0.26
17	0	0	22.65	0.19	20.49	0.26
18	0	0	22.77	0.20	20.49	0.26
Time	Rain [Ltr/m²h]	Radiation [W/m^2]	T_{out} [°C]	RH_{out} [%]	T_{in} [°C]	RH_{in} [%]

The simulated solar radiation intensity was 850 W/m^2 This value was smaller than the radiation value generated by the heat lamps (1313 W/m^2) in the experiments, since not all radiation generated by the heat lamps fell on the wood siding surface. WUFI simulation provides siding surface temperature in Figure 5.2. An infrared camera was used to measure the siding surface temperature at the first three hours of an experiment. Figure 5.3 shows the average siding surface temperature monitored by the infrared camera. These profiles of the WUFI simulation results and the experimental measurements were similar.

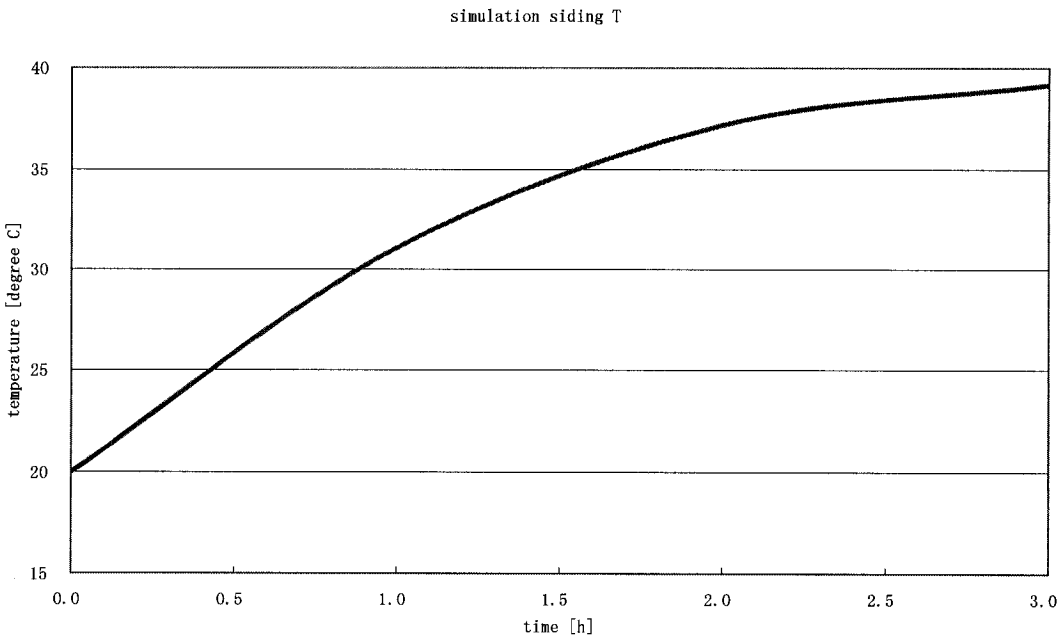

Figure 5.2. Siding surface temperatures by WUFI simulation

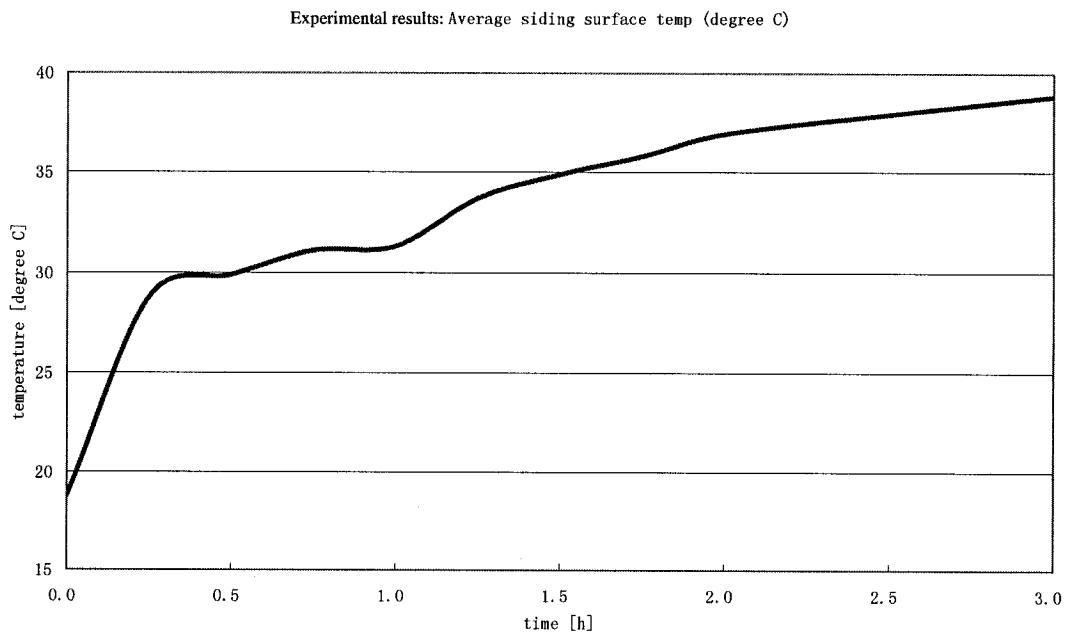

Figure 5.3. Siding surface temperatures by experimental measurements

Once all input were determined, the simulations were run. For each wall component, the initial temperature was set at 20 °C for all the layers. The simulation duration was 18 hours, which was the same as the experimental duration, and the calculation time step was one hour.

WUFI provides the mean water content of each layer after each calculation time step (one hour in this simulation case). This provides users with data to assess the behavior of the components during the simulation (e.g., drying or accumulating moisture).

After summing up the weight change of the layers of the backwall except the sheathing and the polyethylene sheet, i.e. the fibreglass insulation, the back finishing paper, the gypsum plaster and the front finishing paper after each time step, the maximum moisture content changes per square meter were established as shown in Table 5.5.

Table 5.5. The WUFI simulation results (with three-layer gypsum): the maximum moisture accumulation (g/m^2) as calculated by WUFI vs. as measured in the gravimetric sample (g/m^2)

Wall assemblies with sheathing	3h/closed		6h/closed	
	Experimental data	Simulation results	Experimental data	Simulation results
Fiberboard as sheathing	7.56	9.79	5.78	5.84
Plywood	4.00	5.72	3.56	3.43
OSB	3.56	4.63	2.67	3.16
Fiberboard-no polyethylene	16.44	15.05	24.44	16.78

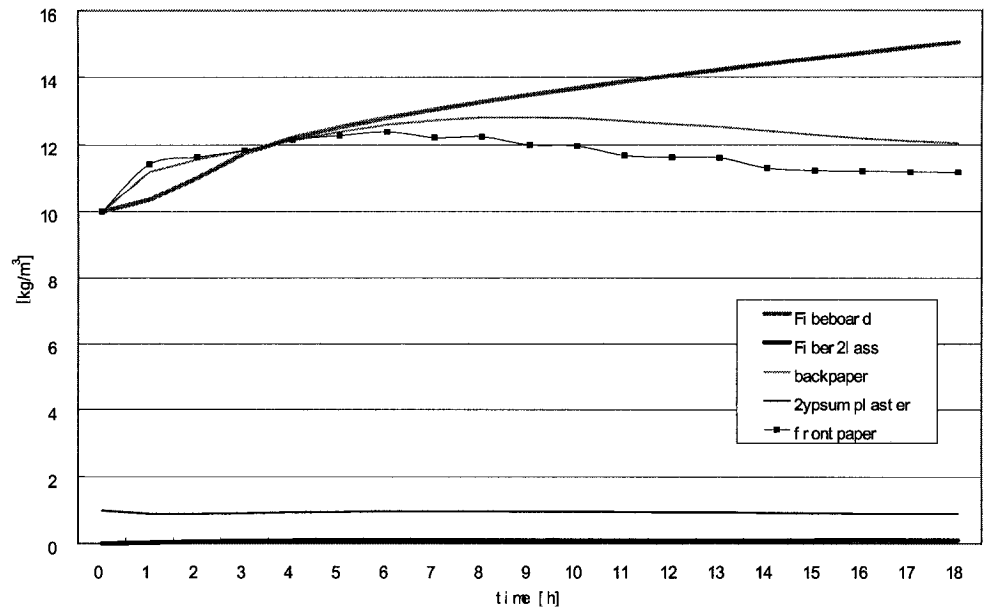

Figure 5.4. Moisture content of the wall components for the wall with fibreboard as the sheathing material

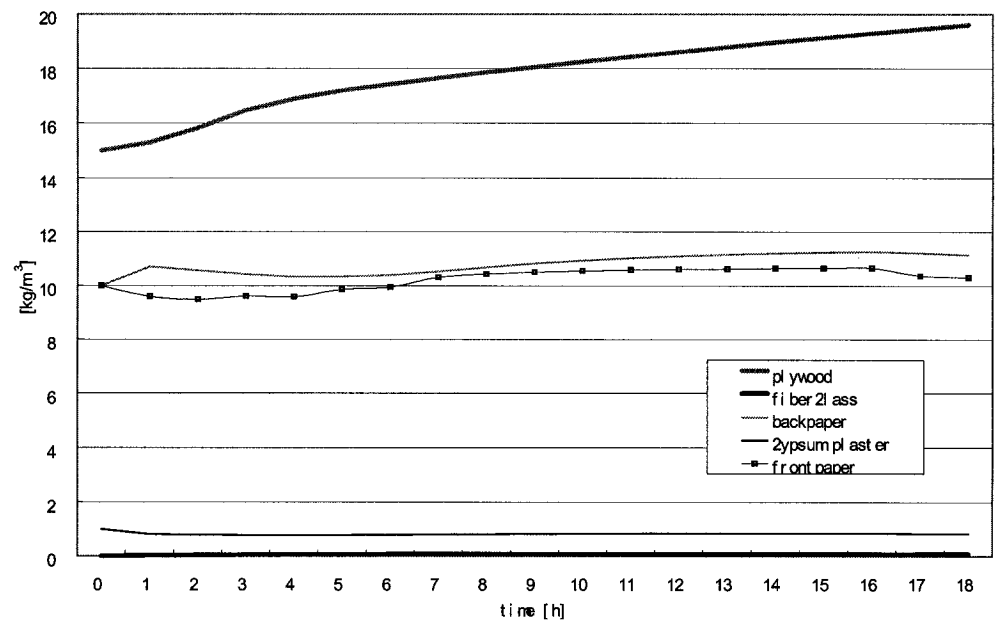

Figure 5.5. Moisture content of the wall components for the wall with plywood as the sheathing material

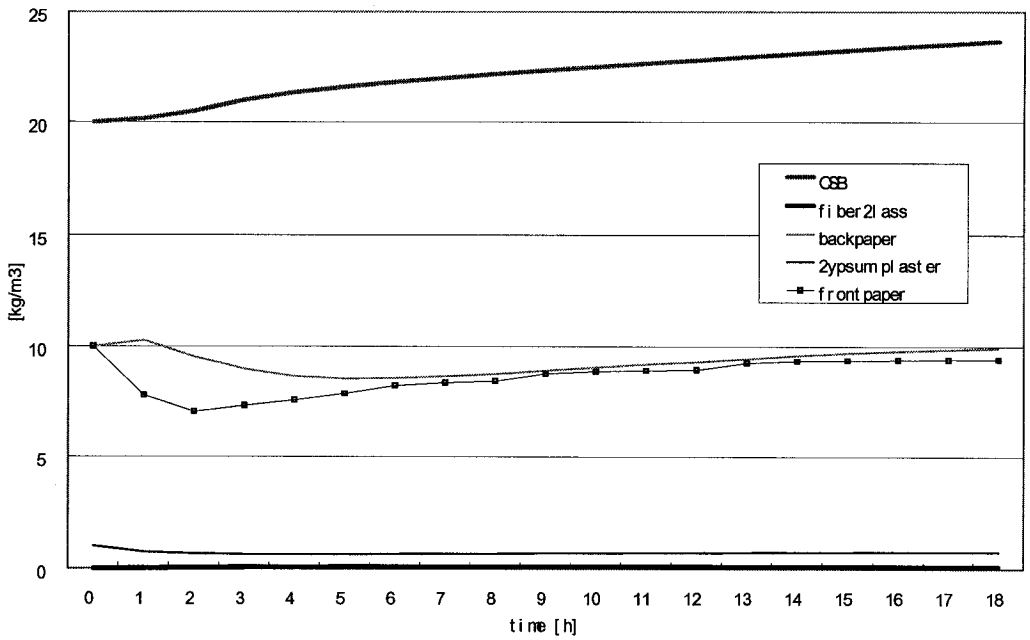

Figure 5.6. Moisture content of the wall components for the wall with OSB as the sheathing material

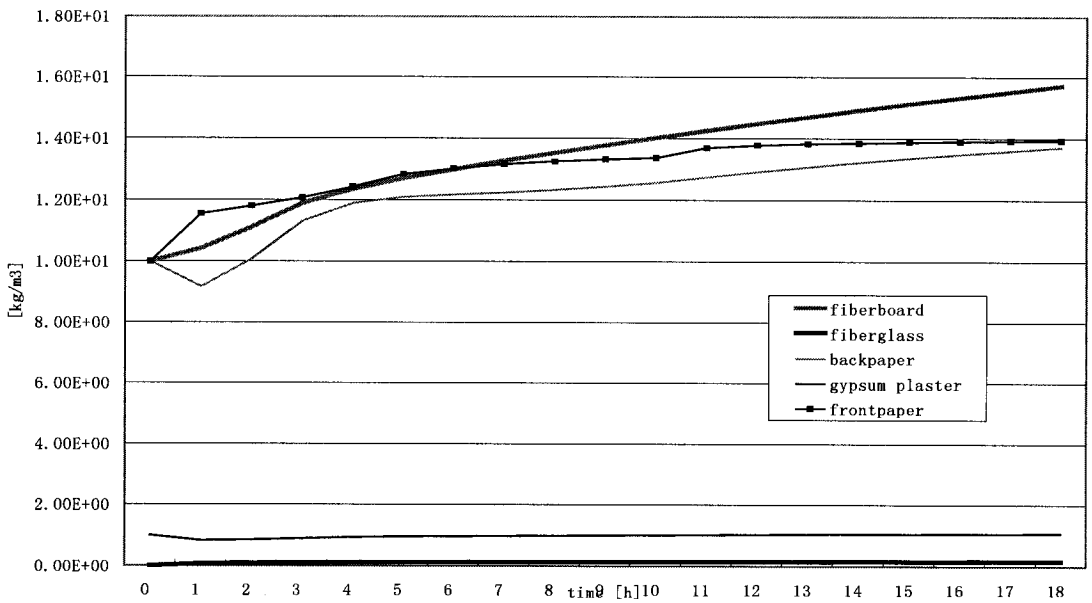

Figure 5.7. Moisture content of the wall components for the wall with fiberboard as the sheathing material and no polyethylene sheet

Comparing the WUFI simulation results with the experimental results, there was just a small difference between each other. WUFI provides a moisture content profile of each layer. Figures 5.4 to 5.7 show moisture content vs. time. These figures are for the wall assemblies with three-hour radiation and a closed air cavity. From the figures, it is shown clearly that most of the moisture transferring to the back wall is absorbed by the sheathing material. When the wall is more vapor permeable, there is more moisture accumulation in the finishing paper of the gypsum board. As shown in figure 5.7, the wall without polyethylene has the maximum moisture content increase of the finishing paper.

5.3 Parametric analysis with simulation using weather data

The sets of input developed in the previous sections provided results in close agreement with the experimental results. The same sets of input on the wall assemblies was used for different loading conditions. WUFI-pro has a database which includes the weather data of 4 Canadian cities and 49 US cities. The June and July weather data of five cities was selected to simulate the summer conditions. Simulation results and comparisons are presented in this section. This succinct parametric comparison aimed at verifying the possibility of extending the work done to full summer conditions.

5.3.1 The chosen cities

The five selected North American cities are Montreal (Canada), Boston (US), Baltimore (US), Charleston (US) and Tampa (US). They are in different latitudes but in a similar longitude. The typical hottest year was selected as the reference year.

The simulation duration was two months: June and July. The simulation time step was one hour. For each wall assembly, a wood siding with initial moisture content of 10%, instead of extremely wet condition, was applied in the simulation. The interior side was an air-conditioned space with medium moisture load: 21 °C, 50% RH.

5.3.2 Initial conditions of the different layers

Table 5.6. Initial conditions of the different layers

Number	Material Layer	Density (kg/m^3)	Thickness (m)	Initial Water Content (kg/m^3)
1	Spruce	400	0.001	40
2	Spruce	400	0.017	40
3	Spruce	400	0.001	40
4	Air Space	1.3	0.02	0
5	Spun Bonded Polyolefin	590	0.001	0
6	Wood Fibreboard Plywood OSB	300 500 600	0.011 0.011 0.011	10 10 20
7	Fibre Glass	30	0.089	0
8	Polyethylene	130	0.00015	0
9	Back Paper	120	0.0005	10
10	Gypsum Plaster	1721	0.0115	1
11	Front Paper	120	0.0005	10

5.3.3 Simulation results

For each simulation, the change of moisture content in the insulation and gypsum board was summed.

Table 5.7. Simulation results from WUFI. All data are in g/ m^2

	Fiberboard	Plywood	OSB	Fiberboard without polyethylene sheet
Montreal	115.35	81.27	78.74	62.99
Boston	130.87	87.78	85.36	64.29
Baltimore	151.51	93.98	90.76	57.94
Charleston	182.80	123.83	114.34	52.01
Tampa	169.84	114.55	106.31	51.48

From the WUFI simulation results, when the sheathing is less vapor permeable, there was less moisture accumulation. The influence of weather on the maximum moisture accumulation is strong. Finally, when there is polyethylene sheet on the inner side of the wall assembly, the maximum moisture accumulations in warmer locations are higher than in cooler locations. When there is no polyethylene sheet on the inner side of the wall assembly, there are no big differences on the moisture accumulation between different cities, and the amount is smaller than in the wall panels with polyethylene sheet as vapor barrier.

The differences between the experimental results and the WUFI simulation results using weather data were caused by the following reasons:

- The indoor air relative humidity was around 20%, which was much lower than the simulation condition (50%). This would increase the actual vapor pressure difference between the air cavity and the indoor conditions.
- The experiments were under extreme conditions, with the limitations shown in chapter 3.

- The loading conditions in the simulation is more complex that in the tests. For example, not only solar radiation is present, also cyclic air temperature and relative humidity conditions are present.
- In the walls without polyethylene simulation, it should be borne in mind that the absorption capacity of paper is limited. As a result, in long period simulations, the absorption does not seem to play such an important role anymore as compared with the experimental data.

Although the wall assembly without polyethylene has lower moisture accumulation, the back finishing paper of the gypsum board was under temperature and relative humidity conditions favourable to mold growth (figure 5.8 & 5.9). The following figures are from a test panel with fibreboard as the sheathing material but no polyethylene on the inner side. This simulation location is Charleston. All the figures of moisture accumulation do not include sheathing materials, e.g., fiberboard.

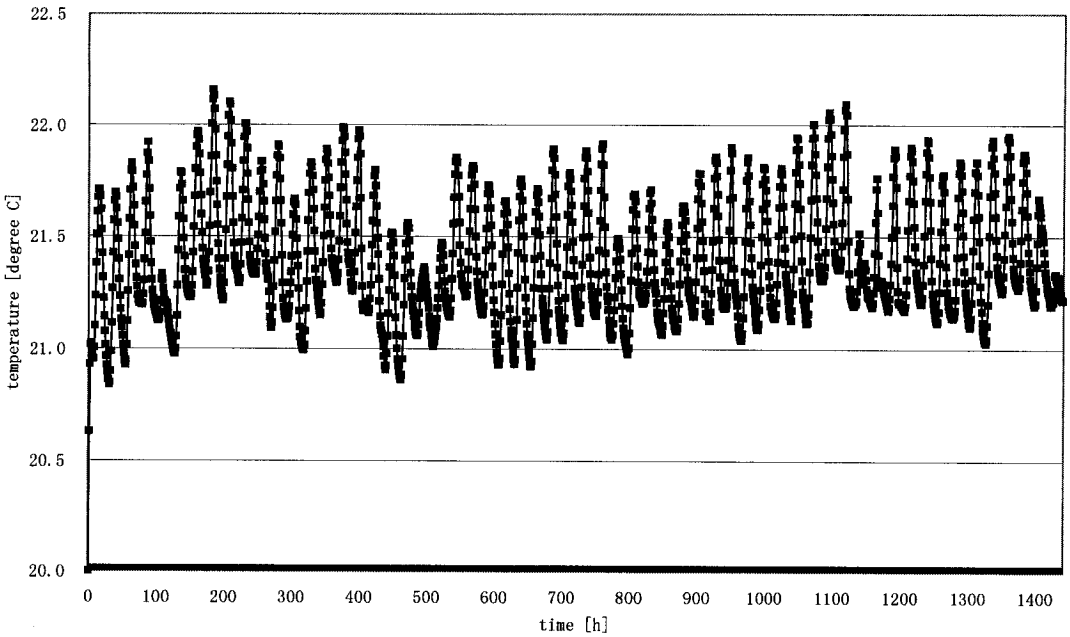

Figure 5.8. Temperature near the backpaper

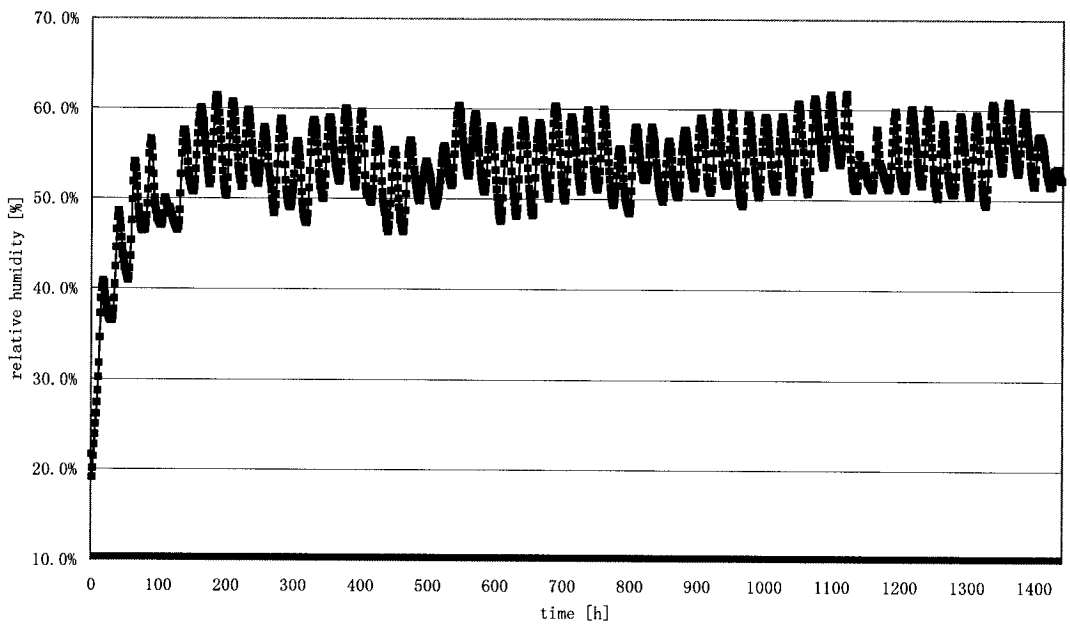

Figure 5.9. Relative humidity near the backpaper

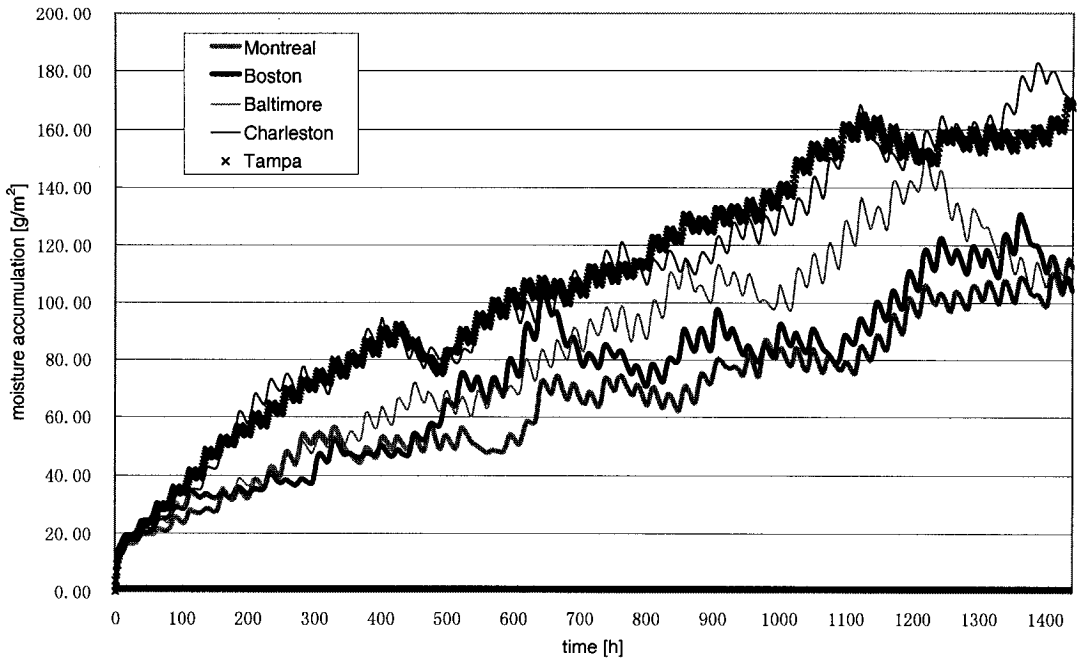

Figure 5.10. Moisture accumulation (insulation; PE, gypsum board) in wall with fiberboard as the sheathing material

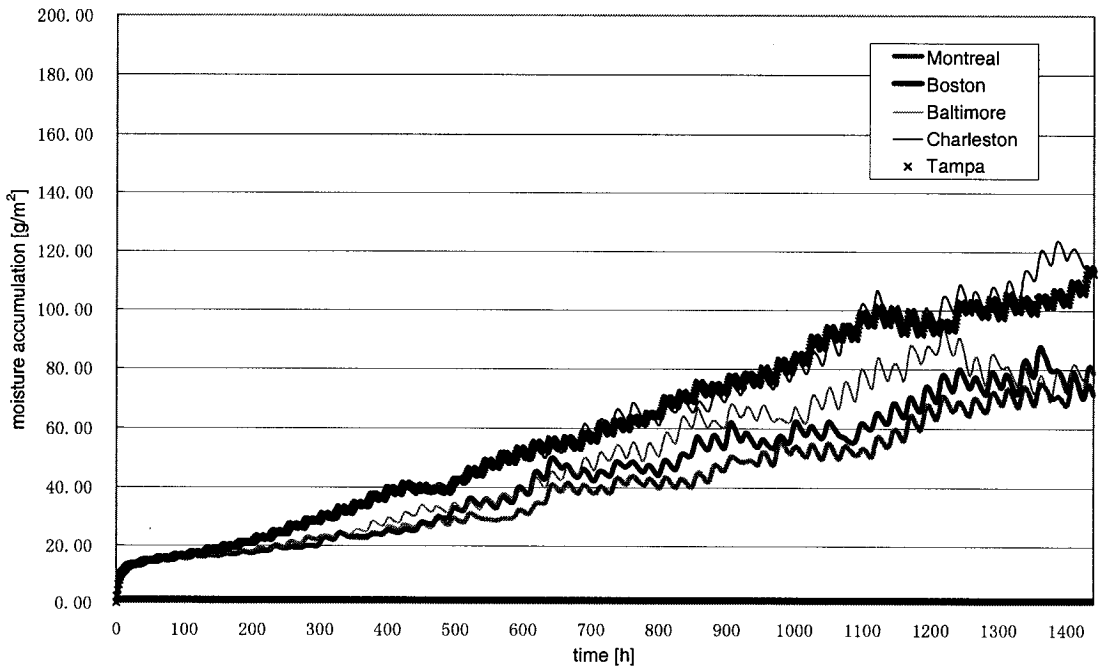

Figure 5.11. Moisture accumulation (insulation; PE, gypsum board) in wall with plywood as the sheathing material

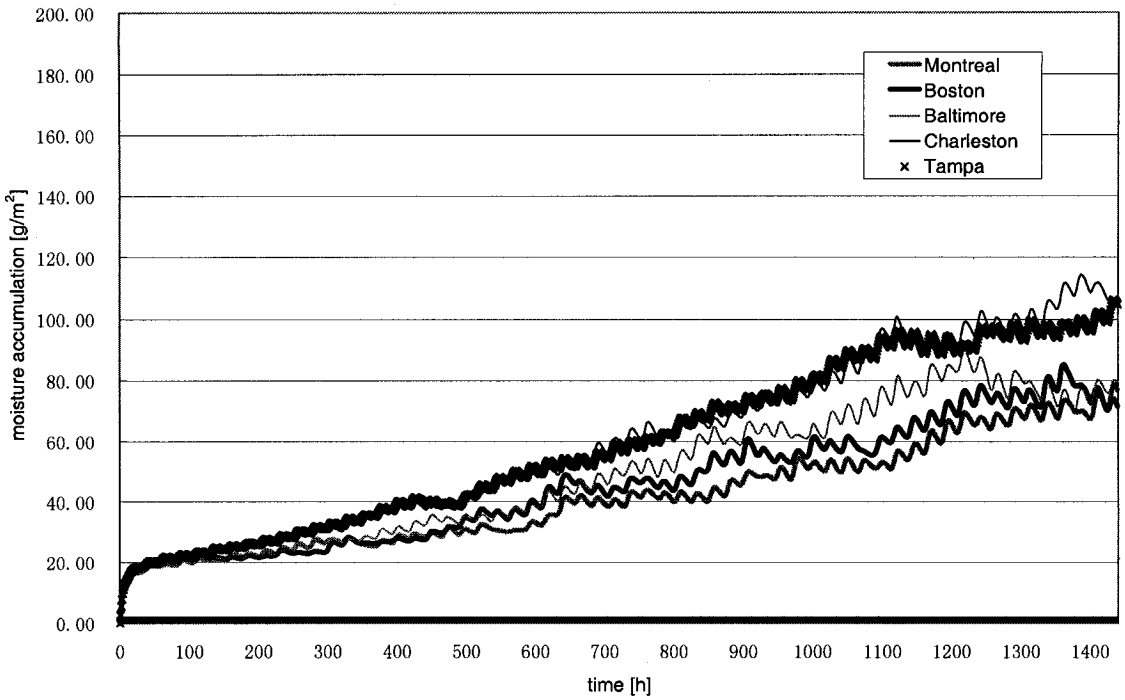

Figure 5.12. Moisture accumulation (insulation; PE, gypsum board) in wall with OSB as the sheathing material

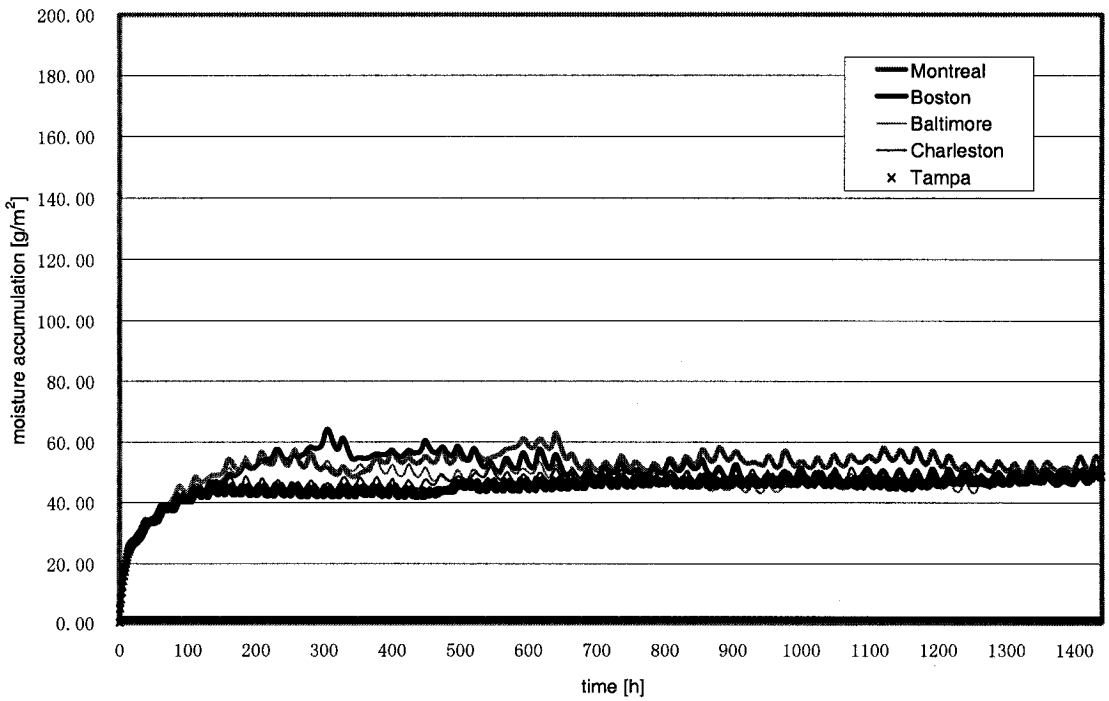

Figure 5.13. Moisture accumulation (insulation; PE, gypsum board) in wall with fiberboard as the sheathing material and without polyethylene membrane

The moisture accumulation is still increasing over all the periods in the wall assemblies with polyethylene (figure 5.10, 5.11, 5.12), and is stable after 10 days in the walls without polyethylene membrane (figure 5.13). The wall assembly with high permeance sheathing (e.g. fibreboard) has more moisture accumulation if there is polyethylene sheet in the wall assembly.

WUFI provides simulation results that can be analyzed to provide more understanding of the distribution of moisture accumulation within assemblies exposed to solar-driven moisture flows. More parameters and loadings conditions could be studied.

5.4 Surface coefficient of vapor transfer β

During the experimental procedure, moisture from the wet wood siding would be transported in two directions: some would evaporate into ambient air; some would evaporate into the air space. In this research project, the amount of moisture added into the air space greatly influences the hygrothermal performance of the test wall assemblies. Surface coefficient of vapor transfer β is an important factor to evaluate this process. Experiments were applied to determine β as shown in Chapter 4. Theoretical estimation of β using the experimental data and comparison between these two β are presented in this chapter.

The air conditions in the air cavity influence the whole hygrothermal performance of the wall assemblies. During the first several hours of the experiments, air in the air space has

a higher temperature and relative humidity than the outside and the inside of the test hut. The main moisture flows in the air cavity of the test panel were as follows: some evaporated moisture from the wet wood siding went to the air cavity and, at the same time, some moisture in the air cavity would diffuse to the back wall and to the outside of the test panel.

The calculation below aims at comparing the surface coefficients of vapor flow, β, which are from different air conditions. Moisture balance in the air cavity is investigated in the following section.

5.4.1 Moisture from the siding to the air space

According to section 4.5, the density of moisture flow rate is:

$$g_v = \beta \cdot (p - p_s) \tag{4.1}$$

where

g_v = density of moisture flow rate (kg/m^{2}s)

β = surface coefficient of vapor transfer (s/m)

p = vapor pressure outside the boundary layer (Pa)

p_s = vapor pressure on the surface

5.4.2 Moisture diffusion from the air space to the back wall system and to the outside of the test panel

According to Fick's equation, $W = M \cdot A \cdot \theta \cdot \Delta P$

where

W = Total mass of vapor transferred (ng)

A = Cross section area of flow path (m^2)

θ = Time of flow (seconds)

ΔP = Vapor pressure difference (Pa)

At the beginning of the experiment in the air cavity, air temperature was 22 °C, and relative humidity was 60%. This initial relative humidity was higher than the ambient air was because after the wet wood siding was installed, it took several minutes to start the tests. This process made the air inside the air space more humid than the outside. From the hourly average temperature and relative humidity data, humidity ratio change or net moisture change in the air space according to time was determined. Since vapor flow by diffusion to the back wall and to the outside could be calculated, the density of moisture flow rate from the wet wood siding to the air space g_v was then finalized. Surface coefficient of vapor transfer β was calculated from g_v. The values of β are shown in table 5.8.

Table 5.8 Surface coefficient of vapor transfer β-from calculation

Time [h]	β [s/m]
1	1.19E-9
2	2.23E-9
3	1.94E-9
4	1.48E-9
5	1.43E-9

The difference between this calculated β and β from the small scale experiments (section 4.5) is shown in figure 5.14. They are from 6-hour radiation experiments. In the small experiment, the wet wood siding faced an open space, which has much drier air (21 ^{o}C, 30%); in the main experiments, the closed air cavity has more humid air than the ambient air, this would delay the process of vapor flow from the siding to the air cavity.

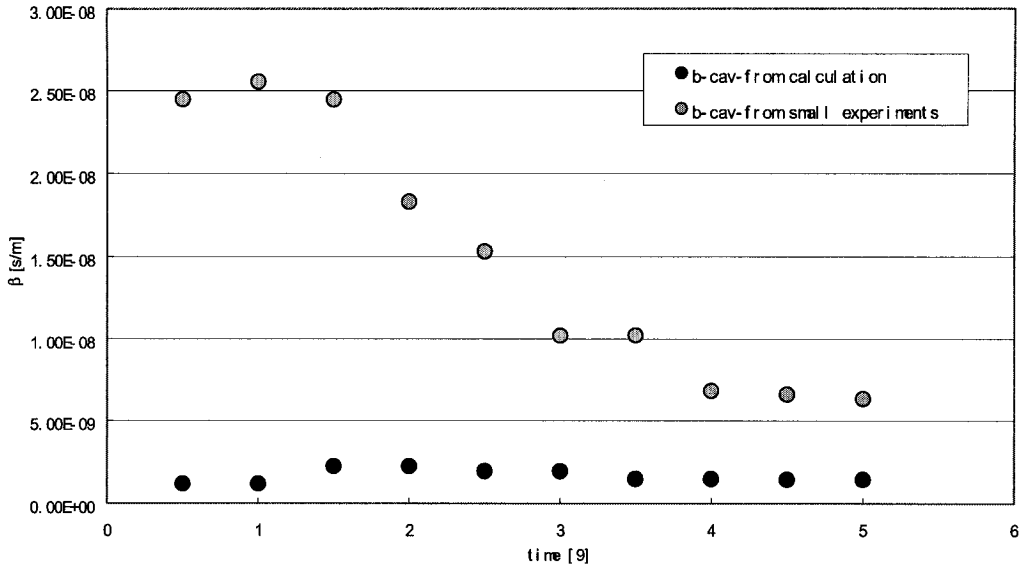

Figure 5.14. Surface coefficient of vapor flow β

From Figure 5.14, both βcav increase at the beginning and then decrease. βcav from the small experiment is much higher than βcav from calculations during the whole process. In the small experiment, as described in section 4.5, the siding sample was placed in very dry ambient air (21 °C, 30%). The density of moisture flow rate in the small experiment, g_v, was much higher than the moisture flow rate from the wet wood siding to the closed air cavity in the main experiment, which has a high temperature and relative humidity.

CHAPTER 6 CONCLUSIONS AND FUTURE WORK

This project studied the moisture movement and accumulation in wood frame wall assemblies exposed to simulated solar radiation from an experimental approach. Two analytical tools, a steady-state method and a commercial heat and mass transfer model, were applied in data analyses. This project developed a better understanding of the nature and significance of solar-driven inward vapor diffusion through the investigation of hygrothermal performance of different wood-framed wall assemblies under summer conditions, with considerations of a cold climate for loading and assembly design.

6.1 Conclusions

This study has the following conclusions:

- The experiments simulated extreme conditions of solar-driven moisture flow. It was demonstrated that solar-driven moisture accumulation may occur, and this phenomenon should be taken into account at the design stage. Sheathing materials with higher water vapour permeance incur bigger amount of moisture accumulation;
- Air cavity ventilation plays an important role in minimizing solar-driven vapour flow;
- With solar radiation, moisture accumulation within the wall assemblies could occur, although there is only small difference between the indoor and the outdoor air conditions (temperature and relative humidity);

- During summer conditions, moisture problems, e.g. mold problems, can still occur, when there is no low permeance polyethylene sheet on the inner side of the wood-frame wall assemblies.

6.2 Contributions of the research

The contributions of the research are:

- The development of an experimental methodology to study the behaviour of wall assemblies with wet cladding exposed to simulated solar-driven moisture flow;
- The production of a documented set of experimental data on 12 test panels exposed to simulated solar radiation;
- The demonstration of the influence of three wall parameters - permeance of sheathing, presence of inner vapour barrier, presence of ventilation;
- The analysis of the experimental data using two methods, steady-state method and transient model, to illustrate further the role of different parameters.

6.3 Recommendations for future work

Through this research work, a clear direction to the future work has been provided. Future work could focus on the study of the following subjects:

- The influence of different moisture storage capacity of the cladding material on the water vapor transportation;
- The selection of different vapor diffusion retarder based on climatic load;

- An efficient and more accurate way of simulating solar radiation;
- The influence of solar-driven vapor flow on sheathing materials;
- Field tests on the significance of inward vapor drives across different climatic regions;
- The performance of assemblies under complete loading condition;
- Development of a model to simulate ventilation in air space in combination with moisture flows;
- Further study of the occurrence of thermal-induced moisture flow versus vapor differential-induced moisture flow;
- Further study of the ratio of moisture accumulation due to absorption in the hygroscopic range versus the accumulation due to vapor condensation;
- Further study of the influence of night temperatures on the hygrothermal performance of wall assemblies.

REFERENCES

Anderson, N.E. 1985 "Sommerkondens (summer condensation)" In Danish with an English Summary Statens Byggeforskningsinstitut (State Building Research Institute), Report 171, Horsholm, Denmark

Andersen, N.E., 1988 Summer Condensation in an Unheated Building Proceeding of Symposium and Day of Building Physics Stockholm: Swedish Council for Building Research, p164-p16

ASHRAE Handbook of Fundamental 2001

Building Research Establishment 1989 "Solid External Walls: Internal Dry-Lining-Preventing Summer Condensation" BRE Defect Action Sheet (Design) DAS 133, Garston, Watford, UK

Burmeister, L.C. 1983. Convective heat transfer. John Wiley and Sons, New York

Christensen, Georg, "Summer Condensation in Post-Insulated Exterior Walls- Some Results from Measurement in a Test House", CIB/W61, Building Physics Division, Danish Building Research Institute, Horsholm, Denmark, 1985, p1-p7

de Wit, M. H. 2004 Heat and Moisture in Building Envelopes

Hutcheon, N.B., 1953 Fundamental Considerations in the Design of Exterior Walls for Buildings, NRC Paper No. 3087, DBR No. 37. Ottawa: Division of Building Research

Kan, L. 1999. An Investigation of Measure's to Reduce Summer Condensation in Walls A M.A.Sc Thesis from University of Toronto

Kan, V. Controlling Sun Driven Moisture: A Laboratory Investigation A M.A.Sc Thesis from University of Toronto 2002 p42

Kays, W.M. and M.Crawford. 1980. Convective heat and mass transfer, 2nd ed. McGraw-Hill, New York

Kumaran, M. K. et al. 2002 A Thermal and Moisture Transport Property Database for Common Building and Insulating Materials, Final Report from ASHRAE Research Project 1018-RP

Lstiburek, J. and Pettit, B. 2004 EEBA Builder's Guide 2004

Pressnail K., Timusk J., Kan, L. Dong, B. Kan, V. Feb. 2003 In Search of a Wall for All Seasons: Controlling Sun-Driven Moisture Proceedings of the Ninth Canadian Conference on Building Science and Technology National Building Envelope Council, p157-p170

Roels, S. and Carmeliet, J. 2005, Water Vapour Permeability and Sorption Isotherm of Coated Gypsum Board, Proceedings of the 7th Symposium on Building Physics in the Nordic Countries, Reykjavik, Iceland, June 13-15 2005 p609~p616

Rose, W.B., 1997 Control of Moisture in the Modern Building Envelope: The History of the Vapor Barrier in the United States 1923-1953 APT Bulletin 18 (4)

Sandin, K. 1993 Moisture Conditions in Cavity Walls with Wooden Framework Building Research and Information 21 (4): p235-p238

Sandin, K. Skalmurskonstruktionens fukt- och temperatur-betingelser. Rapport R43: 1991 Byggforskningsradet, Stockholm, Sweden.

Straube, J.F. December 2001 "The Influence of Low-Permeance Vapour Barriers on Roof and Wall Performance", Conference Proceedings Performance of Exterior Envelopes of Whole Buildings VIII

Straube, J.F., and Burnett, E.F.P., 1995 Moisture Migration in Screened Wall Systems, Proceedings of BETEC/ASHRAE/DOE Thermal Performance of Building Envelopes VI, p177-p188

Straube, J.F. and Burnett, E.F.P. 1998. Drainage, Ventilation Drying, and Enclosure Performance. Thermal Performance of the Exterior Envelopes of Buildings VII. Atlanta: American Society of Heating, Refrigerating and Air-Conditioning Engineers, Inc., p189-p198

Straube, J.F. and Burnett, E.F.P., Vents, Ventilation and Masonry Veneer Wall Systems, Proc. of the Eighth Canadian Masonry Symposium, Jasper, Alta., Canada, May 31-June 3, 1998, p194-p207.

Tenwolde, A., and Mei, H.T., 1985 Moisture Movement in Walls in a Warm Humid Climate. Proceedings of ASHRAE/ DOE/ BTECC Thermal Performance of the Exterior Envelopes of Buildings III, p570-p582, Atlanta: American Society of Heating, Refrigerating and Air-Conditioning Engineers, Inc

Vinha, J. and Kalamees, T., Feb. 2003. Principles to Analyse The Moisture Performance of Timber-Frame External Wall Asembly Due to Diffusion Proceedings of the Ninth Canadian Conference on Building Science and Technology National Building Envelope Council, p123-p140

Wilson, A.G. 1965. Condensation in Insulated Masonry Walls in the Summer Proceedings of RILEM/ CIB Symposium, p2-p7

Appendix A

Sheathing Tape
Application temperature: 0 °F (-18 °C) ~ 260 °F (126 °C)
Weather and UV resistant; Adheres to Poly Plastic; Powerful Adhesive
Venture Tape (brand name): CMHC Evaluation/ Report No. 11362R
Made in U.S.A. Rockland, MA 02370
Dimension: 60 mm x 66 m

XPS on the outside of the test hut
2'' XPS R=10.0 (RSI=1.76)

Weight Scale A (for wood siding)
HOWE Richardson Company
Clifton, N.J.
Model No. SSD-900
Serial No. 6244
Volts 117
Amps 0.05
Capacity 99.99 x 0.01 kg
Platform size 14 x 17

Weight Scale B (for gravimetric sample)
Voyager Pro
Model No. VP6102CN
Max 6100 g
D 0.01 g
E 0.1 g
Temp range 10 °C / 30 °C
Power required: 12V 1A
Geneq inc (www.geneq.com)

Data Logger
Agilent Benchlink Data Logger

T/RH Sensor
HUMITTER Humidity and Temperature Transmitter
0~100% RH measurement
-10~60 °C
±3% RH accuracy with better than ±1% RH stability per year (claimed by the manufacturer)

Thermocouple
T type thermocouple (copper and constantan) gauge 30, with 0.5°C accuracy, with reference junction having 0.2°C accuracy.

Air Conditioner

6000 BTU

Air Velocity Meters
From TSI Incorporated (www.tsi.com)
Model: 8346-E-GB
S/N: 03060073
Range: 0 to 30 m/s
Accuracy: 3.0% of reading or ±0.015 m/s, whichever is greater

Wood Moisture Meter
DELMHORST
Model: J-2000
Range: 6 ~ 40 %
(When using uninsulated pins, push them in to the wood to their full length, if possible. This will give you the highest measured reading.)

Appendix B

temperature swing of room with one exterior wall

place .. Montreal .. (latitude .. 45) .. deg height above sea $Hs := 0.057$ km

date .. July21 have following cinditions;

$L := 45$ deg $n := 202$ day $\beta := 90$ deg $\psi := 0$ $\rho := 0.2$

declination angle

$$\delta := 23.45 \sin\left[360 \frac{(284 + n)}{365 \cdot 57.3}\right]$$

deg

$\delta = 20.449$

timeset time

$$ts1 := 57.3 \frac{\operatorname{acos}\left(-\tan\left(\frac{L}{57.3}\right) \cdot \tan\left(\frac{\delta}{57.3}\right)\right)}{15}$$

$ts1 = 7.46$

$$ts2 := 57.3 \frac{\operatorname{acos}\left(-\tan\left(\frac{L - \beta}{57.3}\right) \cdot \tan\left(\frac{\delta}{57.3}\right)\right)}{15}$$

$ts2 = 4.541$

$$ts := \begin{cases} ts1 & \text{if } ts1 - ts2 \le 0 \\ ts2 & \text{otherwise} \end{cases}$$

$ts = 4.541$

time interval $ti := \frac{ts}{8}$

$i := -8 .. 8$

solar altitude α

$$\alpha(i) := 57.3 \operatorname{asin}\left(\cos\left(\frac{L}{57.3}\right) \cdot \cos\left(\frac{\delta}{57.3}\right) \cdot \cos\left(\frac{ti \cdot i \cdot 15}{57.3}\right) + \sin\left(\frac{L}{57.3}\right) \cdot \sin\left(\frac{\delta}{57.3}\right)\right)$$

$$f(i) := \sin\left(\frac{\alpha(i)}{57.3}\right) \cdot \sin\left(\frac{L}{57.3}\right) - \sin\left(\frac{\delta}{57.3}\right)$$

$$fo(i) := \cos\left(\frac{L}{57.3}\right) \cdot \cos\left(\frac{\alpha(i)}{57.3}\right)$$

$$\phi(i) := 57.3 \operatorname{acos}\left(\frac{f(i)}{fo(i)}\right)$$

$\gamma(i) := \phi(i) - \psi$ deg

incidence angle θ

$$\theta(i) := 57.3\text{acos}\left(\cos\left(\frac{\alpha(i)}{57.3}\right)\cdot\cos\left(\left|\frac{\gamma(i)}{57.3}\right|\right)\cdot\sin\left(\frac{\beta}{57.3}\right) + \sin\left(\frac{\alpha(i)}{57.3}\right)\cos\left(\frac{\beta}{57.3}\right)\right)$$

during clear day, there are following parameters needed to be calculate

$$a0 := 1.03\left[0.4327 - 0.00821(6 - 0.057)^2\right] \qquad a0 = 0.147$$

$$a1 := 1.01\left[0.5055 + [0.00595(6.5 - 0.057)]^2\right] \qquad a1 = 0.512$$

$$k := 0.2711 + [0.01858((2.5 - 0.057))]^2 \qquad k = 0.273$$

transmittance for beam radiation tb

$$tb(i) := a0 + a1\cdot\exp\left(\frac{-k}{\sin\left(\frac{\alpha(i)}{57.3}\right) + 0.000001}\right)$$

the extraterrestrial solar radiation Ion

$$Ion := 1353\left(1 + 0.033\cos\left(\frac{360\cdot n}{365\cdot 57.3}\right)\right)$$

$$Ib(i) := Ion\cdot tb(i)\cos\left(\frac{\theta(i)}{57.3}\right)$$

$$td(i) := 0.271 - 0.294\,tb(i)$$

$$Fws := 0.5\left(1 + \cos\left(\frac{\beta}{57.3}\right)\right)$$

$$Fwg := 0.5\cdot\left(1 - \cos\left(\frac{\beta}{57.3}\right)\right)$$

$$Ids(i) := Ion\cdot td(i)\cdot Fws\cdot\sin\left(\frac{\alpha(i)}{57.3}\right)$$

$$Idg(i) := Ion\cdot(tb(i) + td(i))\cdot\rho\cdot Fwg\cdot\sin\left(\frac{\alpha(i)}{57.3}\right)$$

so, the total radiation It

$$It(i) := Ib(i) + Ids(i) + Idg(i)$$

$$num := -8..7$$

$$It(0) = 432.606$$

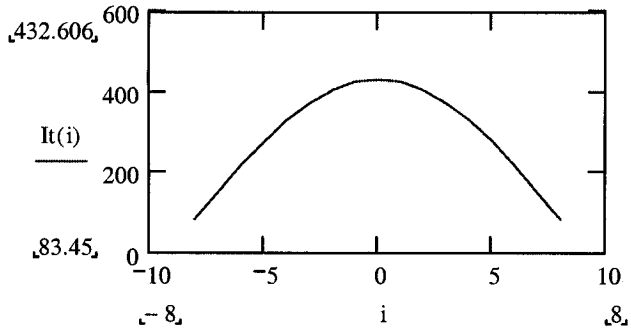

For July 21, Montreal:

$$\alpha \cdot S = ho \cdot (Tsol - To)$$

Where

α = Absorptance for solar radiation
S = solar radiation (W/m^2)
ho = Coefficient of heat transfer by long-wave radiation and convection at outer surface, $W/(m^2 \cdot K)$
Tsol = sol-air temperature, °C
To = outdoor air temperature, °C
α / ho = 0.053 for dark-colored walls

$Tsol - To$ = 0.053 x 433 = 23 °C

Appendix C

In Straube's paper (2001), in the "Example Calculations" part, the author uses Glaser method to calculate vapor-diffusion through several wall assemblies under the weather conditions of Omaha, Nebraska. These calculations are in order to prove the author's point of view: With a vapor barrier, there is a moisture problem; without a vapor barrier, no moisture problem or only a minor moisture problem occurs. The calculation analyses part is shown in Appendix C.

For table 1, with vapor retarder (M=60) and plywood (M=40), condensation occurs. This is under extreme conditions: temperature: 21/ -19°C. Although -19°C is under very cold weather, further calculation shows that condensation will also occur under outdoor temperatures as warm as 5°C, as shown in table 2.

		TABLE 1							
	First Pass Calculation for Omaha, Nebraska								
Element	R	ΔT	t °C	M	Rv	Pv Diff	Pv	Psat	RH
			21.00				990	2474	40%
Inside Film	0.120	1.80		10000	0.000	2			
			19.20				988	2212	45%
Vapor Retarder	0.000	0.00		60	0.017	344			
			19.20				643	2212	29%
Batt Insulation	2.500	37.58		2000	0.001	10			
			-18.38				633	143	443%
				Flow to back of sheathing					
				Permeance=57.9		Pv Diff:847			
				Flow to:0.1765 g/m2h					
Plywood	0.012	0.18		40	0.025	516			
			-18.56				117	141	83%
Outside Film	0.029	0.44		20000	0.000	1			
			-19.00				116	136	85%
SUM	2.661	40.00		23.631	0.042	874			
				Flow away from back of sheathing					
				Permeance=39.92		Pv Diff:27			
				Flow away:0.004					
				Net Accumulation:0.172 g/m2h					

For table 3, without vapor retarder, but with painted drywall and fiberboard (permeance: 180 vs. 1666), no condensation occurs under temperature: 21/ -19°C, 30% RH interior conditions. If indoor relative humidity is increased to 40%, although condensation occurs, the rate is very low, and it will not be a severe problem, as shown in table 13.

		TABLE 3							
	Calculation of Vapor Diffusion with Fiberboard Sheathing								
Element	R	ΔT	t °C	M	Rv	Pv Diff	Pv	Psat	RH
			21.00				742	2474	30%
Inside Film	0.120	1.67		10000	0.000	9			
			19.33				733	2231	33%
Painted drywall	0.000	0.00		180	0.006	511			
			19.33				222	2231	10%
Batt Insulation	2.500	34.72		2000	0.001	46			
			-15.39				175	184	95%
Fiberboard	0.231	3.21		1666	0.001	55			
			-18.60				120	141	85%
Outside Film	0.029	0.40		20000	0.000	5			
			-19.00				116	136	85%
SUM	2.880	40.00		146.93	0.007	627			

		TABLE 13							
	based on table 3, for interior humidity of 40% RH								
Element	R	ΔT	t °C	M	Rv	Pv Diff	Pv	Psat	RH
			21.00				990	2474	40%
Inside Film	0.120	1.67		10000	0.000	13			
			19.33				977	2231	44%
Painted drywall	0.000	0.00		180	0.006	727			
			19.33				249	2231	11%
Batt Insulation	2.500	34.72		2000	0.001	65			
			-15.39				184	184	100%
Sub Total				162.45	0.006	806			
				Flow to back of sheathing					
				Permeance=162.45		Pv Diff:806			
				Flow to:	0.471	g/m2h			
Fiberboard	0.231	3.21		1666	0.001	63			
			-18.60				121	141	86%
Outside Film	0.029	0.40		20000	0.000	5			
			-19.00				116	136	85%
Sub Total				1537.89	0.001	68			
SUM	2.880	40.00		2.07	0.484	874			
				Flow away from back of sheathing					
				Permeance=1537.89		Pv Diff:68			
				Flow away	0.379	g/m2h			
				Net Accumulation:	**0.092**	**g/m2h**			

For table 5, with vapor retarder and fiberboard (permeance: 60 vs.1666), severe condensation occurs under temperature: 22/ 40°C.

		TABLE 5										
	Calculation of Summer Condensation											
				Flow into building								
				Permeance: 59.6		Pressure:1175						
				Flow away	0.25	g/m2h						
				Net Accumulation: 13.64 g/m2h								
Sub Total							59.6	0.017	1175			
Element	t(mm)	k	C	R	ΔT	t °C	M	Rv	Pv Diff	Pv	Psat	RH
						22.0				1579	2631	60%
Inside Film	2	NA	8.30	0.120	-0.75		10000	0.000	7			
						22.8				1586	2754	58%
Vapor Retarder	0	NA	0.00	0.000	0.00		60	0.017	1168			
						22.8				2754	2754	100%
				Flow from back of sheathing								
				Permeance:869		Pressure: 4438						
				Flow away	13.89	g/m2h						
Sub Total							869	0.001	4438			
Batt Insulation	90	0.04	0.40	2.500	-15.62		2000	0.001	1929			
						38.4				4683	6727	70%
Fiberboard	12.7	0.06	4.33	0.231	-1.44		1666	0.001	2316			
						39.8				6999	7267	96%
Outside Film	2	NA	34.00	0.029	-0.18		20000	0.000	193			
						40.0				7192	7339	98%
SUM				2.881	-18.00		52.45	0.019	5614			

From these calculations, the author concludes that the wall with a vapor retarder encounters a condensation problem (no matter it is serious or not), on the other side, the wall assembly without a vapor retarder works well. These calculations are simple steady-state vapor diffusion calculations, which are easy to understand, and the results are apparent. A very important assumption is that there are good air barrier systems in these wall assemblies.

The author mentions five kinds of wall assemblies for four kinds of different environmental conditions, as shown in the table "Summary- Calculation for Omaha, Nebraska (a cold climate). From Table 1 to Table 5, these tables are included in the paper, Table 6 to Table 13, and the author showed their calculation results. Besides these tables, there should be other tables for the wall assemblies under all these four environmental conditions. To get an overall view of the influence of vapor retarders, calculation for the "missed" tables should be undertaken, as shown in table from 14 to 24, using dew point method.

For Table 9, another vapor retarder (vapor permeance is 1.5 metric perms) substitutes the vapor barrier used in table 1 (vapor permeance is 60 metric perms), other conditions are maintained the same, and then almost no condensation occurs. For several cases in Wall 1, because the permeance of the vapor retarder and plywood is very low, and the values are close to each other, if water vapor goes between them, it is hard for it to dry to the outside or to the inside. (Shown in Table 1, 2, 7 and 14) So to prevent condensation problem, there should be a wall component with relatively small vapor permeance compared to other wall components.

		TABLE 9							
	First Pass Calculation for Omaha, Nebraska								
Element	R	ΔT	t °C	M	Rv	Pv Diff	Pv	Psat	RH
			21.00				990	2474	40%
Inside Film	0.120	1.80		10000	0.000	0			
			19.20				989	2224	44%
Vapor Retarder	0.000	0.00		1.5	0.667	860			
			19.20				129	2224	6%
Batt Insulation	2.500	37.58		2000	0.001	1			
			-18.38				129	120.5	107%
Plywood	0.012	0.18		40	0.025	32			
			-18.56				97	118.5	81%
Outside Film	0.029	0.44		20000	0.000	0			
			-19.00				96	113.5	85%
SUM	2.661	40.00		1.444	0.692	893.125			

		TABLE 7							
	First Pass Calculation for Omaha, Nebraska								
Element	R	ΔT	t °C	M	Rv	Pv Diff	Pv	Psat	RH
			21.00				990	2474	40%
Inside Film	0.120	0.72		10000	0.000	1			
			20.28				989	2379	42%
Vapor Retarder	0.000	0.00		60	0.017	98			
			20.28				891	2379	37%
Batt Insulation	2.500	15.03		2000	0.001	3			
			5.25				888	887.6	100%
Plywood	0.012	0.07		40	0.025	147			
			5.17				741	882.6	84%
Outside Film	0.029	0.17		20000	0.000	0			
			5.00				741	871.9	85%
SUM	2.661	16.00		23.631	0.042	248.485			

		TABLE 14							
	based on table 1, temp: 22/40°C								
				flow into building					
				Permeanc	59.64	Pv Diff:	1198.9		
				flow away:	0.257	g/m2h			
				Net Accumulation:		**0.370**	**g/m2h**		
Sub Total				59.64	0.017	1198.9			
Element	R	ΔT	t °C	M	Rv	Pv Diff	Pv	Psat	RH
			22.00				1578.6	2631	60%
Inside Film	0.120	-0.81		10000.00	0.000	7.2			
			22.81				1585.8	2777	57%
Vapor Retarder	0.000	0.00		60.00	0.017	1191.7			
			22.81				2777.5	2777	100%
				flow from back of sheathing					
				Permeanc	39.14	Pv Diff:	4453.0		
				flow away:	0.627	g/m2h			
Sub Total				39.14	0.026	4453.0			
Batt Insulation	2.500	-16.91		2000.00	0.001	87.1			
			39.72				2864.6	7270	39%
Plywood	0.012	-0.08		40.00	0.025	4357.1			
			39.80				7221.7	7301	99%
Outside Film	0.029	-0.20		20000.00	0.000	8.7			
			40.00				7230.4	7378	98%
SUM	2.661	-18.00		0.03	39.835	5651.8			

For Wall 2, vapor permeance of the painted drywall and fiberboard is 180 vs. 1666. In this case, the vapor permeance of the painted drywall is much smaller than the fiberboard. Here painted drywall acts as a vapor retarder in this wall assembly. No condensation occurs, as shown in table 3, 15 and table 16. Condensation occurs in summer because moisture flow reverses, as shown in table 17.

		TABLE 15							
	based on table 3, temp: 21/ -4°C								
Element	R	ΔT	t °C	M	Rv	Pv Diff	Pv	Psat	RH
			21.00				742	2474	30%
Inside Film	0.120	1.04		10000	0.000	5			
			19.96				737	2331	32%
Painted drywall	0.000	0.00		180	0.006	303			
			19.96				434	2331	19%
Batt Insulation	2.500	21.70		2000	0.001	27			
			-1.74				407	529	77%
Fiberboard	0.231	2.01		1666	0.001	33			
			-3.75				374	447	84%
Outside Film	0.029	0.25		20000	0.000	3			
			-4.00				372	437	85%
SUM	2.880	25.00		146.93	0.007	371			

		TABLE 16							
	based on table 3, temp: 21/ 5°C								
Element	R	ΔT	t °C	M	Rv	Pv Diff	Pv	Psat	RH
			21.00				742	2474	30%
Inside Film	0.120	0.67		10000	0.000	1			
			20.33				741	2386	31%
Painted drywall	0.000	0.00		180	0.006	72			
			20.33				669	2386	28%
Batt Insulation	2.500	13.89		2000	0.001	6			
			6.44				662	964	69%
Fiberboard	0.231	1.28		1666	0.001	8			
			5.16				655	882	74%
Outside Film	0.029	0.16		20000	0.000	1			
			5.00				654	872	75%
SUM	2.880	16.00		146.93	0.007	88			

		TABLE 17							
	based on table 3, temp: 22/ 40°C								
				flow into building					
				Permeanc	176.8173	Pv Diff:	-1189		
				flow away:	-0.75679	g/m2h			
				Net Accumulation:		**13.1**	**g/m2h**		
Sub Total				176.8173	0.006	-1189			
Element	R	ΔT	t °C	M	Rv	Pv Diff	Pv	Psat	RH
			22.00				1579	2631	60%
Inside Film	0.120	-0.75		10000	0.000	-21			
			22.75				1600	2768	58%
Painted drywall	0.000	0.00		180	0.006	-1168			
			22.75				2768	2768	100%
				flow from back of sheathing					
				Permeanc	869.000	Pv Diff:	-4425		
				flow away:	-13.848	g/m2h			
Sub Total				869.3837	0.001	-4425			
Batt Insulation	2.500	-15.63		2000	0.001	-1923			
			38.38				4691	6765	69%
Fiberboard	0.231	-1.44		1666	0.001	-2309			
			39.82				7000	7309	96%
Outside Film	0.029	-0.18		20000	0.000	-192			
			40.00				7192	7339	98%
SUM	2.880	-18.00							

For Wall 3, the vapor permeance of vapor retarder and expanded polystyrene (EPS) is approximately the same (180 vs. 150). There should be moisture problem according to previous analysis, but EPS is an insulating sheathing, it greatly increases the temperature of the first cold weather condensation plane. Saturation pressure is increased at the same time. Relative humidity becomes less, so condensation problem becomes less, too. Shown in table 4, table 18, table 19, and table 20.

		TABLE 4							
	Calculation of Vapor Diffusion with EPS Insulating Sheathing								
Element	R	ΔT	t °C	M	Rv	Pv Diff	Pv	Psat	RH
			21.00				990	2474	40%
Inside Film	0.120	0.82		10000	0.000	5			
			20.18				985	2532	42%
Vapor Retarder	0.000	0.00		180	0.006	261			
			20.18				724	2352	31%
Batt Insulation	2.500	17.13		2000	0.001	24			
			3.05				700	757	93%
EPS sheathing	1.000	6.85		150	0.007	314			
			-3.80				387	459	84%
Outside Film	0.029	0.20		20000	0.000	2			
			-4.00				384	452	85%
SUM	3.649	25.00		77.69	0.013	606			

		TABLE 18							
	based on table 4, temp: 21/ -19°C								
Element	R	ΔT	t °C	M	Rv	Pv Diff	Pv	Psat	RH
			21.00				990	2474.00	40%
Inside Film	0.120	1.32		10000	0.000	11			
			19.68				979	2291.88	43%
Vapor Retarder	0.000	0.00		180	0.006	607			
			19.68				372	2291.88	16%
Batt Insulation	2.500	27.40		2000	0.001	55			
			-7.72				318	317.60	100%
Sub Total				162.4549	0.006	672			
				flow to back of sheathing					
				Permeanc	162.455	Pv Diff:	672		
				flow to :	0.393	g/m2h			
EPS sheathing	1.000	10.96		150	0.007	219			
			-18.68				98	117.12	84%
Outside Film	0.029	0.32		20000	0.000	2			
			-19.00				96	113.50	85%
SUM	3.649	40.00		0.01	162.867	894			
Sub Total				148.88	0.007	221			
				flow away from back of sheathing					
				Permeanc	148.88	Pv Diff:	221		
				flow away:	0.118449	g/m2h			
				Net Accumulation:		**0.27**	**g/m2h**		

		TABLE 19							
	based on table 4, temp: 21/ 5°C								
Element	R	ΔT	t °C	M	Rv	Pv Diff	Pv	Psat	RH
			21.00				990	2474.00	40%
Inside Film	0.120	0.53		10000	0.000	3			
			20.47				987	2407.03	41%
Vapor Retarder	0.000	0.00		180	0.006	145			
			20.47				842	2407.03	35%
Batt Insulation	2.500	10.96		2000	0.001	13			
			9.51				829	1187.80	70%
EPS sheathing	1.000	4.38		150	0.007	174			
			5.13				655	880.06	74%
Outside Film	0.029	0.13		20000	0.000	1			
			5.00				654	871.90	75%
SUM	3.649	16.00		77.69	0.013	336			

		TABLE 20							
	based on table 4, temp: 22/ 40°C								
				flow into building					
				Permeanc	176.8	Pv Diff:	1162		
				flow away:	-0.73988	g/m2h			
				Net Accumulation:		**1.48**	**g/m2h**		
Sub Total				176.8173	0.006	-1162			
Element	R	ΔT	t °C	M	Rv	Pv Diff	Pv	Psat	RH
			22.00				1578.6	2631.00	60%
Inside Film	0.120	-0.59		10000	0.000				
			22.59				1579	2740.94	58%
Vapor Retarder	0.000	0.00		180	0.006				
			22.59				2741	2740.94	100%
				flow from back of sheathing					
				Permeanc	138.570	Pv Diff:	4451		
				flow away:	-2.220	g/m2h			
Sub Total				138.5681	0.007	-4451			
Batt Insulation	2.500	-12.33		2000	0.001	-308			
			34.92				3049	5599.68	54%
EPS sheathing	1.000	-4.93		150	0.007	-4112			
			39.86				7161	7324.10	98%
Outside Film	0.029	-0.14		20000	0.000	-31			
			40.00				7192	7339.00	98%
SUM	3.649	-18.00		0.01	136.370	-5614			

For Wall 4, with vapor retarder and fiberboard (permeance: 60 vs. 1666), no condensation in winter, as shown in table 21, 22, and 23. Summer condensation occurred because water vapor, which entered the wall assembly, cannot get to the inside because of low permeance of vapor retarder, as shown in table 5.

		TABLE 21										
	based on table 5, temp: 21/ -19°C											
Element	t(mm)	k	C	R	ΔT	t °C	M	Rv	Pv Diff	Pv	Psat	RH
						21.0				990	2474	40%
Inside Film	2	NA	8.30	0.120	1.67		10000	0.000	5			
						19.3				985	2238.3	44%
Vapor Retarder	0	NA	0.00	0.000	0.00		60	0.017	831			
						19.3				154	2238.3	7%
Batt Insulation	90	0.04	0.04	2.500	34.71		2000	0.001	25			
						-15.4				129	159.36	81%
Fiberboard	12.7	0.06	4.33	0.231	3.21		1666	0.001	30			
						-18.6				99	118.02	84%
Outside Film	2	NA	34.00	0.029	0.41		20000	0.000	2			
						-19.0				96	113.5	85%
SUM				2.881	40.00		55.81	0.018	893			

		TABLE 22										
	based on table 5, temp: 21/ -4°C											
Element	t(mm)	k	C	R	ΔT	t °C	M	Rv	Pv Diff	Pv	Psat	RH
						21.0				990	2474	40%
Inside Film	2	NA	8.30	0.120	1.05		10000	0.000	3			
						20.0				986	2337	42%
Vapor Retarder	0	NA	0.00	0.000	0.00		60	0.017	575			
						20.0				411	2337	18%
Batt Insulation	90	0.04	0.04	2.500	21.70		2000	0.001	17			
						-1.7				394	530.8	74%
Fiberboard	12.7	0.06	4.33	0.231	2.00		1666	0.001	21			
						-3.7				373	448.75	83%
Outside Film	2	NA	34.00	0.029	0.26		20000	0.000	2			
						-4.0				372	437.2	85%
SUM				2.881	25.00		55.81	0.018	618			

		TABLE 23										
	based on table 5, temp: 21/ 5°C											
Element	t(mm)	k	C	R	ΔT	t °C	M	Rv	Pv Diff	Pv	Psat	RH
						21.0				990	2474	40%
Inside Film	2	NA	8.30	0.120	0.67		10000	0.000	2			
						20.3				988	2381.7	41%
Vapor Retarder	0	NA	0.00	0.000	0.00		60	0.017	312			
						20.3				675	2381.7	28%
Batt Insulation	90	0.04	0.04	2.500	13.88		2000	0.001	9			
						6.4				666	961.22	69%
Fiberboard	12.7	0.06	4.33	0.231	1.28		1666	0.001	11			
						5.2				655	884.46	74%
Outside Film	2	NA	34.00	0.029	0.16		20000	0.000	1			
						5.0				654	871.9	75%
SUM				2.881	16.00		55.81	0.018	336			

For Wall 5, with gypsum drywall and plywood (permeance: 180 vs. 40), because the permeance of plywood is lower than gypsum drywall, so in this case, plywood actually acts as a vapor retarder in this wall assembly. In winter, it is not easy for water vapor to dry to the outside, as shown in table 10 and table 12, but in summer, no condensation problem at all (as shown in table 24).

		TABLE 10							
based on table 1, a layer of primer and two coats of latex paint over gypsum drywall substitute code-approved vapor retarder									
Element	R	ΔT	t °C	M	Rv	Pv Diff	Pv	Psat	RH
			21.00				990	2474	40%
Inside Film	0.120	1.75		10000	0.000	14			
			19.25				975	2212	44%
Gypsum Drywal	0.079	1.15		180	0.006	785			
			18.09				191	2075	9%
Batt Insulation	2.500	36.50		2000	0.001	71			
			-18.40				120	120.3	100%
Sub Total				162.455	0.006	869			
				Flow to back of sheathing					
				Permeance=5162.5		Pv Diff:847			
				Flow to:	0.508	g/m2h			
Plywood	0.012	0.18		40	0.025	5			
			-18.58				116	141	82%
Outside Film	0.029	0.42		20000	0.000	0			
			-19.00				116	136	85%
Sub Total				39.920	0.025	5			
SUM	2.740	40.00		1.832	0.546	874			
				Flow away from back of sheathing					
				Permeance=39.92		Pv Diff:5			
				Flow away	0.001	g/m2h			
				Net Accumulation:		**0.508**	**g/m2h**		

		TABLE 12							
based on table 2, a layer of primer and two coats of latex paint over gypsum drywall substitute code-approved vapor retarder									
Element	R	ΔT	t °C	M	Rv	Pv Diff	Pv	Psat	RH
			21.00				990	2474	40%
Inside Film	0.120	1.09		10000	0.000	9			
			19.91				981	2324	42%
Gypsum Drywal	0.079	0.72		180	0.006	486			
			19.18				495	2221	22%
Batt Insulation	2.500	22.81		2000	0.001	44			
			-3.63				451	451.4	100%
Sub Total				162.455	0.006	538			
				Flow to back of sheathing					
				Permeance=5162.5		Pv Diff:847			
				Flow to:	0.315	g/m2h			
Plywood	0.012	0.11		40	0.025	167			
			-3.74				285	447.2	64%
Outside Film	0.029	0.26		20000	0.000	0			
			-4.00				284	437.2	65%
Sub Total				39.920	0.025	167			
SUM	2.740	25.00		2.840	0.352	705.42			
				Flow away from back of sheathing					
				Permeance=39.92		Pv Diff:5			
				Flow away	0.024	g/m2h			
				Net Accumulation:		**0.291**	**g/m2h**		

		TABLE 24							
based on table 10, a layer of primer and two coats of latex paint over gypsum drywall substitute code-approved vapor retarder									
	22/ 40°C								
Element	R	ΔT	t °C	M	Rv	Pv Diff	Pv	Psat	RH
			22.00				1579	2631.0	60%
Inside Film	0.120	-0.79		10000	0.000	-18			
			22.79				1597	2774.14	58%
Gypsum Drywal	0.079	-0.52		180	0.006	-999			
			23.31				2596	2862.94	91%
Batt Insulation	2.500	-16.42		2000	0.001	-90			
			39.73				2686	7274.05	37%
Plywood	0.012	-0.08		40	0.025	-4497			
			39.81				7183	7304.85	98%
Outside Film	0.029	-0.19		20000	0.000	-9			
			40.00				7192	7339	98%
SUM	2.740	-18.00		32.046	0.031	-5613.62			

According to the analyses from above, an important principle came into being. Vapor barriers cannot only be understood as several kinds of materials, of which their vapor permeance is lower than 60 metric perms. A lot of wall components, which have relatively smaller vapor permeance compared to other wall components, actually work as vapor barriers in their wall assemblies to reduce the occurrence or intensity of condensation.

The following table is a summary of calculation for Omaha, Nebraska (a cold climate)

Summary

Calculation for Omaha, Nebraska (a cold climate)

Wall 1	**Temperature**	**Temp: 21/ -19°C**	**Temp: 21/ -4°C**	**Temp: 21/ 5°C**	**Temp: 22/ 40°C**
	Element Inside film **Vapor retarder** Batt insulation **Plywood** Outside film	Table 1 Condensation Rate: 0.172 g/m2h Mvapor retarder:**60** **M**plywood:**40** MR (plywood)=2% Table 9 Condensation Rate:0 very small Vapor retarder: **M=1.5**	Table 2 Condensation Rate: 0.10 g/m2h MR (plywood)=1.05%	Table 7 Condensation Rate:0 very small	Table 14 Condensation Rate: 0.370 g/m2h MR(spruce)=1.75%
Wall 2	Element Inside film **Painted drywall** Batt insulation **Fiberboard** Outside film	Table 3 No condensation in door RH=30% **M**painted drywall:**180** **M**fiberboard:**1666** Table 13 Condensation Rate: 0.092 g/m2h in door RH=40% MR (fiberboard)=1.69%	Table 15 No condensation in door RH=30%	Table 16 No condensation in door RH=30%	Table 17 Condensation Rate: 13.1 g/m2h MR (painted drywall)= 87.33%
Wall 3	Element Inside film **Vapor retarder** Batt insulation **EPS sheathing** Outside film	Table 18 Condensation Rate: 0.270 g/m2h **M**vapor retarder:**180** **M**eps:**150** MR (spruce)=1.28%	Table 4 No condensation Vapor retarder: **M=180**	Table 19 No condensation	Table 20 Condensation Rate: 1.48 g/m2h MR (spruce)=7.01%
Wall 4	Element Inside film **Vapor retarder** Batt insulation **Fiberboard** Outside film	Table 21 No condensation **M**vapor retarder: **60** **M**fiberboard: **1666**	Table 22 No condensation	Table 23 No condensation	Table 5 Condensation Rate: 13.64 g/m2h MR (spruce)=64.61%
Wall 5	Element Inside film **Gypsum drywall** Batt insulation **Plywood** Outside film	Table 10 Temp: 21/ -19°C Condensation Rate: 0.508 g/m2h **M**gypsum:**180** **M**plywood:**40** MR (plywood)=5.33%	Table 12 Temp: 21/ -4°C Condensation Rate: 0.291 g/m2h MR(plywood)=3.06%	Table 11 Temp: 21/ 6°C No condensation	Table 24 Temp: 22/ 40°C No condensation

Note: means tables the author mentioned in the paper

means tables the author only mentioned their results in the paper

means relevant tables the author didn't mentioned in the paper

MR Moisture Content Rise For One Month

Appendix D
FIBERBOARD-3H-OPEN

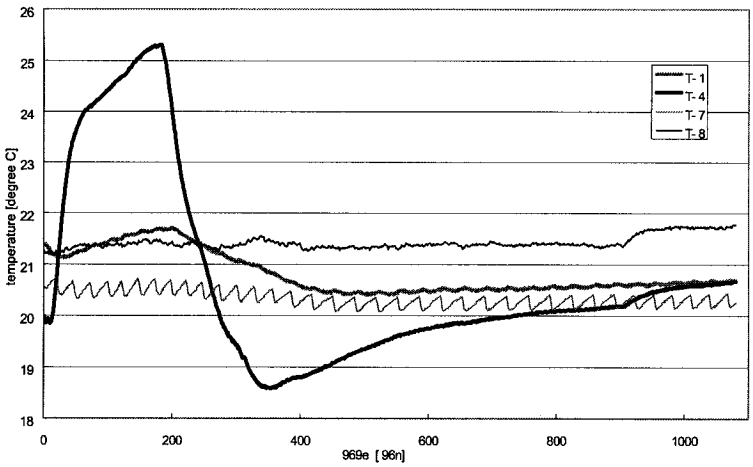

Sensors location:

1- near PE-Membrane
4- in the air cavity
7- inside the test hut
8- outside the test hut

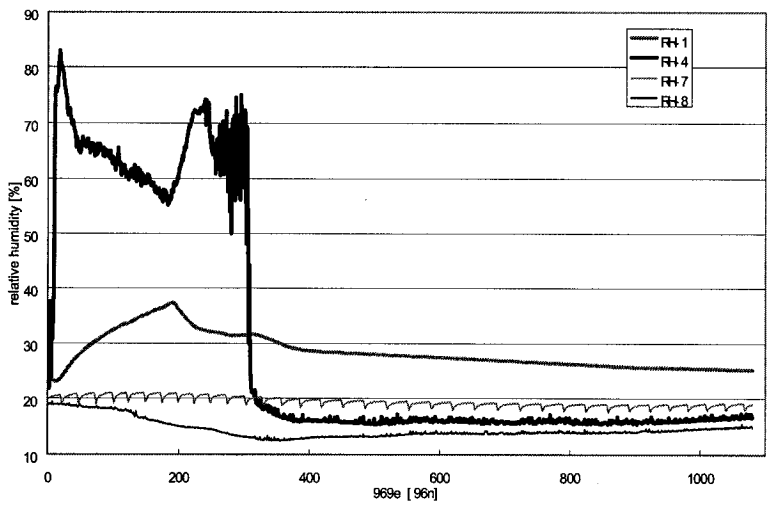

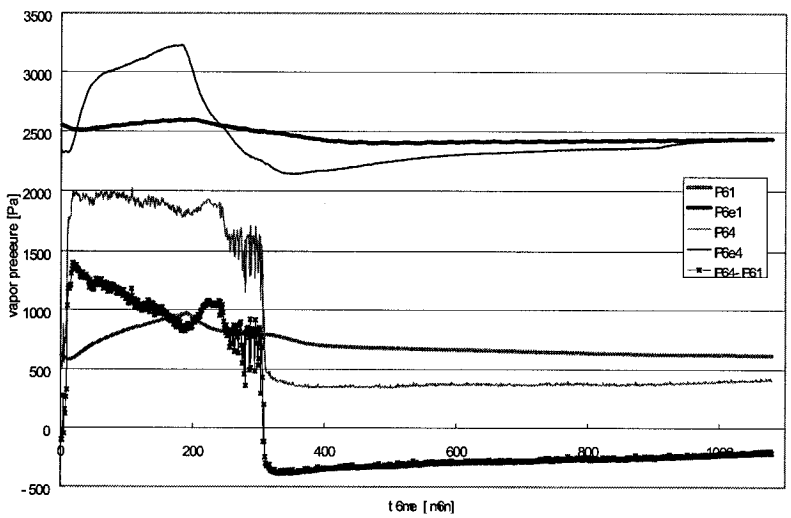

FIBERBOARD-3H-CLOSED

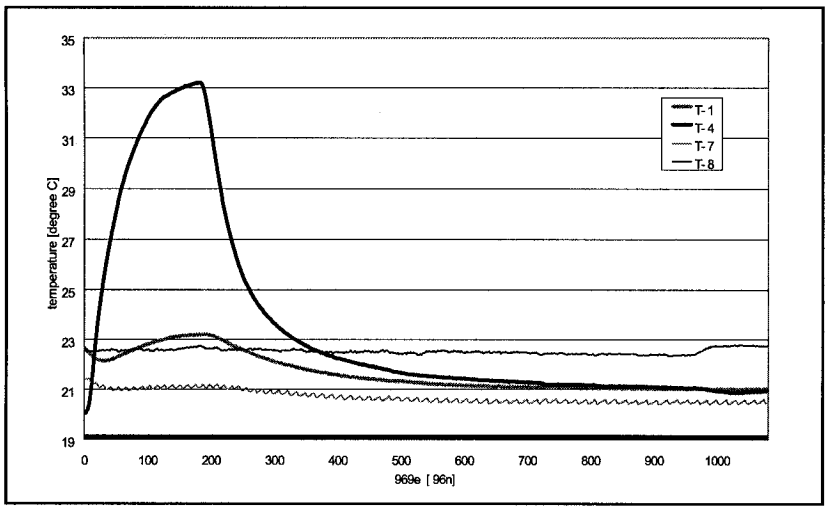

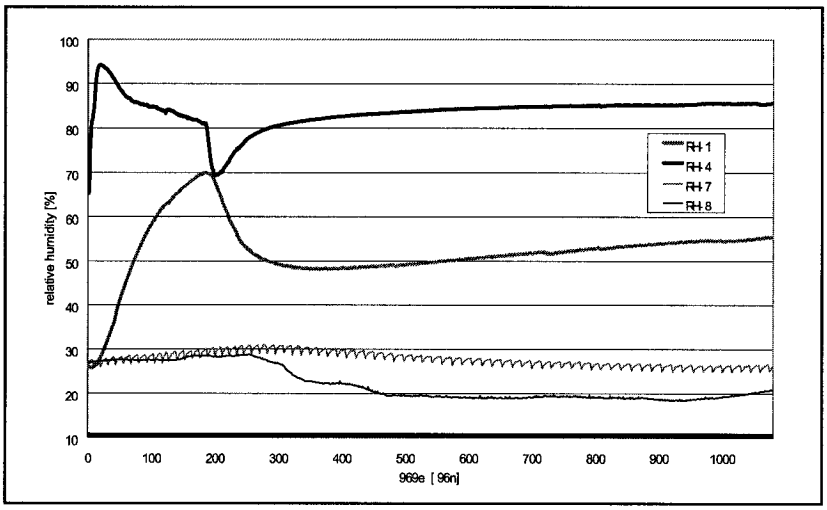

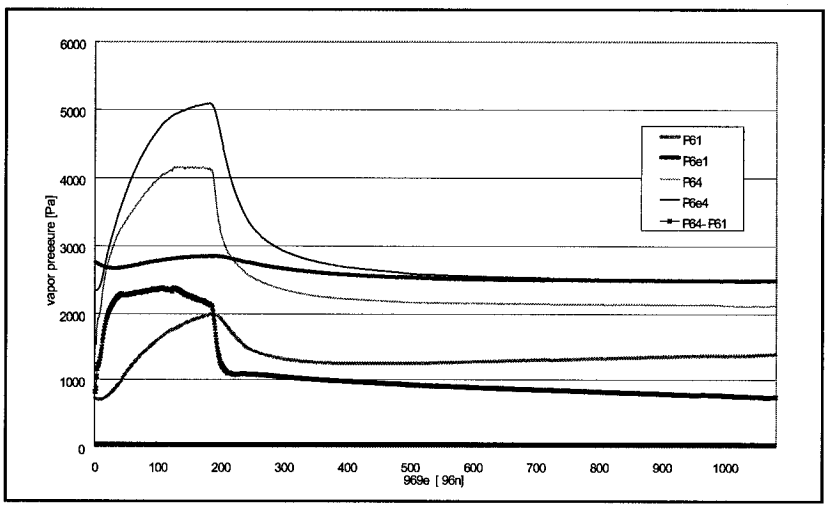

FIBERBOARD-6H-CLOSED

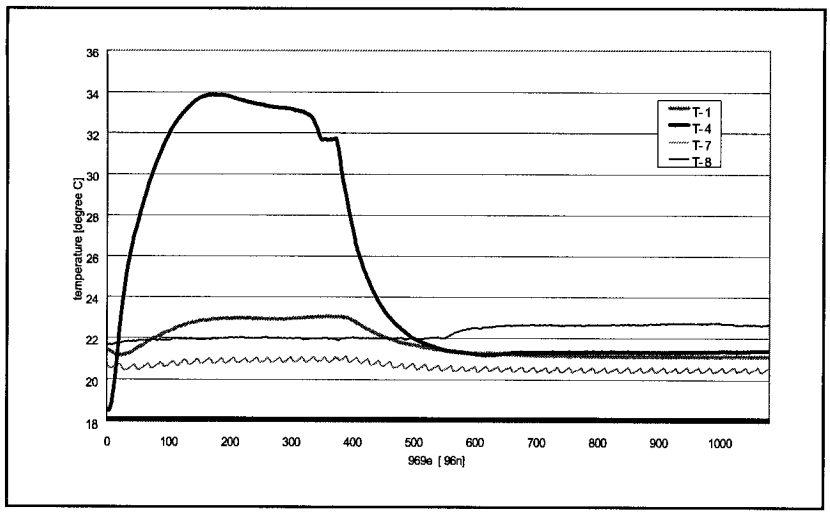

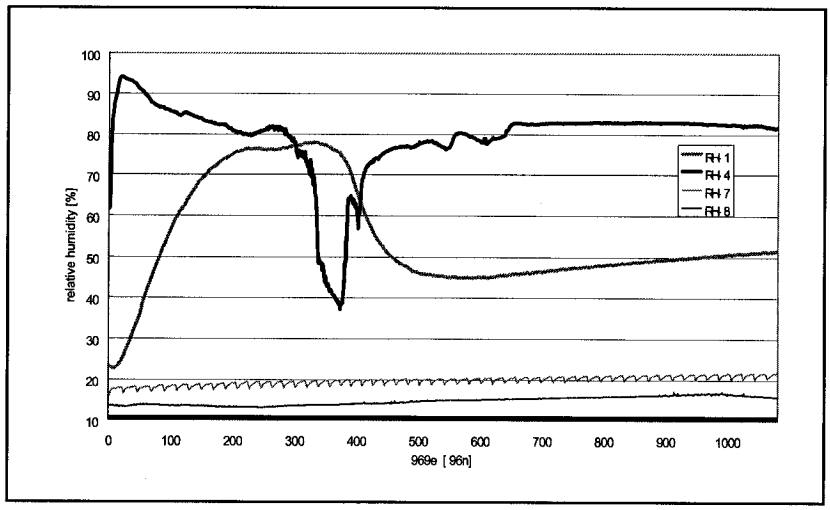

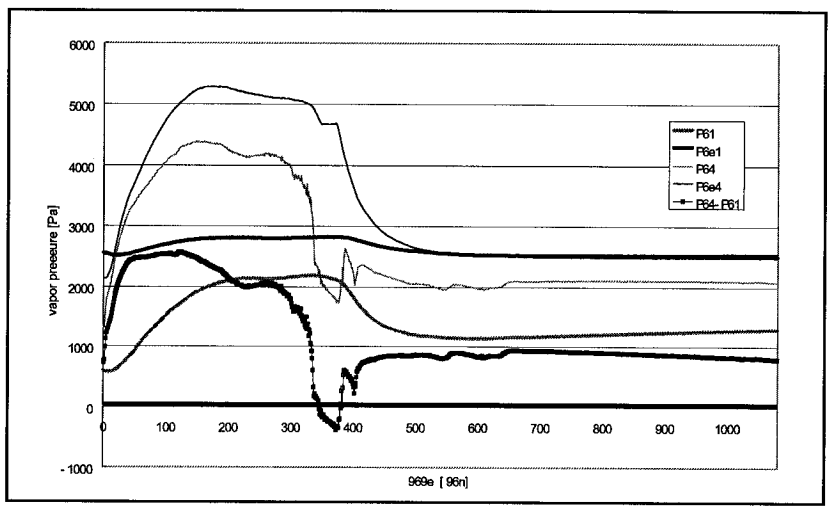

PLYWOOD-3H-OPEN

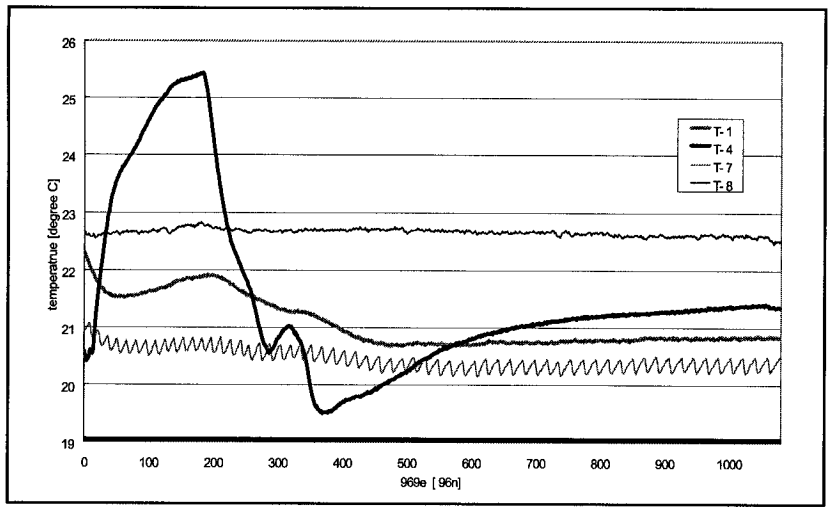

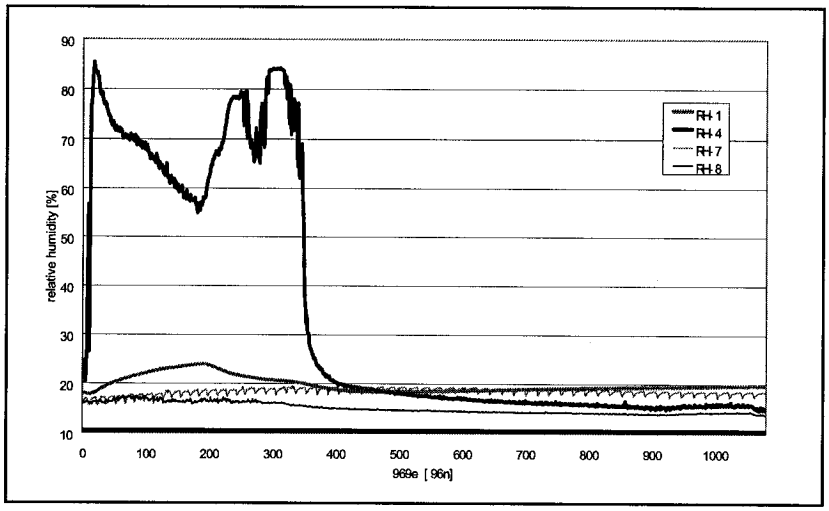

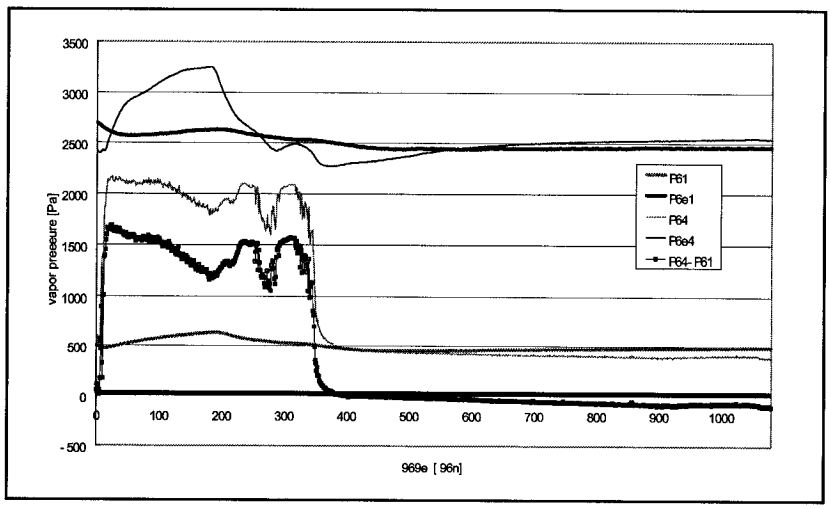

PLYWOOD-3H-CLOSED

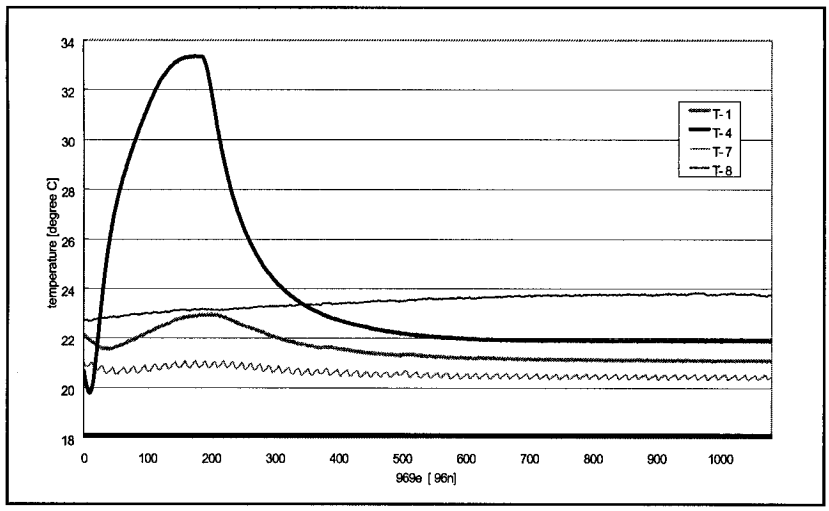

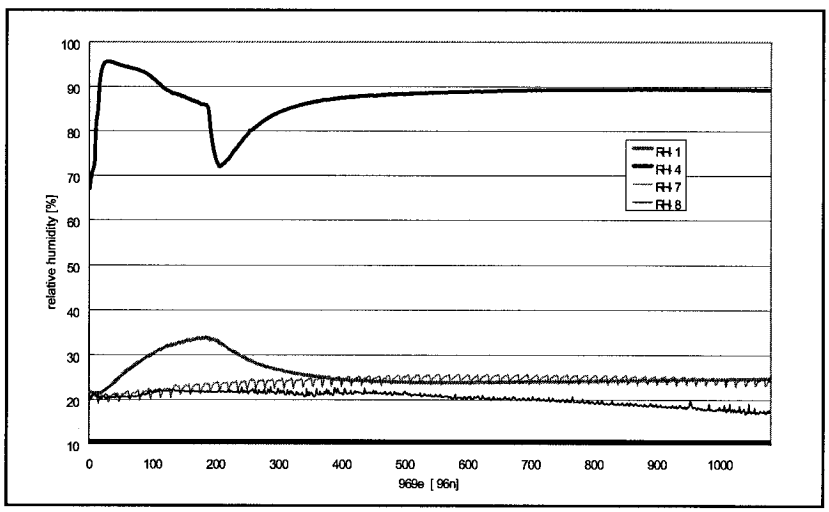

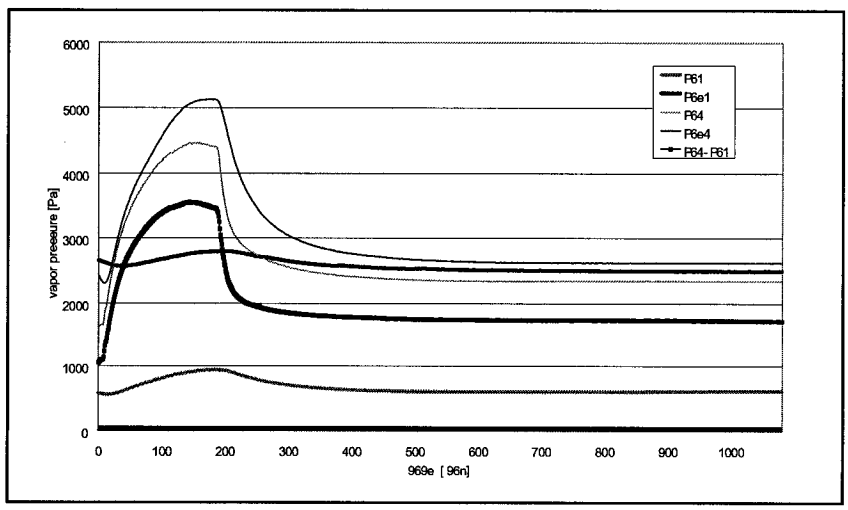

PLYWOOD-6H-CLOSED

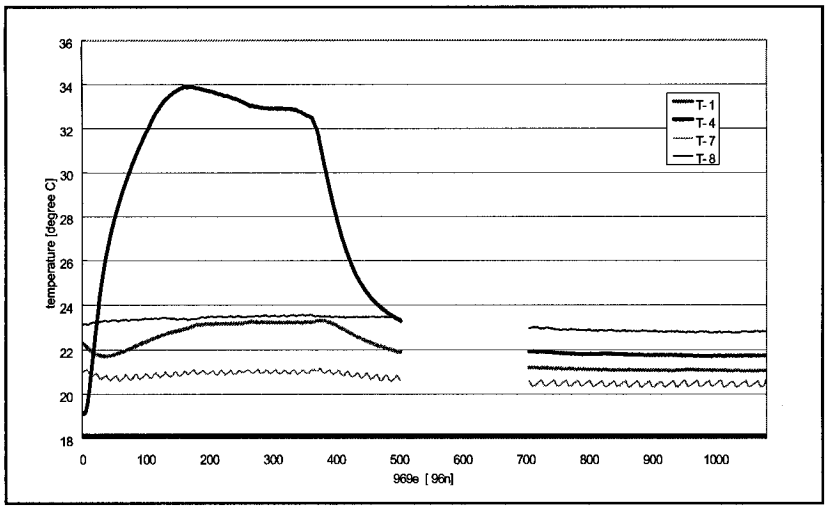

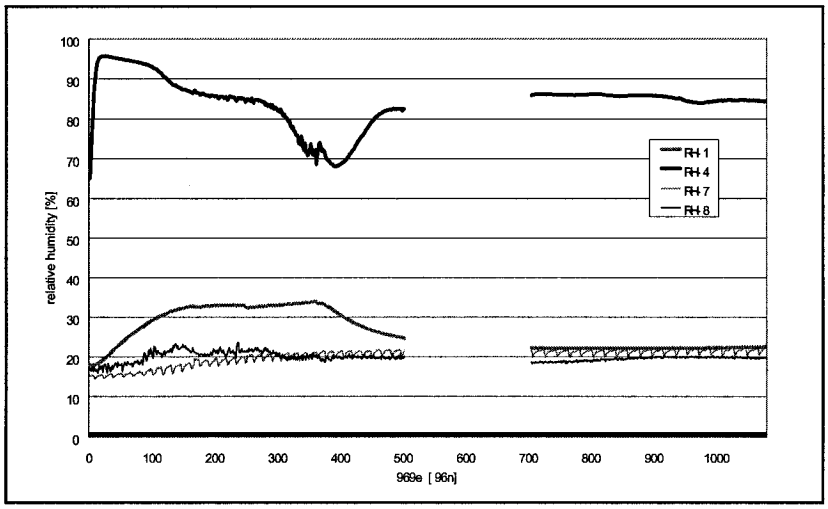

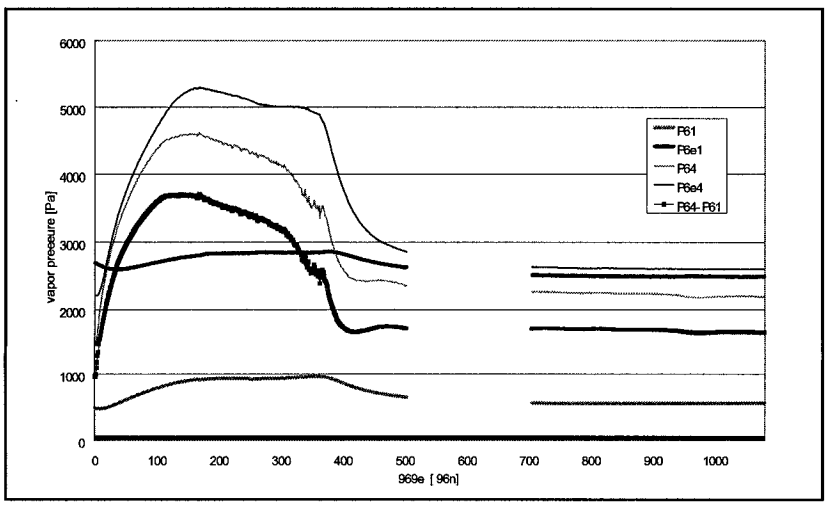

OSB-3H-OPEN

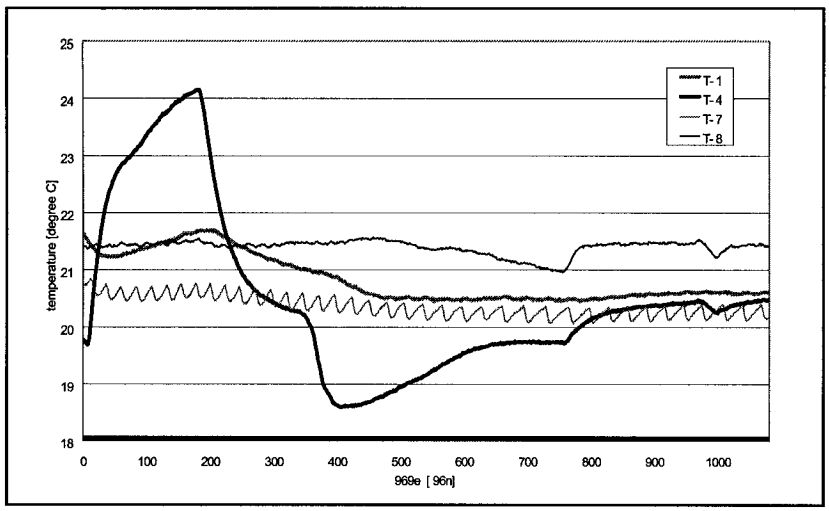
T-1
T-4
T-7
T-8
temperature [degree C]
969e [96n]

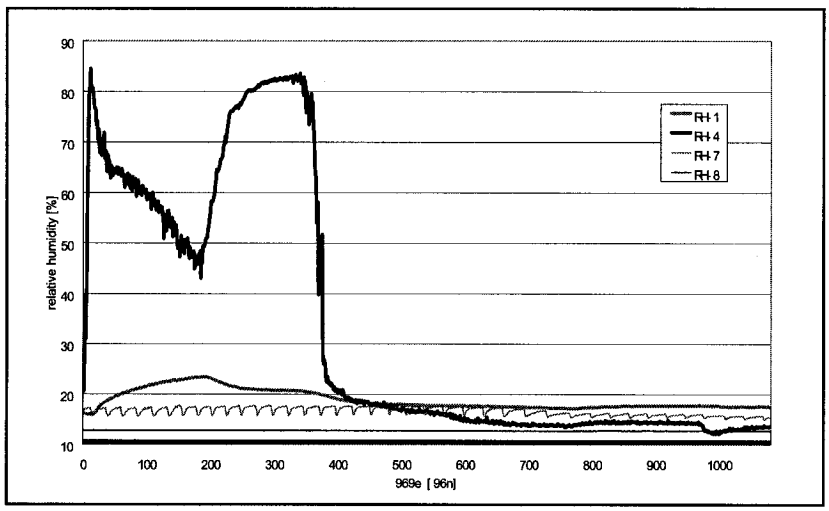
RH-1
RH-4
RH-7
RH-8
relative humidity [%]
969e [96n]

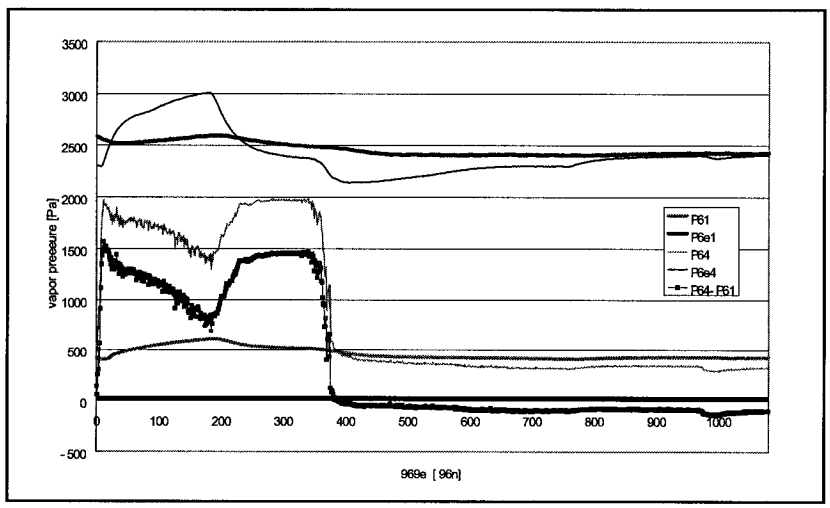
P61
P6e1
P64
P6e4
P64-P61
vapor preseure [Pa]
969e [96n]

OSB-3H-CLOSED

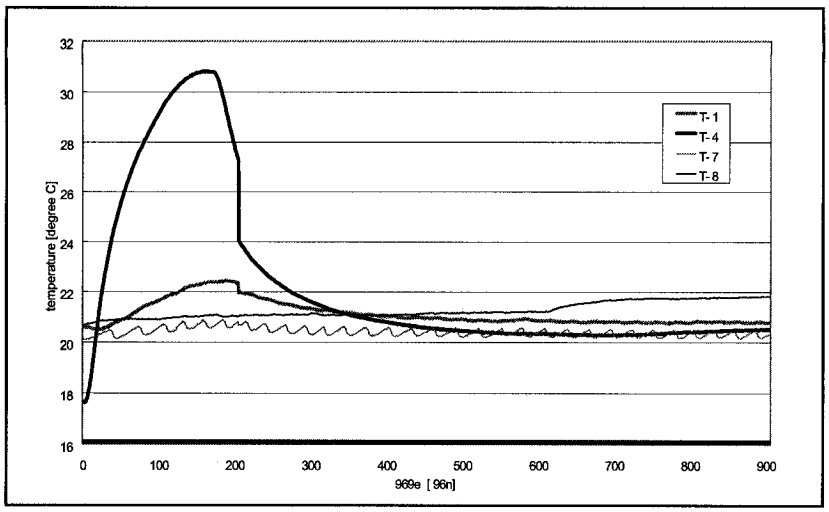

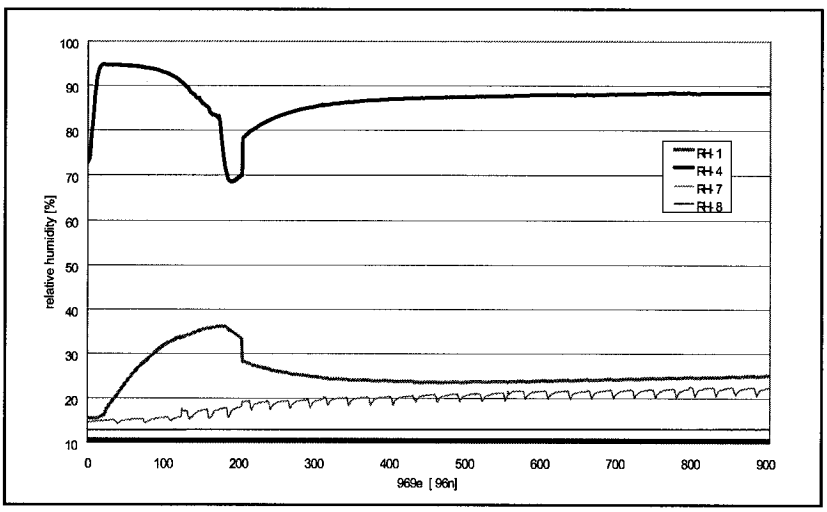

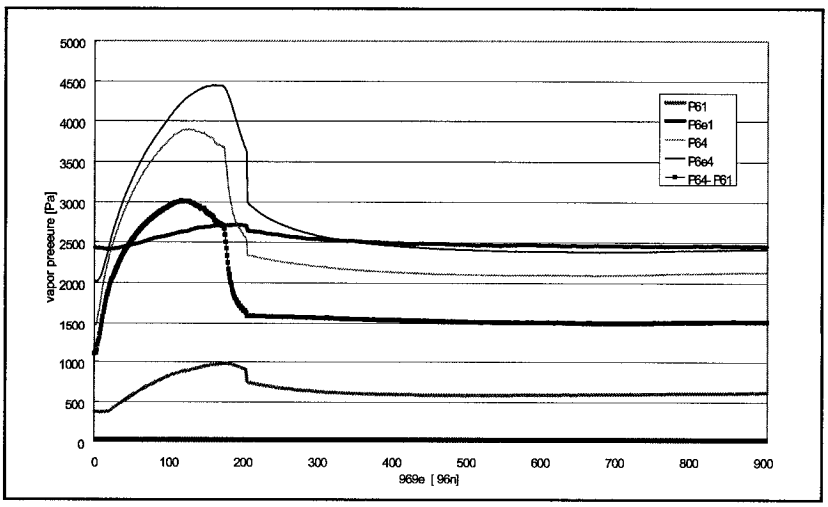

OSB-6H-CLOSED

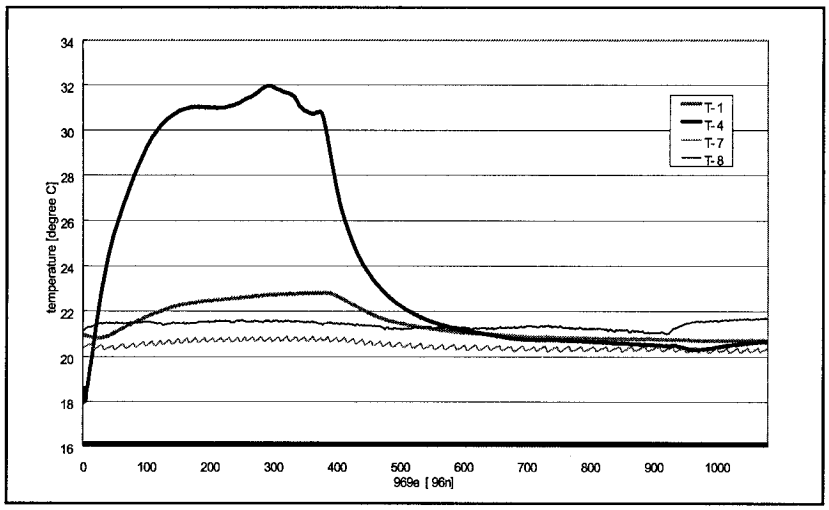

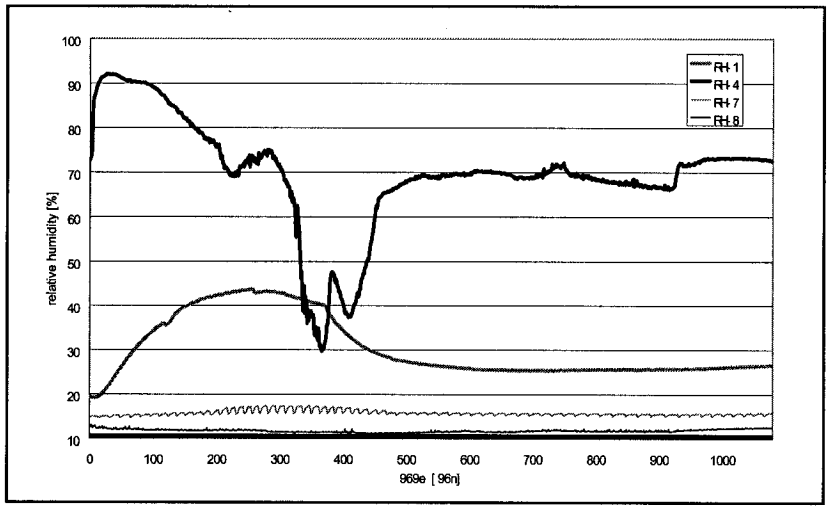

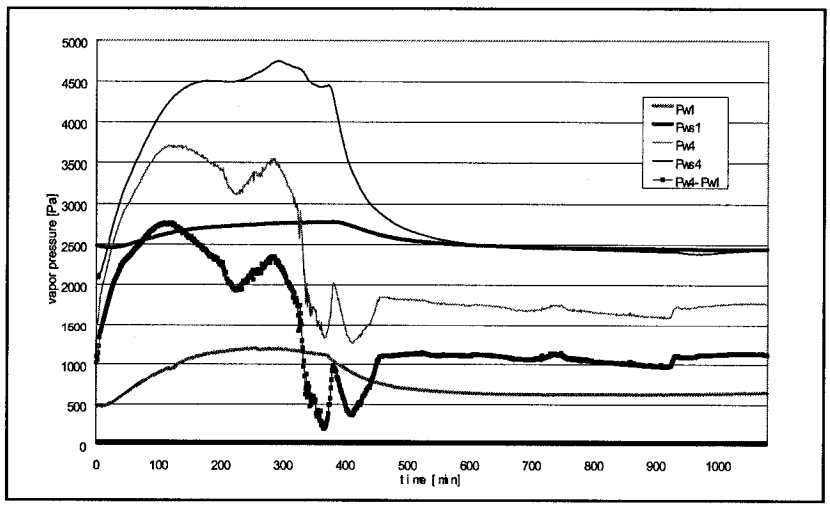

FIBERBOARD-3H-OPEN-NO PE

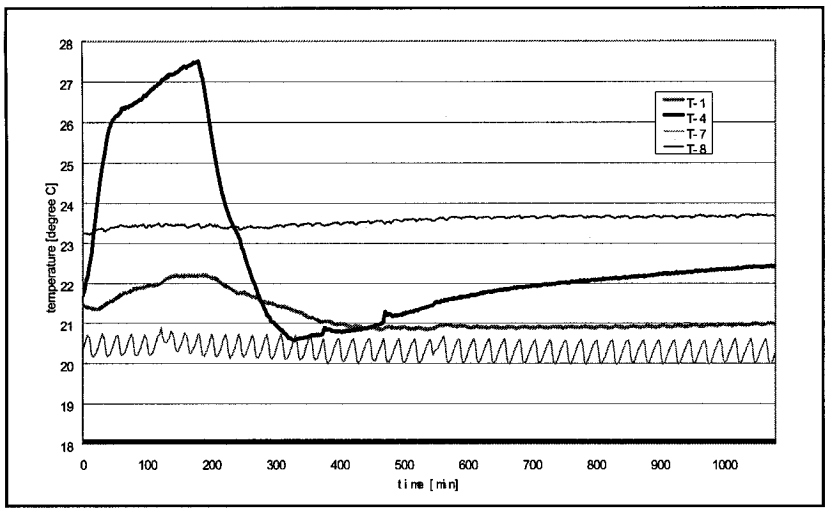

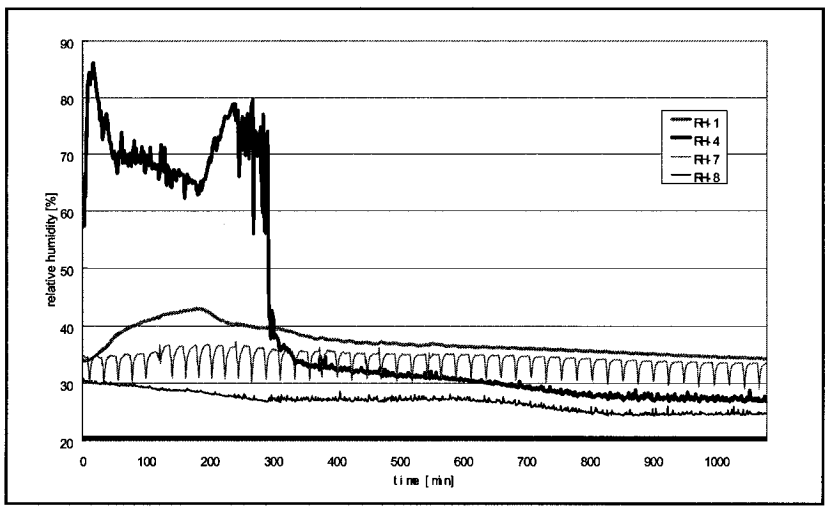

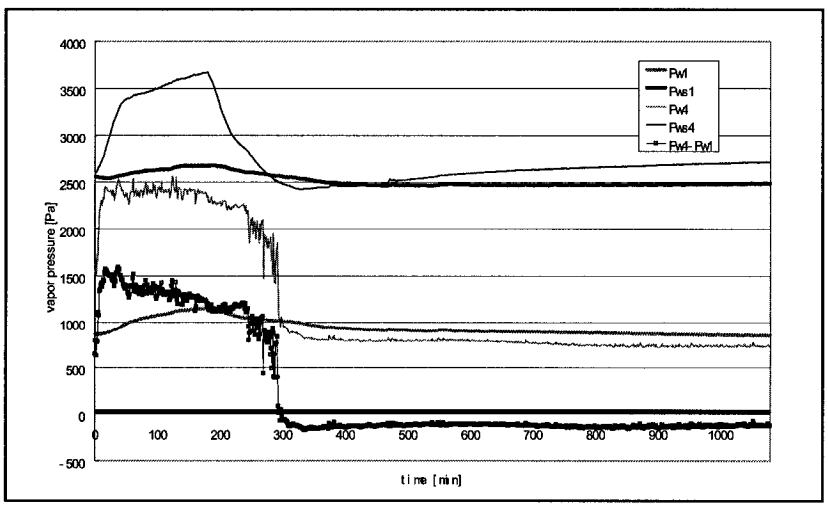

FIBERBOARD-3H-CLOSED-NO PE

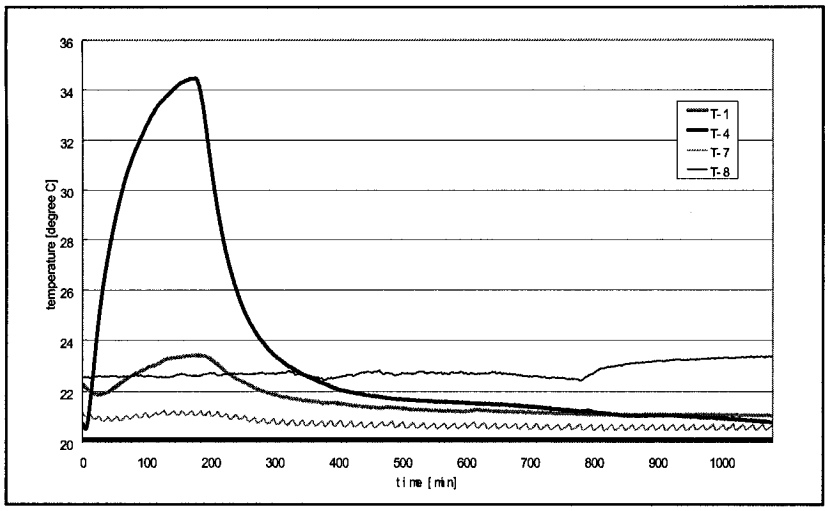

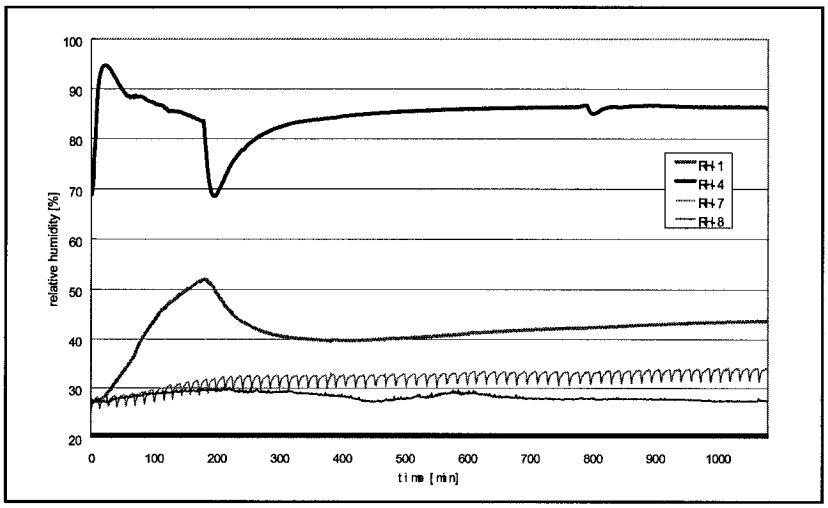

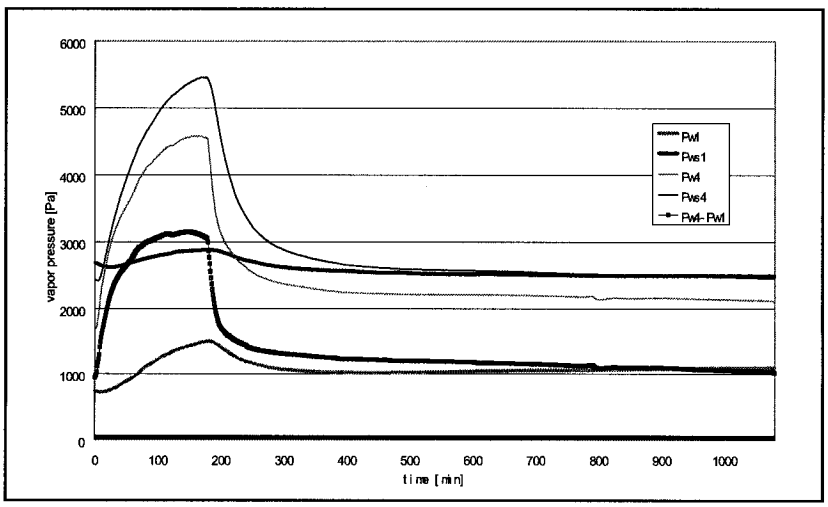

FIBERBOARD-6H-CLOSED-NO PE

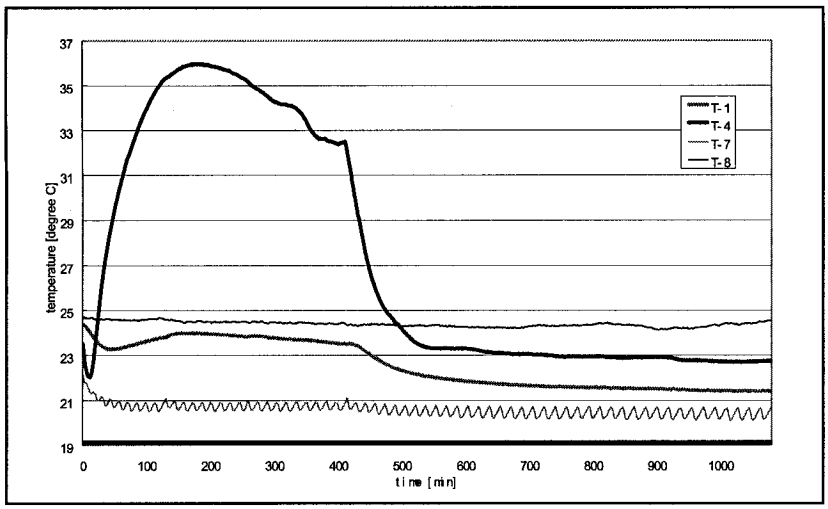

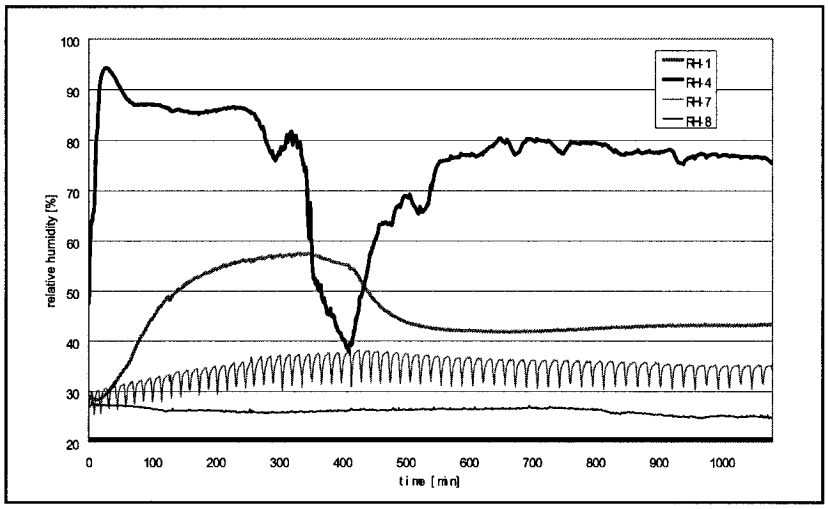

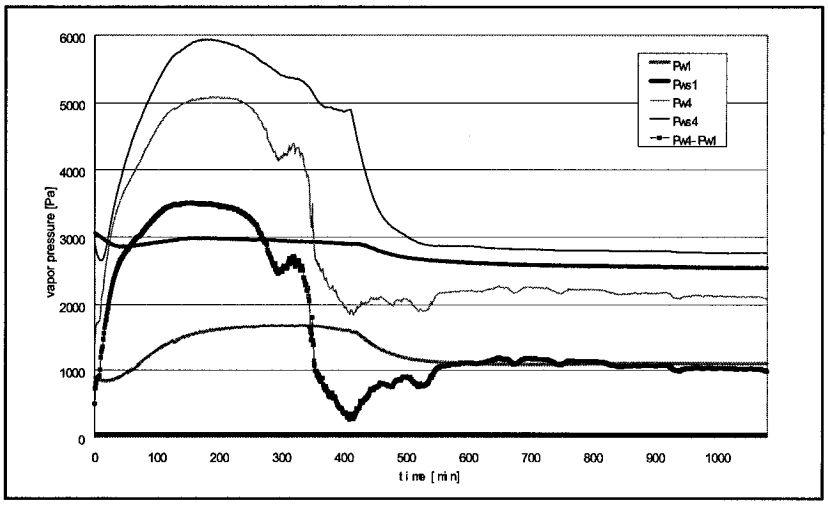

Appendix E

Paper backside (0.5 mm)

No.	RH	Water Content [kg/m^2]
1	0.325	0.0075
2	0.550	0.0076
3	0.800	0.0110
4	0.940	0.0230

Interior gypsum layer (11.5 mm)

No.	RH	Water Content [kg/m^2]
1	0.325	0.013
2	0.550	0.014
3	0.800	0.024
4	0.940	0.052

Paper frontside (0.5 mm)

No.	RH	Water Content [kg/m^2]
1	0.325	0.007
2	0.550	0.0076
3	0.800	0.0110
4	0.940	0.0200

The tables can be rewritten in the following format.

Paper backside (0.5 mm)

No.	RH	Water Content [kg/m^3]
1	0.325	15
2	0.550	15.2
3	0.800	22
4	0.940	46

Interior gypsum layer (11.5 mm)

No.	RH	Water Content [kg/m^3]
1	0.325	1.13
2	0.550	1.22
3	0.800	2.09
4	0.940	4.52

Paper frontside (0.5 mm)

No.	RH	Water Content [kg/m^3]
1	0.325	14
2	0.550	15.2
3	0.800	22
4	0.940	40